DISSERTATION

BIOCHEMICAL, BIOPHYSICAL AND FUNCTIONAL CHARACTERIZATION OF HISTONE CHAPERONES

Submitted by

Ling Zhang

Department of Biochemistry and Molecular Biology

In partial fulfillment of the requirements

For the Degree of Doctor of Philosophy

Colorado State University

Fort Collins, Colorado

Spring 2014

Doctoral committee:

Advisor: Karolin Luger

Diego Krapf
Jennifer Nyborg
Alan van Orden
Laurie Stargell

ABSTRACT

BIOCHEMICAL, BIOPHYSICAL AND FUNCTIONAL CHARACTERIZATION OF HISTONE CHAPERONES

Nucleosomes, the basic repeating unit of chromatin, are highly dynamic. Nucleosome dynamics allow for various cellular activities such as replication, recombination, transcription and DNA repair, while maintaining a high degree of DNA compaction. Each nucleosome is composed of 147 bp DNA wrapping around a histone octamer. Histone chaperones interact with histones and regulate nucleosome assembly and disassembly in the absence of ATP. To understand how nucleosome dynamics are regulated, it is essential to characterize the functions of histone chaperones.

The first project of my doctoral research focused on the comparison of different nucleosome assembly proteins employing various biochemical and molecular approaches. Nucleosome assembly proteins (Nap) are a large family of histone chaperones, including Nap1 and Vps75 in *Saccharomyces cerevisiae*, and Nap1 (also Nap1L1), Nap1L2-6 (Nap1-like 2-6, with Nap1L4 being Nap2) and Set in metazoans. The functional differences of nucleosome assembly proteins are thus interesting to explore. We show that Nap1, Nap2 and Set bind to histones with similar and high affinities, but Nap2 and Set do not disassemble non-nucleosomal DNA-histone complexes as efficiently as Nap1. Also, nucleosome assembly proteins do not display discrepancies for histone variants or different DNA sequences.

In the second project, we identified Spn1 as a novel histone chaperone and look into new functions of Spn1 on the regulation of chromatin structural states. Spn1 was identified as a transcription regulator that regulates post-recruitment of RNA polymerase II in yeast. We demonstrated that Spn1 is a H3/H4 histone chaperone, a novel finding that was not observed previously. Spn1 also interacts with Nap1, and forms ternary complexes with Nap1 and histones. We also show that Spn1 has chromatin assembly activity and N- and C- terminal domains of Spn1 are required for its histone chaperone properties. At the same time, we had an interesting observation that Spn1 potentially has topoisomerase/nuclease activity, which is dependent on magnesium ions. This activity of Spn1 can also help answer questions raised by *in vivo* assays related to Spn1, including its correlation with telomere length, the heat sensitivity in the reduction of function yeast strains, and the elongated lifespan in the Spn1ΔNΔC strain.

Our studies on the functional comparison of nucleosome assembly proteins revealed their distinct roles in the regulation of nucleosome dynamics. Our findings on the histone chaperone functions and nuclease/topoisomerase activities disclosed new roles of Spn1 in chromatin regulation, by regulating histone-DNA interaction and also maintenance of DNA integrity.

Ling Zhang

Department of Biochemistry and Molecular Biology

Colorado State University

Fort Collins, Colorado 80523

Spring 2014

ACKNOWLEDGEMENTS

I owe my deepest gratitude to my advisor Professor Dr. Karolin Luger, for her mentorship on my graduate research. It has been an honor for me to have the chance to pursue my graduate degree in the Luger lab. Professor Luger has always been encouraging, while offering generous advice, suggestions and support towards my projects. She is an excellent scientist and her passion for science has always inspired me.

I am also grateful to members of my graduate student advisory committee, Professor Dr. Diego Krapf, Professor Dr. Jennifer Nyborg, Professor Dr. Alan van Orden and Professor Dr. Laurie Stargell. I thank all of them for their advice, comments and critiques over the years. Not only did they offer suggestions for my research, they also helped me improving my presentation and writing skills, from which I will benefit for the rest of my research career.

I want to thank people in the Luger lab. Everybody is always nice and willing to help. Pam Dyer was my first mentor and taught me various techniques. Dr. Vidya Subramanian, a former graduate student, helped me a lot when I just started my graduate project. All the former and present members of the Luger lab are awesome people to work with, be friends with and learn from, including Dr. Andy Andrews, Dr. Serge Bergeron, Kitty Brown, Dr. Xu Chen, Dr. Nick Clark, Dr. Sheena D'Arcy, Dr. Meckonnen Lemma Dechassa, Yajie Gu, Dr. Aaron Hieb, Dan Krizizike, Dr. Wayne Lilyestrom, Uma Muthurajan, Dr. Young-jun Park, Dr. Mary Robinson, Tao Wang, Alison

White, Dr. Duane Winkler, Dr, Mark van der Woerd, Kat Wyns, Dr. Chenghua Yang and Keda Zhou.

I would like to thank my collaborators from other labs, Dr. Qian Zhang from Nyborg lab, Adam Almeida and Dr. Cathy Radebaugh from Stargell lab, Dr. Ferdinand Kappes From Markovitz lab in University of Michigan Medical Center. Collaboration with them was pleasant and enjoyable, and I appreciate the opportunity not only to work on various interesting projects, but also to learn from and exchange ideas with other scientists.

I also want to thank members of the P01 group. My collaborators and I have presented our research several times among the group and also the microgroups. Members in the P01 group have expertise in various areas, and offered insights in different aspects, which helped us to improve on the designing of the projects and understanding of experimental results.

I want to thank American Heart Association for providing me with the predoctoral fellowship (AHA-10PRE4160125). This rare opportunity offered financial support for the research I have done.

Last but not least, I want to thank my family, especially my parents, for their understanding during the time of my oversea studies. They appreciated my devotion for science, and showed generous support towards all the decisions I have made. Their unconditional love got me through tough times during my graduate studies and allowed me to carry on.

TABLE OF CONTENTS

PROJECT I.

TITLE: FUNCTIONAL STUDIES OF NUCLEOSOME ASSEMBLY PROTEIN FAMILY MEMBERS

CHAPTER 1

REVIEW OF LITERATURE

1.1 Chromatin architecture and dynamics

Deoxyribonucleic acid (DNA) is the major carrier of the genetic information. DNA strands are composed of nucleotides, deoxyribose and phosphate groups. Genetic information stored in DNA is encoded by a combination of four nucleotides (guanine, adenine, thymine and cytosine).

In eukaryotic cells, the genetic material DNA is organized into chromatin and stored in the nucleus of a cell. In mammalian cells, approximately 2 meters length of linear DNA is packed into a nucleus of about 10 μm diameter. The formation of chromatin allows DNA to package into a much smaller volume to fit into the cell nucleus. Yet at the same time, chromatin has to be dynamic, allowing enzymatic activities during replication, recombination, transcription and DNA repair (Luger, 2003). Proper regulation of chromatin dynamics is essential for proper functions of living organisms. Based on the local structure, chromatin is divided into two groups: euchromatin is comparatively loosely

packaged, and DNA coding genes are actively regulated (Hsu, 1962); heterochromatin is tightly packaged, and DNA is generally inaccessible for gene transcription (Frenster et al, 1963; Grewal & Elgin, 2002).

The regulation of chromatin dynamics is essential for cellular processes such as transcription, achieved via the regulation of nucleosome dynamics. Nucleosomes are the basic repeating units of chromatin. In the nucleosome, 147 bp of DNA is wrapped around a histone octamer which consists of two copies of each histone H2A, H2B, H3, H4 (Luger et al, 1997). During the assembly of the nucleosome, a $(H3/H4)_2$ tetramer (or two half-tetramers) is first deposited onto the DNA, followed by the deposition of two heterodimers of H2A/H2B (Kleinschmidt et al, 1990). Nucleosomes form a 'beads on a string' or nucleosome array structure, and then are further compacted into structures of various hierarchies (Luger & Hansen, 2005) (figure 1.1). The process of nucleosome compaction is aided by linker histone H1 and additional protein factors. Nucleosome dynamics can be regulated by DNA methylation, histone modifications (Kouzarides, 2007), histone variant incorporation (Kamakaka & Biggins, 2005), ATP-dependent chromatin remodelers (Cairns, 2005), and histone chaperones which modulate the DNA-histone interactions in an ATP-independent manner (Eitoku et al, 2008; Ito et al, 1997).

The first atomic resolution crystal structure was published in 1997 (figure 1.2) (Luger et al, 1997). It revealed the architecture of the histone octamer and how the 146 bp α-

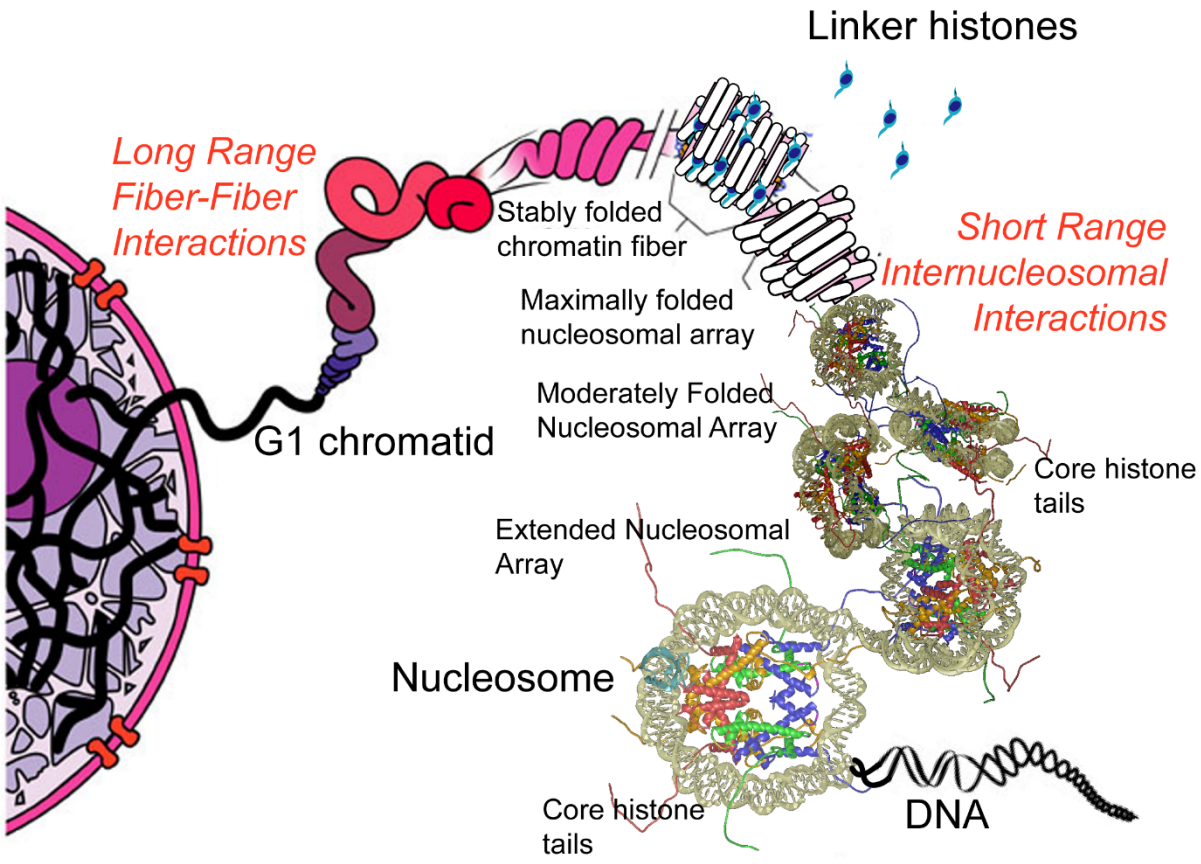

Figure 1.1. Chromatin organization in the cell nucleus. Core histone octamers and DNA form nucleosomes. Nucleosomes then form an array. Nucleosome arrays are then folded further into higher-order structures with linker histones such as H1 (figure adapted from (Hansen, 2002)).

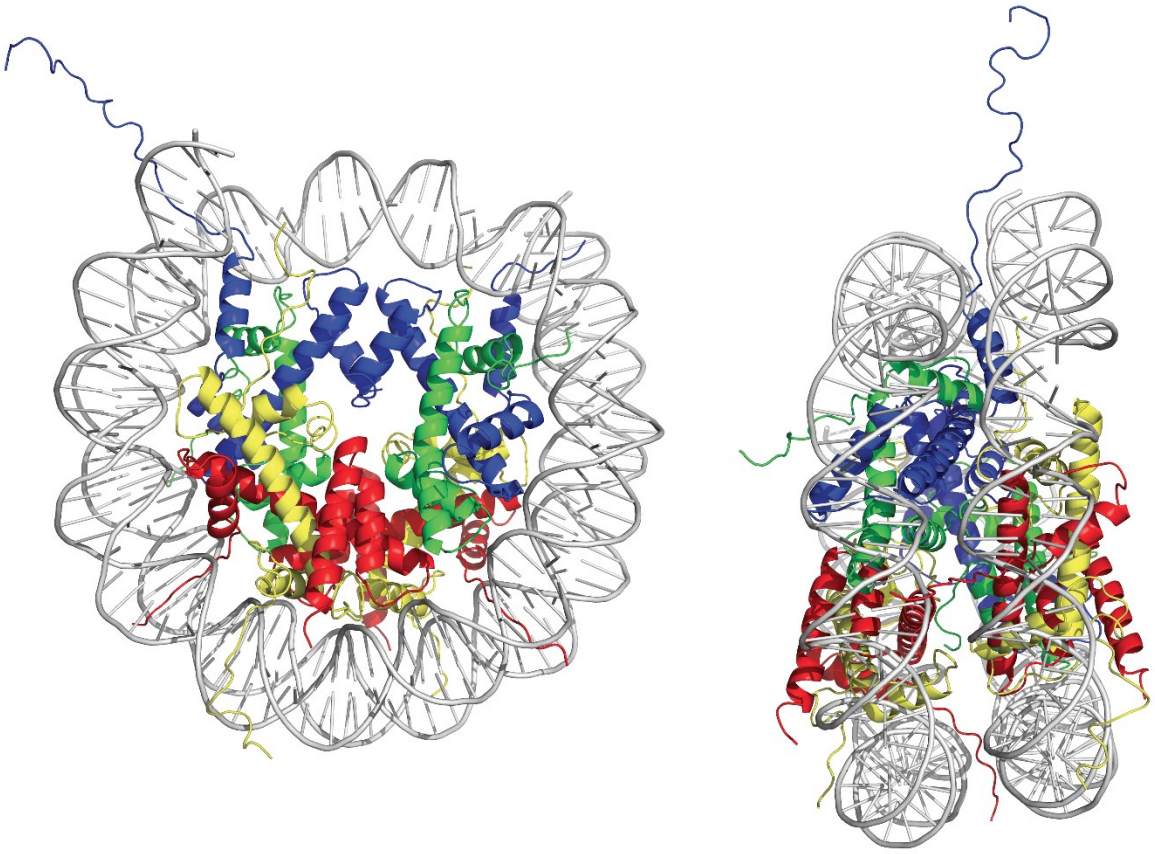

Figure 1.2. Crystal structure of the nucleosome core particle (NCP) (Luger et al, 1997) (PDB ID: 1AOI). *Xenopus laevis* H2A, H2B, H3 and H4 are shown in yellow, red, blue and green respectively. 146 bp α-satellite DNA is shown in grey. Views are shown down the superhelical axis of the DNA (left) and rotated 90 degrees horizontally (right).

satellite sequence DNA is organized within the nucleosome. The histone fold of all four histones contains three alpha helices connected by two loops. Histone tails are largely unstructured and are the major targets for post-translational modifications. Later, structures were determined for nucleosomes containing different DNA sequences, including the '601' positioning sequence (Vasudevan et al, 2010). Crystal structures are also available for nucleosomes with histone variants, for example, H2A/Z-containing nucleosome (Suto et al, 2000), macroH2A-containing nucleosome (Chakravarthy et al, 2005) and H3T-containing nucleosome (Tachiwana et al, 2010); also with histone modifications such as methylation of H3/H4 (Lu et al, 2008); with histones from various species, including yeast (White et al, 2001), chicken (Harp et al, 2000), *Drosophila* (Clapier et al, 2008) and humans (Tsunaka et al, 2005). Crystal structures of nucleosomes with other proteins bound have also been solved, including the RCC1-nucleosome complex (Makde et al, 2010), and the Sir3 BAH domain-nucleosome complex (Armache et al, 2011). The crystal structure of the nucleosome is remarkably conserved throughout, despite the known stability and functional differences (reviewed in (Luger et al, 2012; Tan & Davey, 2011)), indicating that these structures represent one possible state (likely the most stable state due to crystallization conditions).

Alternative nucleosome structures have also been described, which suggested that DNA ends partially dissociate from the nucleosomes in solution, using small-angle X-ray scattering technique. Interestingly, this conformation is dependent on DNA sequence, and

can be observed for nucleosome reconstituted with alpha-satellite DNA, but not 601-sequene (Yang et al, 2011). FRET-based assays also indicated that H2A/H2B histone dimers can partially dissociate from the tetrasome, and an estimation of 0.2% of the nucleosome adopts this conformation under physiological conditions (Bohm et al, 2011). The 'open' conformation of nucleosome is thought to be important for nucleosome dynamics. Also, it has become clear that subtle changes in the structure of nucleosome, such as changes caused by modification of histones, histone variants and DNA sequences, can have dramatic effects on the final outcome of the chromatin organization.

1.2 Regulation of nucleosome dynamics

There are five major categories of factors that are involved in the regulation of nucleosome dynamics: DNA methylation, histone modifications, variant histone incorporation, chromatin remodelers and histone chaperones (reviewed in (Avvakumov et al, 2011; Clapier & Cairns, 2009; Henikoff, 2010; Moore et al, 2013; Talbert & Henikoff, 2010; Zentner & Henikoff, 2013)).

DNA methylation is the addition of a methyl group to DNA nucleotides, either cytosine or adenine. DNA methylation can affect gene transcription by inhibiting or recruiting the binding of transcription-related proteins (Choy et al, 2010). In humans, aberrant DNA methylation pattern is associated with oncogenesis (Craig & Wong, 2011).

Histones undergo post-translational modifications, including methylation, acetylation, phosphorylation, ubiquitination and recently identified crotonylation (summarized in (Tan

et al, 2011)). Histone modification can change the nucleosome stability and accessibility by other regulatory factors, and can serve as transcription activation or repression marks.

Variant histones also exist and can be incorporated into nucleosomes. Histone variants are expressed throughout the cell cycle and can be incorporated into nucleosomes independently of DNA replication. Several histone variants have been identified for H2A, H2B and H3. Histone variants play important roles in a wide range of cellular processes, such as DNA repair, chromosome segregation, sex chromosome condensation and sperm chromatin packaging (reviewed in (Henikoff et al, 2004; Jin et al, 2005; Talbert & Henikoff, 2010)).

Chromatin remodelers are ATP-dependent proteins that can move or restructure nucleosomes. Some remodelers promote dense nucleosome packaging, while others move or eject histones to allow transcription factor to access DNA sequences (reviewed in (Clapier & Cairns, 2009)).

1.2.1 Histone chaperones

Definition of histone chaperone has evolved with ongoing studies. Histone chaperones were originally defined as factors that can recover aggregated histones (Laskey et al, 1978). Later more functions of histone chaperones were discovered, including histone shuttling, interaction with chromatin remodelers, and nucleosome assembly and disassembly via its interaction with histones (reviewed in (Avvakumov et al, 2011; Burgess & Zhang, 2013; Eitoku et al, 2008; Elsasser, 2013; Loyola & Almouzni, 2004;

Park & Luger, 2006a; Zlatanova et al, 2007)). They are generally considered as a group of proteins that bind histones and display nucleosome assembly and/or disassembly activity in the absence of ATP (Avvakumov et al, 2011).

Some histone chaperones are considered H2A/H2B chaperones, such as nucleoplasmin, Nap1 and FACT. Some histone chaperones are considered H3/H4 chaperones, such as CAF-1, Vps75, Spt6 and Rtt106. Apart from the interaction with histones, histone chaperones also interact with each other and/or with other chromatin factors, and this property of histone chaperones is also essential for their biological functions (reviewed in (Eitoku et al, 2008)).

Histone chaperones all have acidic overall charge, yet the structures and oligomeric states of histone chaperones are diversified, such as Nap1 (Park & Luger, 2006b), Asf1 (Daganzo et al, 2003) and nucleoplasmin (Dutta et al, 2001). The differences in histone type preference, crystal structures and oligomeric states of histone chaperones all indicate that their functional mechanisms can be diverse.

A lot of efforts have been put into understanding the mechanism of how histone chaperones regulate chromatin dynamics. The available structures of chaperone-histone complexes, including Asf1-H3-H4 (Natsume et al, 2007), HJUP/Scm3-cenH3-H4 (Hu et al, 2011; Zhou et al, 2011) and Chz1-H2A.Z-H2B (Zhou et al, 2008), suggest that the binding of histone chaperones to histones and nucleosome formation are mutually exclusive. Yet the lack of thorough understanding of the structural and molecular basis

for chaperone-histone interactions, and the difficulty to apply the *in vitro* investigation into *in vivo* studies, all complicate the ongoing investigation of the 'chaperone mechanism'.

Nucleosome assembly proteins: Nap1 and Nap2

Nucleosome assembly protein 1 family (Nap1 family) is a large family of histone chaperones. There are two types of Nap1 family proteins in *Saccharomyces cerevisiae*, Nap1 and Vps75. Higher eukaryotes have multiple family members; and in mammals, there are Nap1 (aka Nap1-like 1, Nap1L1), Nap1L2-6 (Nap1-like 2-6), Setα and Setβ (Hansen et al, 2010). Nap1 plays important roles in histone binding, chromatin assembly, disassembly and remodeling (Park & Luger, 2006a). Additional functions of Nap1 and its homologues include tissue-specific transcription regulation, nuclear shuttling, cell-cycle regulation, apoptosis, etc (Park et al, 2005; Park & Luger, 2006a; Rogner et al, 2000; Zlatanova et al, 2007).

Crystal structures have been solved for several Nap1 family members, including *S. cerevisiae* Nap1 (yeast Nap1 or yNap1) (Park & Luger, 2006b), Vps75 (Tang et al, 2008), *Plasmodium falciparum* NapL and NapS (PfNapL and PfNapS) (Gill et al, 2009). They all contain a central domain (a Nap domain, highly conserved among the Nap family), which is considered important for histone binding (Park & Luger, 2006b). Most Nap1 family members also have unstructured N- and C- terminal domains (NTDs and CTDs). The NTD and CTD of yNap1 were shown to contribute synergistically to histone binding (Andrews et al, 2008).

Human Nap1 was first identified in HeLa cells as a nucleosome assembly factor (Ishimi et al, 1983). It binds to both histone H2A/H2B dimers and $(H3/H4)_2$ tetramers with high affinities (Andrews et al, 2008). It also has nucleosome assembly and disassembly activity (Fujii-Nakata et al, 1992; Park et al, 2005; Sharma & Nyborg, 2008). Recently, it was found that Nap1 promotes nucleosome assembly by eliminating non-nucleosomal histone-DNA complexes both *in vivo* and *in vitro*. In *S. cerevisiae*, H2A and H2B levels are enriched significantly at endogenous genes if Nap1 is deleted. Using a fluorescence-based thermodynamic approach, it was also shown that Nap1 can prevent non-nucleosomal H2A/H2B-DNA interactions, and facilitate the formation of nucleosomes (Andrews et al, 2010). Nap1 binds to H2A/H2B in an unconventional tetrameric form and shields histone surface in the nucleosome structure (D'Arcy et al, 2013). In a defined *in vitro* system, the nucleosome disassembly activity of Nap1 is dependent on the acetylation of histone tails (Luebben et al, 2010). Nap1 can also bind linker histone H1, and is thus also a linker histone chaperone (Kepert et al, 2005).

Nap2 (aka Nap1L4) is one type of Nap1-like protein, with about 30% sequence identity to yNap1. Nap2 is highly conserved among mammals. Human Nap2 (hNap2) has 95% amino acid conservation compared to mouse Nap2 (mNap2), but only 63% amino acid conservation to human Nap1 (hNap1) (Figure 1.3). This strongly indicates a conserved role of mammalian Nap2. Nap2 has been shown to catalyze the incorporation of testis-

specific histone variant into nucleosomes *in vitro*, implying that Nap2 may have specific functions in chromatin reorganization during meiosis (Tachiwana et al, 2008).

Both Nap1 and Nap2 undergo post-translational modifications. Both Nap1 and Nap2 can be polyglutamylated on their C-terminal domains by the addition of up to 10 glutamyl residues (Regnard et al, 2000). Studies on polyglutamylation of *Drosophila* Nap1 indicate that this modification changes the histone chaperone activity of Nap1 (Vidya Subramanian et al, data in preparation for submission). Phosphorylation of Nap1 by casein kinase 2 (CK2) was identified in yeast and *Drosophila* (Li et al, 1999; Rodriguez et al, 2000). Phosphorylation of Nap2 in human cells has also been observed (Rodriguez et al, 2000). Phosphorylation promotes the translocation of Nap1 from the cytoplasm to the nucleus during S phase (Calvert et al, 2008; Li et al, 1999).

The coexistence of Nap1 and Nap2 in metazoans indicates that they can potentially perform different functions *in vivo*. Yet functions of Nap2 have not been intensively explored, especially the nucleosome assembly activity of Nap2. The functional differences between Nap1 and Nap2 are of great interest to explore, since this may offer insights into regulation of chromatin dynamics in different contexts.

Nucleosome assembly proteins: Set

Set is a member of the nucleosome assembly protein family and is highly conservedamong higher eukayotes (figure 1.4). Set is expressed ubiquitously in various human cell lines and localized predominantly in the nuclei (Adachi et al, 1994). It is a

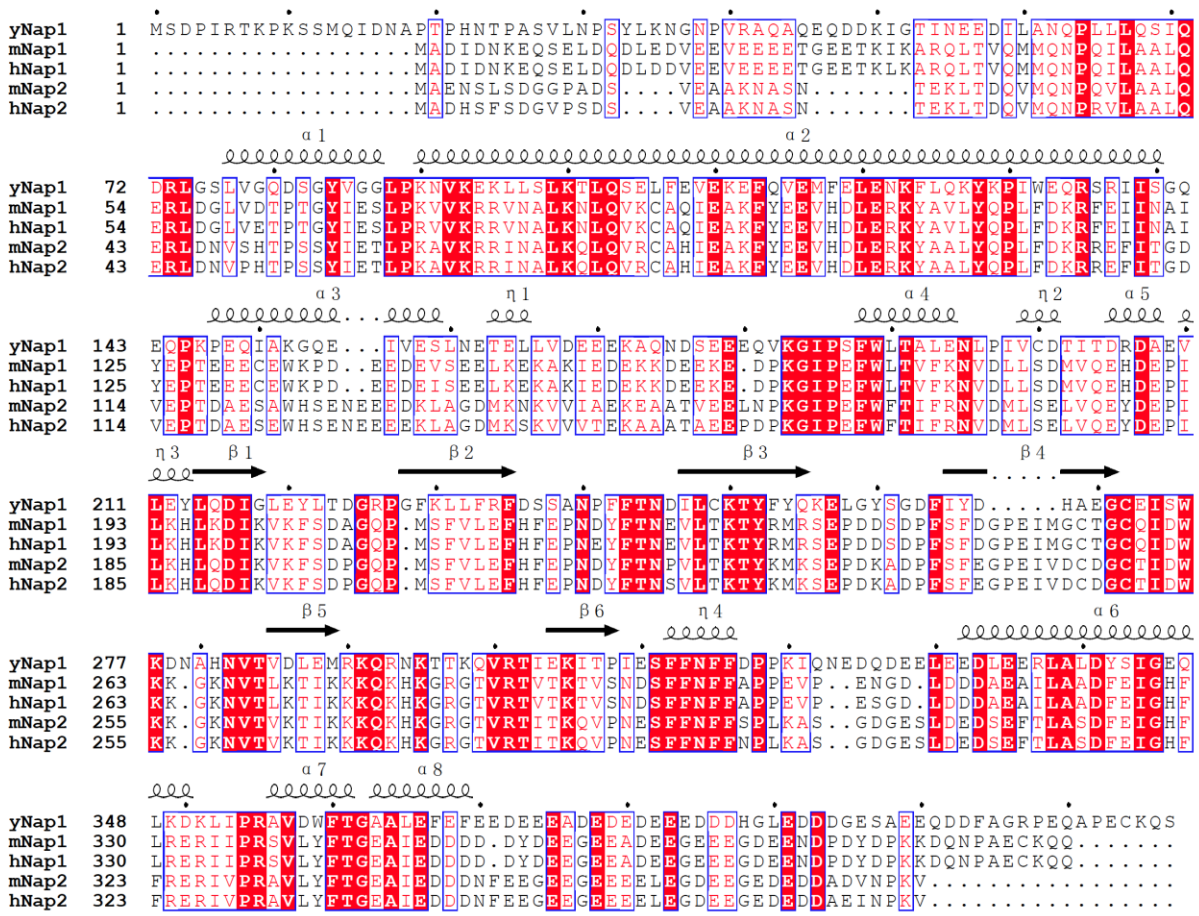

Figure 1.3. Amino acid sequence alignment of Nap1 family proteins. Alignments were performed using *Clustal X* (Thompson et al, 1994), and visualized with *ESPript* (Gouet et al, 1999). Secondary structures are indicated. Blue boxes indicate >70% similarity between aligned sequences. Red indicates identical amino acids among all (shading) or most (letters) of aligned sequences.

multifunctional protein. Set is also designated as template activating factor I (TafI) since it was found to be a host factor required to stimulate the adenovirus core DNA replication (Matsumoto et al, 1993). It is an inhibitor of phosphatase 2A (PP2A) tumor suppressor, and is thus also given the name IPP2A (Li et al, 1996). Set is also a subunit of the INHAT (inhibitor of histone acetyltransferase) complex. Endogenous INHAT is composed of Setα, Setβ and pp32. INHAT inhibits the acetylation of histones by p300/CBP and PCAF, and is proposed to mask histones from acetyltransferase (Seo et al, 2001). Set was also found to be an inhibitor of tumor suppressor NM23-H1 through binding to NM23-H1. Set suppresses the transcriptional activity of steroid hormone receptors on MMTV promoter (Fan et al, 2003). Set preferentially binds to histones H3/H4, but the interaction with H2A/H2B was also identified. Set also binds to linker histone (Muto et al, 2007; Okuwaki & Nagata, 1998; Seo et al, 2001), and has nucleosome assembly activity (Muto et al, 2007). Some research groups indicated the interaction of Set and chromatin or DNA, yet other factors are also present in the set-up of the reaction system and may mediate the binding interactions. The crystal structure of human Set has been solved (Muto et al, 2007), and is folded similarly with the structure of yeast Nap1 (Park & Luger, 2006b) as shown in figure 1.5. Set does not contain the accessory domain (α3 helix of Nap1). Set also forms a dimer via the dimerization helix, and the relative disposition of the dimerization helices and the earmuff domains of Set and Nap1 differ by a rotation of 40 degrees, resulting in a relatively high rmsd value (3 Å) of the corresponding atoms. The

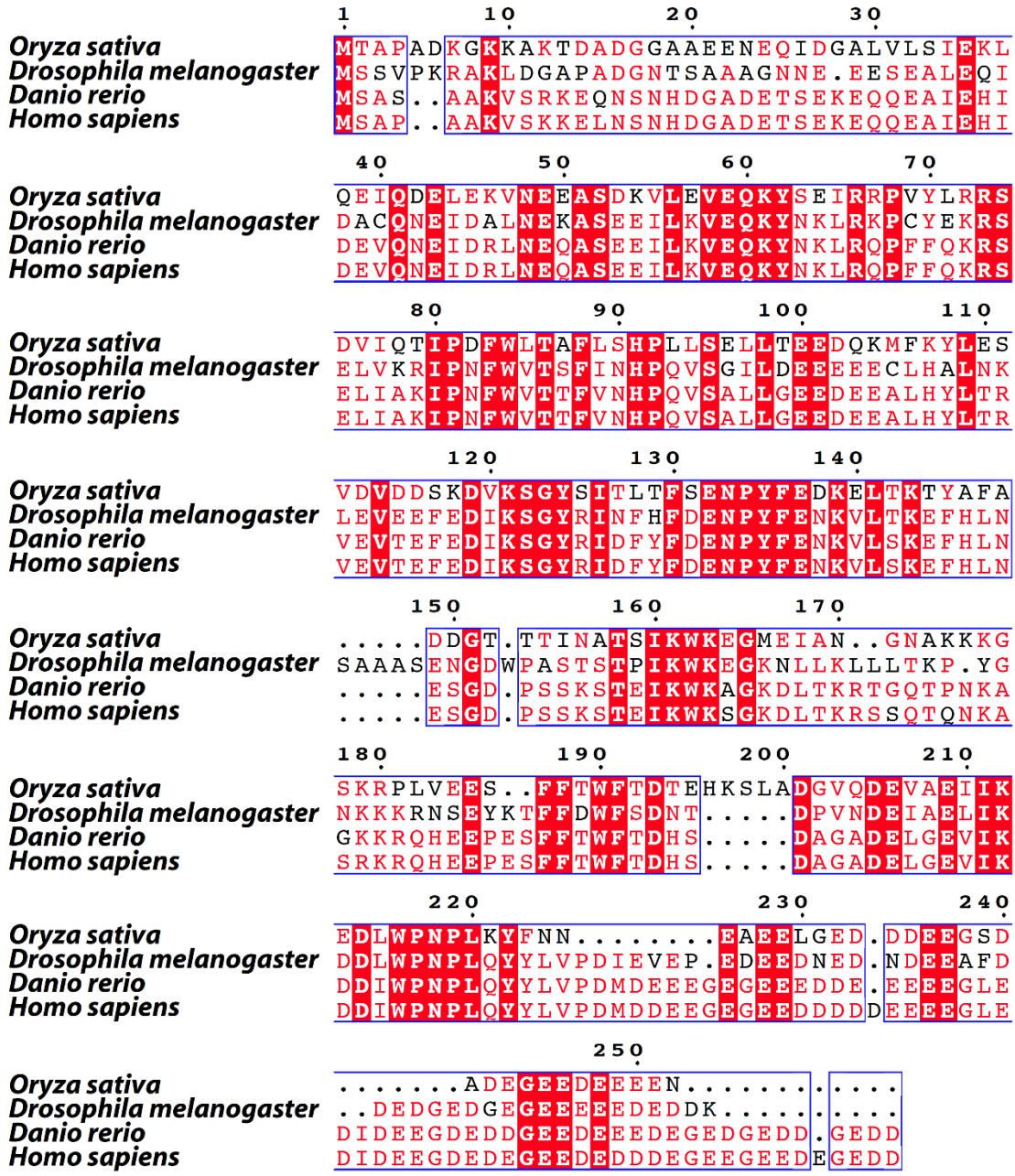

Figure 1.4. Setβ is highly conserved in higher eukaryotes. The amino acid sequences of Setβ in rice (*Oryza sativa*), fruit flies (*Drosophila melanogaster*), Zebra fish (*Danio rerio*) and humans (*Homo sapiens*) are aligned using *clustalX* (Thompson et al, 1994) and then visualized using *ESPript (Gouet et al, 1999)*. Red indicates identical amino acids among all (shading) or most (letters) of aligned sequences.

rest of the two proteins are structurally similar with each other, with an rmsd of 1.9 Å. The structural differences might account for the functional differences between Nap1 and Set.

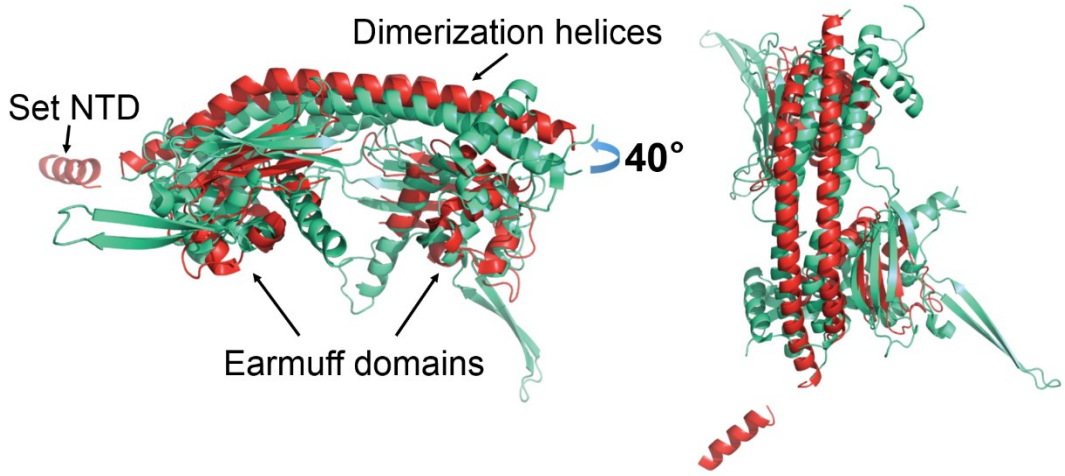

Figure 1.5. Structural alignment of Set (PDB ID: 2E50) and Nap1 (PDB ID: 2Z2R). Set is shown in red, and Nap1 is shown in green. Structural comparison is shown from side view of the dimerization helix (left) and rotated 90° (right). Dimerization helices, earmuff domains, and NTD of Set are indicated.

CHAPTER 2

FUNCTIONAL COMPARISON OF NUCLEOSOME ASSEMBLY PROTEIN FAMILY MEMBERS[1]

2.1 Summary

Histone chaperones are important factors in the regulation of chromatin dynamics. Multiple isoforms of the histone chaperone Nucleosome Assembly Protein 1 (Nap1) have been identified in eukaryotic cells, yet their functional differences are not clear. Here we investigated and compared the functions of several Nap1 family members, including yeast Nap1 (yNap1), mouse Nap2 (mNap2), human Nap1 (hNap1) and human Set (hSet). We compared their histone binding properties, their ability to dissociate non-nucleosomal complexes, and their nucleosome assembly activities. This study provides us with insight into different *in vivo* functions of Nap1 family members.

2.2 Introduction

In eukaryotic cells, DNA is compacted into chromatin. The basic unit of chromatin is a nucleosome (Oudet et al, 1975). A nucleosome is formed by 147 base pair (bp) of DNA wrapping around a histone octamer, which comprises two H2A/H2B dimers and a

[1] Ling Zhang conducted the experiments. Ling Zhang and Karolin Luger designed the experiments and wrote this chapter.

$(H3/H4)_2$ tetramer (Luger et al, 1997). Formation of the nucleosome starts with $(H3/H4)_2$ tetramer deposition onto the DNA, followed by the deposition of two H2A/H2B dimers (Kleinschmidt et al, 1990). Chromatin structure, and thus DNA accessibility, can be regulated by post-translational modification of histones (Kouzarides, 2007), incorporation of variant histones (Kamakaka & Biggins, 2005), ATP-dependent chromatin remodelers (Cairns, 2005), and ATP-independent histone chaperones (Eitoku et al, 2008).

Histone chaperones are a group of proteins that bind histones, function in nucleosome assembly and possibly disassembly (Eitoku et al, 2008). In many cases, they contribute to transcription regulation. Nucleosome assembly protein 1 (Nap1) is a large family of histone chaperones. While there are two types of Nap1 family members in *Saccharomyces cerevisiae*, Nap1 and Vps75, metazoans have at least six isoforms: Nap1 (aka Nap1-like 1, Nap1L1), Nap1L2-6 (Nap1-like 2-6), and Set (reviewed in (Park & Luger, 2006a)).

Nap1 was first identified as an acidic protein that recovers aggregated histones (Ishimi et al, 1983). Further studies, mostly conducted with yNap1, revealed other functions such as histone shuttling, nucleosome assembly and disassembly, and transcriptional regulation (reviewed in (Park & Luger, 2006a; Zlatanova et al, 2007)). Nap1 binds to both H2A/H2B and H3/H4 with low nM affinities (Andrews et al, 2008). It was shown that Nap1 can prevent non-nucleosomal DNA-H2A/H2B interactions *in vitro*, and facilitate the formation of nucleosomes (Andrews et al, 2010). Nap1 eliminates non-nucleosomal DNA-

H2A/H2B interactions via direct competition for H2A/H2B with DNA (D'Arcy et al, 2013). In *S. cerevisiae*, H2A and H2B levels are enriched significantly at endogenous genes if Nap1 is deleted. Nap2 (also termed Nap1L4) is highly conserved among mammals, suggesting conserved functions. For example, mouse Nap2 and human Nap2 share 97% sequence similarity and are thus nearly identical. In mouse and humans, both Nap1 and Nap2 are expressed ubiquitously (Hu et al, 1996). Set (also known under the names TAF-Iβ) was identified as an oncogene. It is described as a multifunctional protein that exhibits histone chaperone activity and regulates transcription (Loven et al, 2003).

Several structures of Nap1 family members have been obtained by X-ray crystallography, including yeast Nap1 (yNap1) and hSet (Muto et al, 2007; Park & Luger, 2006b). Both exist as homodimers and are structurally similar. To date, no structural information is available for complexes of any Nap1 family member in complex with histones. Researchers have been trying alternative approaches to look into Nap-histone interactions. Recently the binding of Nap1 to H2A/H2B was characterized using hydrogen/deuterium exchange-coupled to mass spectrometry, and it was found that H2A/H2B bound to Nap1 adopts a non-canonical tetrameric conformation, with the histone surface involved in nucleosome formation shielded by Nap1 (D'Arcy et al, 2013). Other research groups showed that Nap1 binds to histones H3/H4 in a tetrameric conformation. The tetrameric state of H3/H4 can serve as substrates for nucleosome assembly (Bowman et al, 2011).

Histone variants are involved in the regulation of chromatin dynamics. H2AL2 and TH2B are both testis-specific histone variants, where Nap2 shows highest levels of expression (Govin et al, 2004; Hwang & Chae, 1989). We thus wondered whether Nap2 has specificity over these histone variants. H2A variant H2AL2-containing nucleosomes has an altered structure, which only protects ~130 bp of DNA (Wu et al, 2008). H2B variant TH2B has a high level of conservation between mammalian species (Choi et al, 1996; Hwang & Chae, 1989; Zalensky et al, 2002). The major difference of TH2B and canonical H2B exists in the N-terminal tails, where most of post-translational modifications have been found (Govin et al, 2004). During spermatogenesis in mouse testis, H2AL2 is found to specifically dimerize with TH2B within an unknown DNA packaging structure, though it is able to from dimers with H2B with much less efficiency. H2AL2/TH2B containing dimers are shown to be less stable than somatic-type histones (Govin et al, 2007).

Although Nap1 family members are closely related evolutionarily, they diverged into playing different roles *in vivo*. For example, Nap1L2 is essential for viability (Rogner et al, 2000), whereas Set is an oncogene (von Lindern et al, 1992). It is intriguing how Nap1 family members are similar and different from each other, including whether they are specific for histone variants, and how they regulate nucleosome dynamics. Here we studied and compared the properties of various Nap1 family members from different species, including Nap1 from both yeast and humans (yNap1 and hNap1), Nap2 from

mouse (mNap2, which is nearly identical to hNap2), and Set from humans (hSet), by looking at their binding to histones, dissociation of non-nucleosomal complexes, and chromatin assembly activities.

2.3 Materials and Methods

2.3.1 Preparation of proteins and reagents

His-tagged H2AL2 was overexpressed in BL21 (DE3) CodonPlus RP cells (Stratagene) for 3 hours (h) and lysed by sonication. It was further purified by Ni-NTA column (Qiagen) under denaturing conditions (Ohara-Imaizumi et al, 2002) followed by Sephacryl S-200 gel filtration chromatography and TSK-GEL SP-5PW ion-exchange chromatography. *Xenopus laevis* H2A, H2B, H2BT112C, H3, H4, H4E63C, *Mus musculus* H2A, H2B, H2B T115C, H3 and H4, TH2B and DNA were purified as described in (Dyer et al, 2004). Histone H2A/H2B dimer, H2AL2/TH2B dimer, $(H3/H4)_2$ tetramer and histone octamer were refolded as described (Dyer et al, 2004). Histones were mixed at equal molar ratios and reconstituted using salt dialysis followed by Superdex 200 chromatography.

Full-length yNap1 and yNap1C200A,C249A,C272A were overexpressed in BL21 (DE3) cells (Stratagene) and purified as described (Andrews et al, 2008; McBryant et al**,** 2003). His-tagged human Nap1 and Nap1C88A,C132A,C255A,C258A, mouse Nap2, Nap2G10C was expressed from a pHAT4 vector and in BL21 (DE3) cells (Stratagene) and purified the same way as Nap1 with his-tag, which was cleaved using TEV protease

before ion-exchange chromatography. Set and SetA94C proteins were expressed in a pET14b vector. The A94 residue was chosen for fluorescence labeling; as it is the structural analog of the yNap1 D201C labeling mutant used in previous research (D'Arcy et al, 2013). The plasmid was transformed into Rosetta pLysS competent cells, incubated at 37°C, and induced at OD (600 nm) 0.6 with 0.4 mM IPTG. The cells were incubated for another 3 h at 37°C before harvesting by centrifugation. Cells were then resuspended in lysis buffer containing 20 mM Tris-HCl, pH 8.0, 300 mM KCl, 10% glycerol, 10 mM imidazole, 0.1 mM AEBSF, 8 µg/ml leupeptin, 8 µg/ml aprotinin, Complete-Mini EDTA-free tablet (Roche) and 4 mM βME. Cells were lysed via sonication, and cell lysates were cleared at 17,000 rpm at 4°C for 15 min. The supernatant was applied onto a HisPrep FF 16/10 column. Gradient buffer contained 20 mM Tris-HCl, pH 8.0, 300 mM KCl, 10% glycerol, 0-500 mM imidazole, 0.1 mM AEBSF and 4 mM βME. Selected fractions from the HisPrep FF 16/10 column were then applied to a Superdex 200 16/60 column in 50 mM Tris-HCl, pH 7.9, 100 mM KCl, 12.5 mM $MgCl_2$, 20% glycerol and 0.2 mM TCEP.

2.3.2 Fluorescence-based de-quenching assays for affinity measurements

The fluorescence-based thermodynamic assays were performed as described (Andrews et al, 2008). *X. laevis* H2BT112C, *M. musculus* H2BT115C and *M. musculus* TH2BC33 were labeled with Alexa 488 before refolding into histone H2A/H2B dimers. Fluorescence was measured using a Horiba Jobin Yvon Fluorolog-3 spectrofluorometer. Reactions were carried out in buffers containing 50 mM Tris-HCl, pH 7.5, 300 mM NaCl,

1 mM EDTA, 100 µg/ml BSA and 1 mM DTT. Fluorescence change was monitored as a function of titrated protein or DNA. Dissociation constants were calculated as described (Andrews et al, 2008).

2.3.3 FRET-based HI-FI assays for affinity measurements

FRET-based thermodynamic assays were carried out as described (Winkler et al, 2012). 1 nM *X. laevis* H2A/H2BT112C-Alexa488 or $(H3/H4\ E63C)_2$-Alexa488 was used as a donor probe, and yNap1C200A,C249A,C272A, human Nap1C88A,C132A,C255A,C258A, mouse Nap2G10C or human SetA94C labeled with Atto647N (acceptor fluorophore) was titrated in buffer containing 300 mM NaCl, 10 mM Tris-HCl, pH 7.5, 5% glycerol, 0.01% CHAPS, 0.01% NP40 and 1 mM DTT.

2.3.4 Electrophoretic mobility shift assays for dissociation of DNA-H2A/H2B complexes by histone chaperones

EMSAs were performed using 7.5 µM Nap1, Nap2 or Set, 1.5 µM 207 bp 601 DNA (Lowary & Widom, 1998) or 588 bp HTLV1 promoter sequence (Luebben et al, 2010), and 0.75, 1.5 or 3 µM *X. laevis* H2A/H2B, mouse H2A/H2B or H2AL2/TH2B. These were mixed in a final buffer containing 20 mM Tris-HCl, pH 7.5, 100 mM NaCl and 0.35 mM EDTA. Reactions were incubated at 25°C for 15 min and then analyzed using 5% polyacrylamide gel electrophoresis.

2.3.5 DNA Supercoiling assays

The DNA supercoiling assay was done as described (Lusser & Kadonaga, 2004). Human Nap1 or mouse Nap2 was added to 18.75 pmol *M. musculus* histone octamer to reach a final Nap: histone octamer ratio of 0.5:1, 2:1, 4:1 and 8:1. Yeast Nap1 or human Set was added to 40 µM histones to a final ratio of 4:1, 8:1 and 16:1. Reactions were incubated at 37°C for 10 min. The relaxed plasmid (1.2 µg of DNA for human Nap1 and mouse Nap2; 0.8 µg of DNA for yeast Nap1 and Set; plasmid relaxed with 3 units of *Escherichia coli* topoisomerase I (NEB) for 2 h at 37°C) was added to the reaction and incubated at 37°C for 1 h in a buffer containing 10 mM Tris-HCl, pH 8.0, 100 mM NaCl, 1 mM EDTA and 100 µg/µl BSA. 8 units of wheat germ topoisomerase I (Promega) was then added and the reaction was incubated at 37°C for an additional 1 h. Final concentrations of 0.5% SDS and 0.2 mg/ml proteinase K were added and the reaction was incubated at 55°C for 30 min. DNA was purified by phenol/chloroform extraction and ethanol precipitation. The final products were analyzed on a 1.2% agarose gel.

2.3.6 Recovery of aggregated chromatin (RAC) assays

48 nM $(H3/H4E63C)_2$-Alexa488 and 300 nM H2A/H2BT112C-Atto647N was incubated with 150, 300 and 450 nM yeast Nap1, human Nap1, mouse Nap2 or human Set, and mixed with 10 nM DNA (165bp-601 sequence). Reaction buffer contained 200 mM NaCl, 10 mM Tris-HCl, pH 7.5, 5% glycerol, 0.05% NP-40, 0.05% CHAPS, 1 mM EGTA, 0.5

mM $MgAc_2$, 0.5 mM imidazole, 0.5 mM DTT, 0.5 mM PMSF, 0.05 µg/ml pepstatin A and 0.05 µg/ml leupeptin.

Reactions were incubated at room temperature for 15 min, and analyzed using 5% PAGE. Gels were scanned using Typhoon Trio multimode imager (GE healthcare) and collected at three excitation/emission wavelengths: for donor channel, 488/520 nm; for acceptor channel, 633/670 nm; for FRET channel, 488/670 nm.

2.3.7 FRET-based Job plot assays

Job plot assays (Olson & Buhlmann, 2011) were carried out in a 384-well microplate with glass bottom. A total concentration of proteins was kept constant, with varying ratios of H2A/H2BT112C-Alexa488 and Nap1, Nap2 or Set labeled with Atto647N fluorophore, in a reaction buffer containing 300 mM NaCl, 10 mM Tris-HCl, pH 7.5, 5% glycerol, 0.01% CHAPS, 0.01% NP40 and 1 mM DTT. The microplate was then scanned on a Typhoon Trio multimode imager (GE healthcare) using the following excitation/emission wavelength settings: donor channel, 488/520 nm; for acceptor channel, 633/670 nm; for FRET channel, 488/670 nm. FRET signals were corrected as described in (Hieb et al, 2012).

2.4 Results

2.4.1 Nap1, Nap2 and Set bind to all histones with similarly high affinity

One essential function of Nap1 family members is to interact with histones. yNap1 binds to histones with high affinity (Andrews et al, 2008), yet affinity numbers of mammalian

Nap1, Nap2 or Set binding to histones have not been available. Here we measured and compared the binding affinities of Nap1, Nap2 and Set to histones H2A/H2B and H3/H4. To do that, we utilized two approaches: fluorescence-based de-quenching assays (Andrews et al, 2008), and FRET-based HI-FI (High-throughput Interactions by Fluorescence Intensity, (Winkler et al, 2012)) assays.

For fluorescence-based de-quenching assays (figure 2.1.A), histones are labeled with fluorophores, and unlabeled nucleosome assembly proteins are titrated. The fluorescent signal change is measured using a spectrofluorometer and plotted against the concentrations of the titrated protein, and the binding affinity can be calculated.

Using de-quenching assays, we measured the affinity of yNap1, hNap1, mNap2 and hSet to canonical histones from various species (Table 2.1). yNap1 does not display preference to histones from different species, nor does mNap2. The affinities we observed for yNap1 binding to *X. laevis* H2A/H2B and H3/H4 are comparable with previously published values (Andrews et al, 2008).

We also tested the affinity of Nap2 to histone variants H2AL2/TH2B. In our *in vitro* assays Nap2 does not distinguish between H2AL2/TH2B compared to canonical H2A/H2B histones, nor does yNap1.

We managed to validate several affinity measurements obtained from de-quenching assays with FRET-based assays. For FRET-based HI-FI assays, histone and nucleosome assembly proteins were labeled with donor and acceptor fluorophores

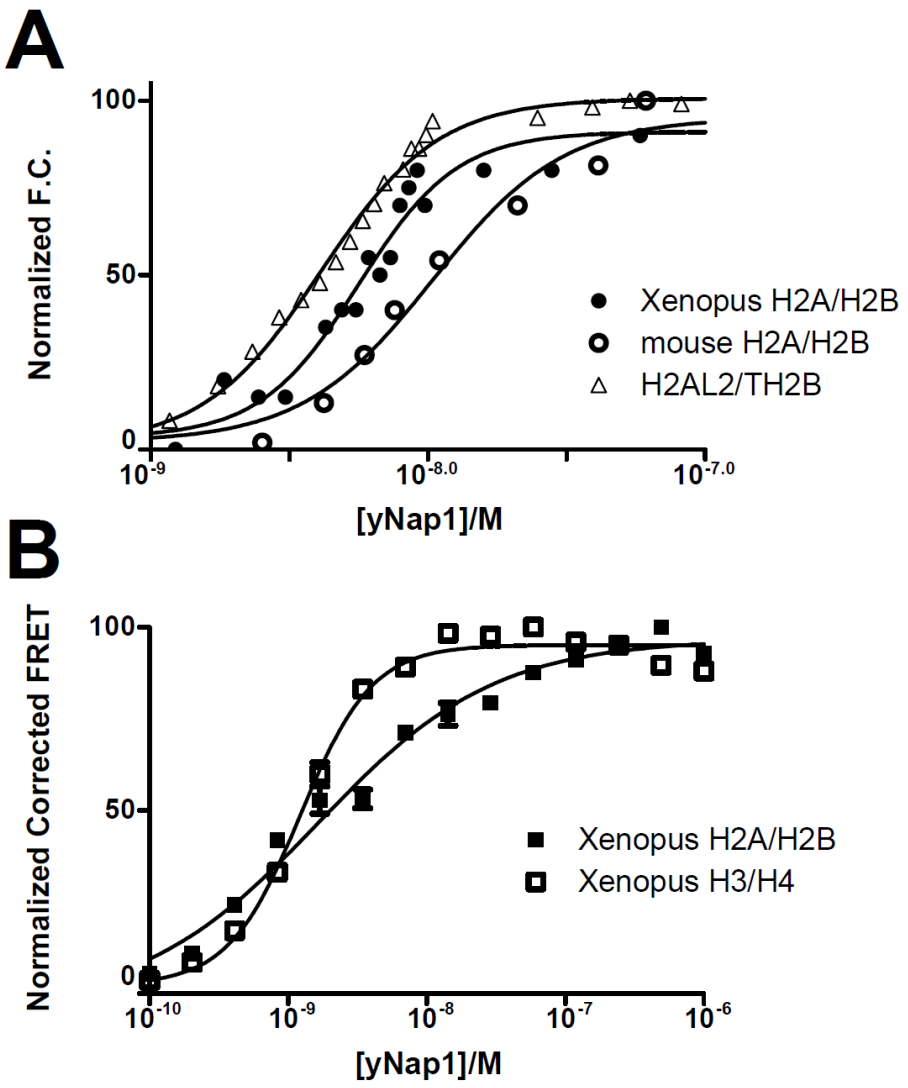

Figure 2.1. Representative curves for histone chaperone and histone interactions. One representative curve is shown of at least three replicates for each affinity measurement. (A) Fluorescence-based de-quenching assays. Normalized fluorescence signal change is plotted as a function of histone chaperone concentration. Unlabeled yNap1 is titrated into 1 nM X. laevis H2A/H2BT112C-Alexa 488, mouse H2A/H2BT115C or mouse H2AL2/TH2BC33. (B) FRET-based HI-FI assays. Normalized corrected FRET signal is plotted as a function of histone chaperone concentration. yNap1C200A,C249A,C272A labeled with Atto647N (acceptor fluorophore) is titrated into 1 nM *X. laevis* H2A/H2BT112C or $(H3/H4E63C)_2$-Alexa488 as donor probe. Measurements were carried out in duplicate.

Table 2.1. Binding affinities of nucleosome assembly proteins and histones. Binding affinities were measured with 1 nM histone probes, and nucleosome assembly proteins were titrated. Apparent affinity numbers shown in the table are average and standard deviation values calculated from at least three independent experiments. Asterisks stand for data not available.

Nap1 family member	Histones (Probe)	K_d / nM (De-quenching assays)	K_d / nM (FRET assays)
yNap1	*X. laevis* H2A/H2B	3.9 ± 1.3	1.4 ± 0.3
	M. musculus H2A/H2B	5.1 ± 3.8	*
	M. musculus H2AL2/TH2B	4.8 ± 1.4	*
	X. laevis H3/H4	*	1.2 ± 0.2
hNap1	*X. laevis* H2A/H2B	5.4 ± 1.1	10.1 ± 2.1
	X. laevis H3/H4	*	37.8 ± 19.6
mNap2	*X. laevis* H2A/H2B	3.5 ± 0.9	10.0 ± 2.2
	M. musculus H2A/H2B	4.7 ± 2.8	*
	M. musculus H2AL2/TH2B	4.6 ± 2.1	*
	X. Laevis H3/H4	*	3.9 ± 2.3
hSet	*X. laevis* H2A/H2B	*	18.1 ± 4.1
	X. laevis H3/H4	*	3.9 ± 0.3

respectively. Histones H2A/H2B or H3/H4 were kept at constant concentrations, with chaperones titrated. Signals are measured with a Typhoon imager with corresponding excitation/emission wavelengths for donor, acceptor and FRET. Corrected FRET can then be calculated by subtracting the donor and acceptor signal noises.

Using FRET assays, we measured affinities of Nap1 family members to histones H2A/H2B and H3/H4. yNap1 shows similar affinity to both H2A/H2B and H3/H4, whereas hNap1 shows slight preference for H2A/H2B. mNap2 and Set both show preference for histones H3/H4.

It is also worth noting that the affinity values are comparable between different instruments (fluorometer vs. Typhoon imager), techniques (fluorescence de-quenching vs. FRET) and buffers, and also between unlabeled wild type proteins and labeled protein mutants (with introduced point mutations to allow fluorophore conjugation). These observations further validated our data collection and analyses.

2.4.2 Nap2 and Set do not disassemble non-nucleosomal DNA-histone complexes

yNap1 was shown to promote nucleosome assembly by eliminating non-nucleosomal DNA-histone interaction, both *in vivo* and *in vitro*. When DNA is bound to H2A/H2B, forming non-nucleosomal complexes, the addition of yNap1 can directly compete for H2A/H2B with DNA (Andrews et al, 2010; D'Arcy et al, 2013).

Here we examined the ability of other histone chaperones to dissociate DNA-H2A/H2B complexes. yNap1 is shown as a positive control. In agreement with previous results

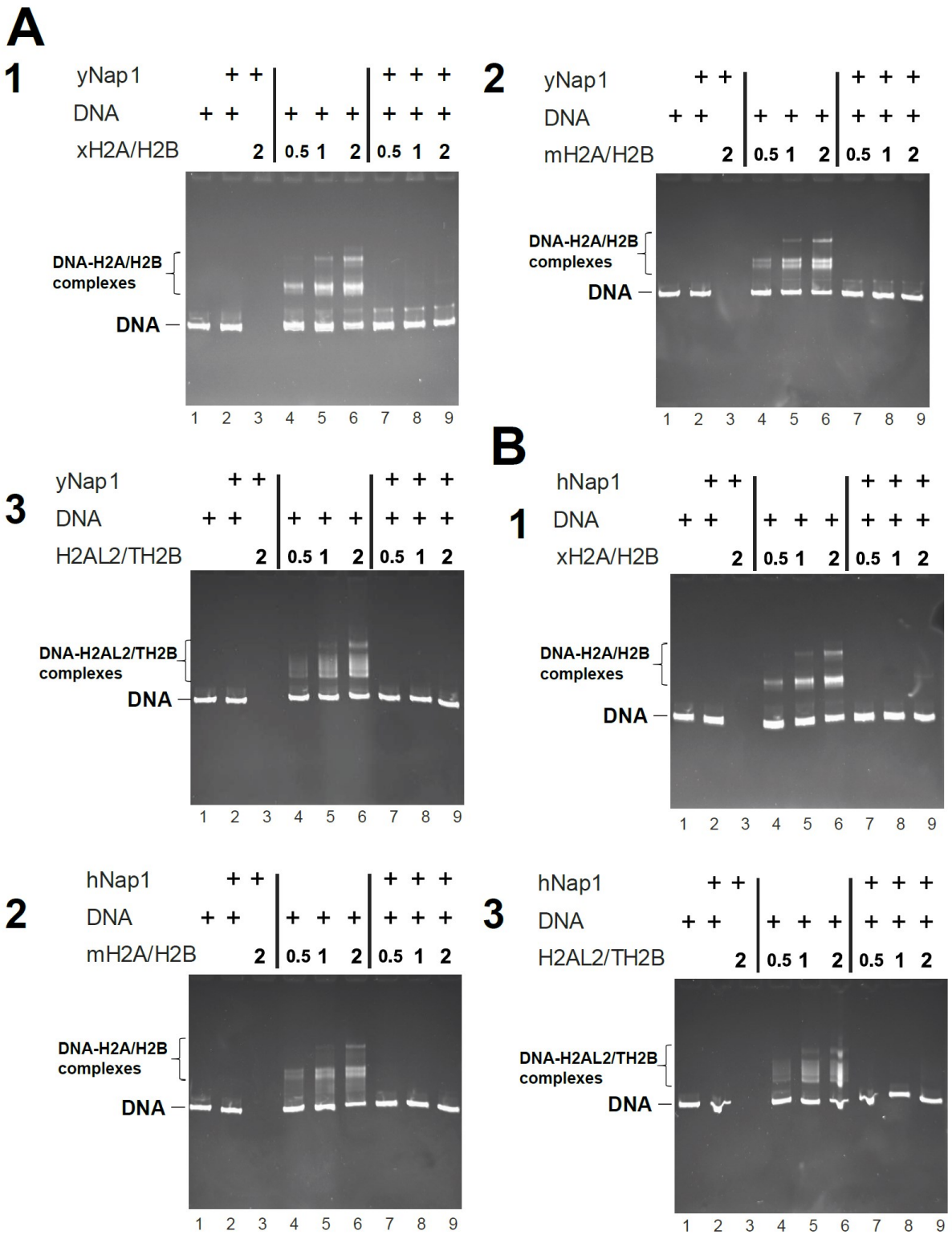
A
1
yNap1 + +
DNA + + + + + + + +
xH2A/H2B 2 0.5 1 2 0.5 1 2
DNA-H2A/H2B complexes
DNA
1 2 3 4 5 6 7 8 9
2
yNap1 + +
DNA + + + + + + + +
mH2A/H2B 2 0.5 1 2 0.5 1 2
DNA-H2A/H2B complexes
DNA
1 2 3 4 5 6 7 8 9
3
yNap1 + +
DNA + + + + + + + +
H2AL2/TH2B 2 0.5 1 2 0.5 1 2
DNA-H2AL2/TH2B complexes
DNA
1 2 3 4 5 6 7 8 9
2
hNap1 + +
DNA + + + + + + + +
mH2A/H2B 2 0.5 1 2 0.5 1 2
DNA-H2A/H2B complexes
DNA
1 2 3 4 5 6 7 8 9
B
1
hNap1 + +
DNA + + + + + + + +
xH2A/H2B 2 0.5 1 2 0.5 1 2
DNA-H2A/H2B complexes
DNA
1 2 3 4 5 6 7 8 9
3
hNap1 + +
DNA + + + + + + + +
H2AL2/TH2B 2 0.5 1 2 0.5 1 2
DNA-H2AL2/TH2B complexes
DNA
1 2 3 4 5 6 7 8 9

C

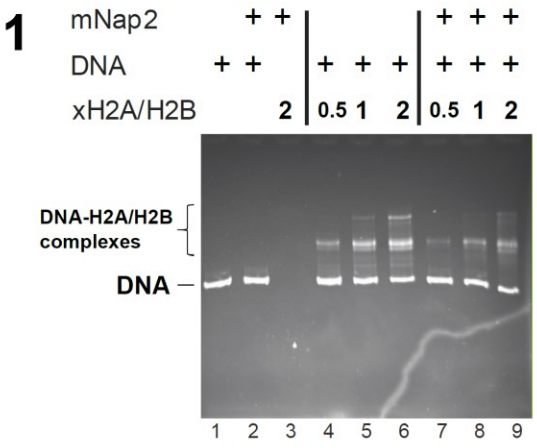
1
mNap2 + +
DNA + + + + + + + + +
xH2A/H2B 2 0.5 1 2 0.5 1 2
DNA-H2A/H2B complexes
DNA
1 2 3 4 5 6 7 8 9

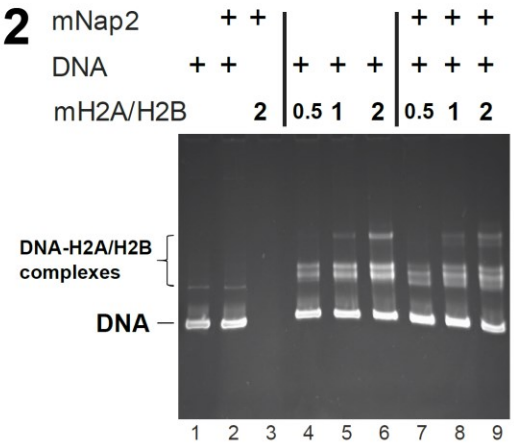
2
mNap2 + +
DNA + + + + + + + + +
mH2A/H2B 2 0.5 1 2 0.5 1 2
DNA-H2A/H2B complexes
DNA
1 2 3 4 5 6 7 8 9

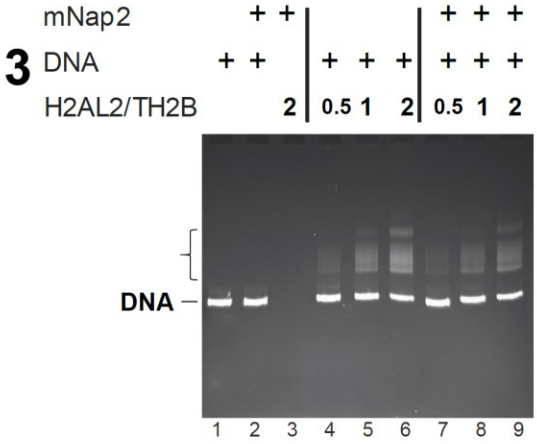
3
mNap2 + +
DNA + + + + + + + + +
H2AL2/TH2B 2 0.5 1 2 0.5 1 2
DNA
1 2 3 4 5 6 7 8 9

D

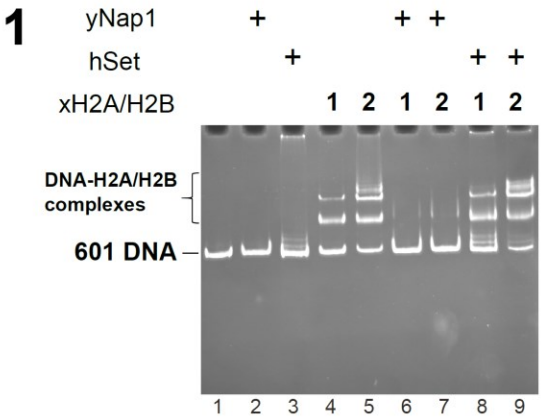
1
yNap1 + + +
hSet + + +
xH2A/H2B 1 2 1 2 1 2
DNA-H2A/H2B complexes
601 DNA
1 2 3 4 5 6 7 8 9

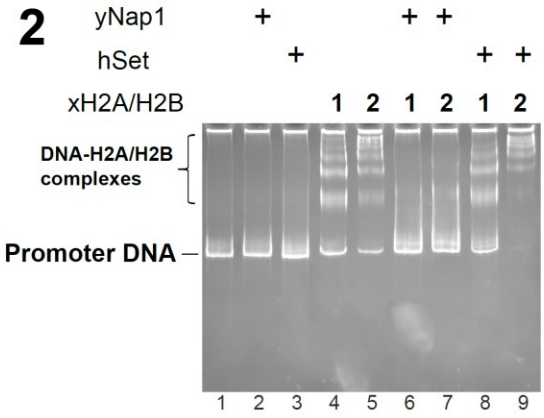
2
yNap1 + + +
hSet + + +
xH2A/H2B 1 2 1 2 1 2
DNA-H2A/H2B complexes
Promoter DNA
1 2 3 4 5 6 7 8 9

Figure 2.2. Nap1 can dissociate non-nucleosomal complexes, whereas Nap2 and Set do not. (A) (B) yNap1 and hNap1 can dissociate H2A/H2B-DNA or H2AL2/TH2B-DNA complexes. (C) mNap2 does not dissociate H2A/H2B-DNA or H2AL2/TH2B-DNA complexes. For (A)-(C), *X.laevis* H2A/H2B (xH2A/H2B), mouse H2A/H2B (mH2A/H2B) or H2AL2/TH2B was added to 1.5 μM DNA as indicated. The molar ratios of H2A/H2B to DNA are 0.5:1, 1:1 and 2:1 (lanes 4-6). Histone chaperones was added in five-fold excess to DNA (lanes 7-9). Histone chaperones do not interact with DNA (lane 2). DNA control (lane 1) and chaperone-histone complexes (lane 3) are shown. (D) hSet does not dissociate H2A/H2B-DNA complexes for 207 bp 601 DNA sequence (D.1) or 588 bp HTLV-1 promoter sequence (D.2). 1- or 2-fold excess of *X. laevis* H2A/H2B was added to 1.5 μM DNA (lanes 4-5). yNap1 or hSet was added in five-fold excess to DNA (lanes 6-7 for yNap1, lanes 8-9 for hSet). yNap1 and Set do not interact with DNA (lane 2-3). DNA control is shown (lane 1). Samples were analyzed on 5% polyacrylamide gels and visualized with ethidium bromide staining.

(Andrews et al, 2010; D'Arcy et al, 2013), as shown by electrophoretic mobility shift assays (EMSAs), the addition of yNap1 eliminates the DNA (207 bp '601' sequence)-H2A/H2B complexes (figure 2.2.A.1 and 2). hNap1 can also disassemble non-nucleosomal complexes (2.2.B). However no disassembly was observed for mNap2 and hSet under the same experimental conditions (2.2.C and 2.2.D).

We also examined if changing to histone variants and different DNA sequence would alter the results in this assay. H2AL2/TH2B histones were used, which binds to DNA, forming DNA-H2AL2/TH2B complexes. The addition of yNap1 or hNap1 again eliminates the non-nucleosomal complexes containing variant histones (2.2.A.3 and 2.2.B.3); whereas mNap2 does not (2.2.C.3). Besides '601' sequence, we also tested 588 bp HTLV1 promoter sequence, for which yNap1 can dissociate the complex with H2A/H2B, whereas hSet still does not (figure 2.2.D.2).

2.4.3 Nap2 and Set have weaker nucleosome assembly activity compared to Nap1

Although it was proposed that yNap1 promotes nucleosome assembly by eliminating non-nucleosomal complexes, there has not been direct evidence for a correlation between the ability to dissociate DNA-H2A/H2B complexes and their nucleosome assembly activity. Here we provide an approach by comparing different histone chaperones in their efficiency to eliminate DNA-H2A/H2B complexes, and their nucleosome assembly activity. To examine the nucleosome assembly activity of different

histone chaperones, we applied two types of assays: the supercoiling assay and 'Recovery of Aggregated Chromatin' ('RAC') assay.

In the supercoiling assay, assembly of one nucleosome on a closed circular DNA plasmid yields one supercoil. After removing histones, supercoils can be analyzed using agarose gel electrophoresis. More supercoiling indicates more histone-DNA association. yNap1 can promote more histones to bind to DNA, as indicated by formation of supercoiled plasmid (figure 2.3.A, lanes 7-9, where 4, 8 or 16-fold of yNap1 over histones is added. Less supercoiling is observed in lane 9, possibly due to excess amount of yNap1 competing for histones with DNA). hSet also has nucleosome assembly activity when a 16-fold excess of Set over histone octamer is used, yet no chromatin assembly was noticed when Set concentration has a ratio to histone octamer as 4:1 or 8:1 (lanes 10 and 11). hNap1 and mNap2 have chromatin assembly activity (figure 2.3.B, lanes 6-9 and 11-14, for which 0.5, 2, 4 or 8-fold of hNap1 or mNap2 over histones is added). At equal concentrations of histone chaperones, mNap2 induces less supercoiling than hNap1 and thus has less efficient nucleosome assembly activity (compare lanes 6-9 and 11-14).

Another assay was also carried out to examine the nucleosome assembly activity of Nap1 and Nap2, which we term removal of aggregated chromatin assay ('RAC' assay). In this assay, DNA is mixed with excess amount of H2A/H2B so an aggregation is noticed in the well when samples are analyzed with native gels (figure 2.4, lane 6). Histones H2B and H4 utilized in this assay are labeled with acceptor and donor fluorophores

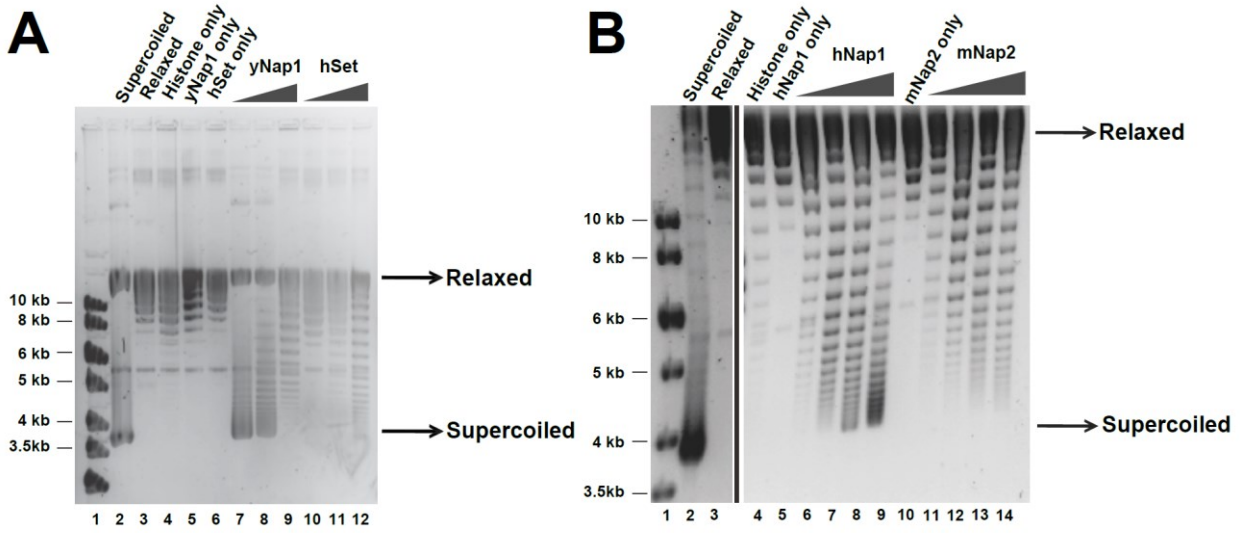

Figure 2.3. Chromatin assembly activity of Nap1 family members shown by supercoiling assay. Nucleosomes were reconstituted by incubating relaxed plasmid with canonical histone octamer and yNap1 or hSet (A), hNap1 or mNap2 (B). The nucleosome reconstitution was analyzed by DNA supercoiling assay on 1.2% agarose gel. (A) The molar ratio of yNap1 or hSet to histone octamer was 0.5:1, 2:1, 4:1 or 8:1 (lanes 6-9 for hNap1, lanes 11-14 for mNap2). Controls of supercoiled (lane 2) and relaxed plasmids (lane 3), with histones (lane 4), Nap1 without histones (lane 5), Nap2 without histones (lane 10) are shown. DNA ladder is indicated (lane 1). (B) hNap1 or mNap2 is titrated to relaxed plasmid in the presence of histone octamer (lanes 7-9 for yNap1, lanes 10-12 for hSet). DNA ladder is shown (lane 1). Supercoiled and relaxed plasmid controls are shown (lane 2 and 3). yNap1 or hSet does not induce supercoiling on relaxed plasmid (lanes 5 and 6).

respectively, so nucleosome formation can be monitored by the appearance of FRET. A nucleosome control reconstituted with salt dialysis method is also performed for which FRET can be monitored as a control for migration of the nucleosome band (lane 5). When yNap1 or hNap1 is added to the reaction, nucleosome formation is observed, as indicated by a band with the same migration as the nucleosome (figure 2.4.A and B, lanes 7-9). Also, FRET signal can be observed between H2B and H4, and the band also has the same migration property as the nucleosome control. These all indicate the formation of nucleosomes. When hSet is added to the reaction, nucleosome formation was not as efficient as yNap1 (figure 2.4.A, lanes 10-12). This again suggests that hSet has weaker nucleosome assembly activity compared to yNap1. mNap2 is also not as efficient in nucleosome assembly as hNap1 (figure 2.4.B).

2.4.4 Nucleosome assembly proteins bind to histones with different stoichiometry

Despite the fact that Nap1, Nap2 and Set bind to histones with similar affinity (table 2.1), the stoichiometry of the interaction has not been investigated for these chaperones with the exception of yNap1 (D'Arcy et al, 2013). Here we used a FRET-based Job plot assay to study the stoichiometry of the interaction. In this assay, the total concentration of Nap and H2A/H2B is kept constant, and the ratios are varied. FRET signal is monitored as change of Nap fraction. The stoichiometry corresponds to the Nap:H2A/H2B ratio for which the maximum FRET signal is achieved. Using the FRET-based Job plot assays,

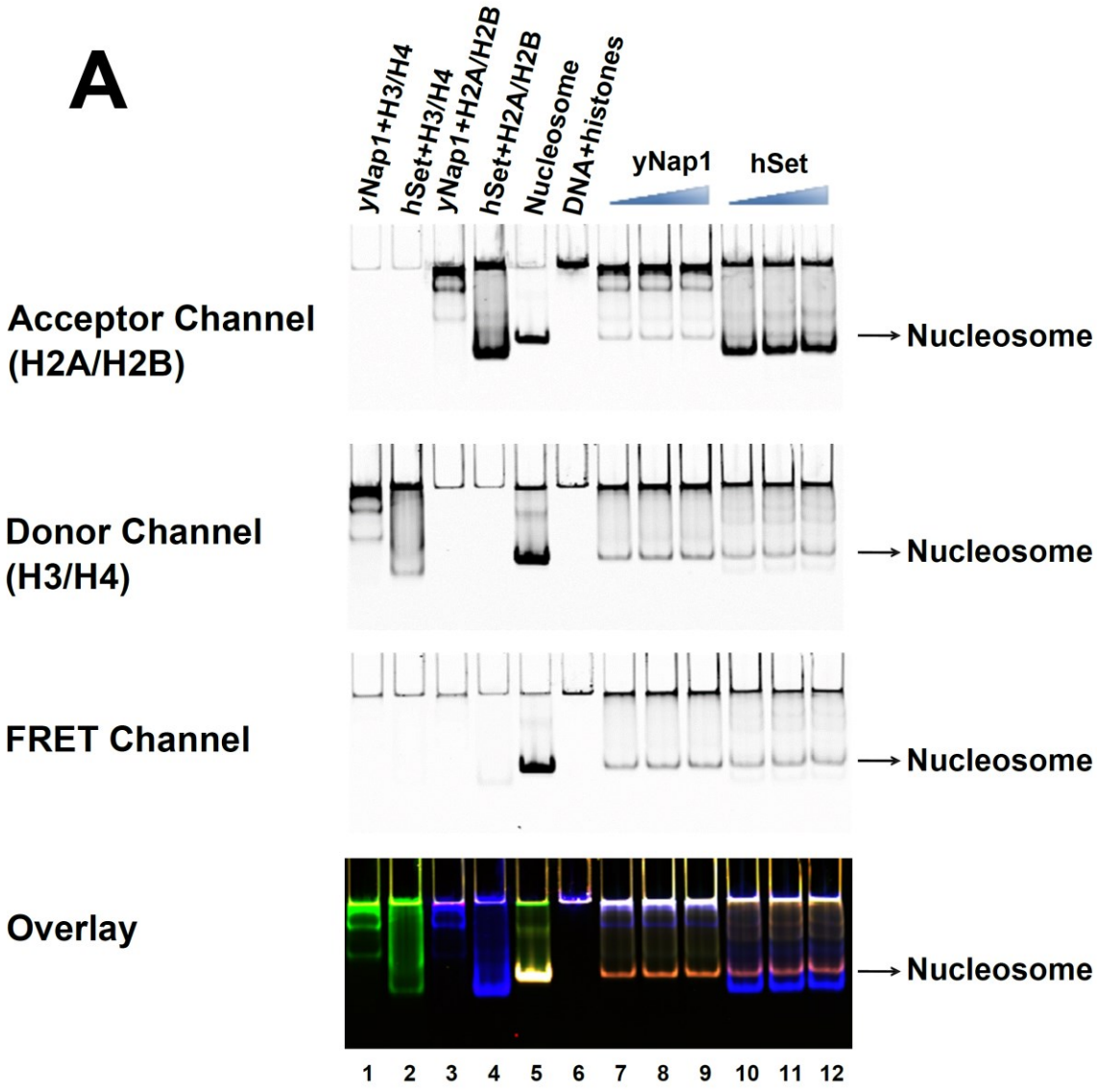
A
yNap1+H3/H4
hSet+H3/H4
yNap1+H2A/H2B
hSet+H2A/H2B
Nucleosome
DNA+histones
yNap1
hSet
Acceptor Channel (H2A/H2B)
Donor Channel (H3/H4)
FRET Channel
Overlay
Nucleosome
1 2 3 4 5 6 7 8 9 10 11 12

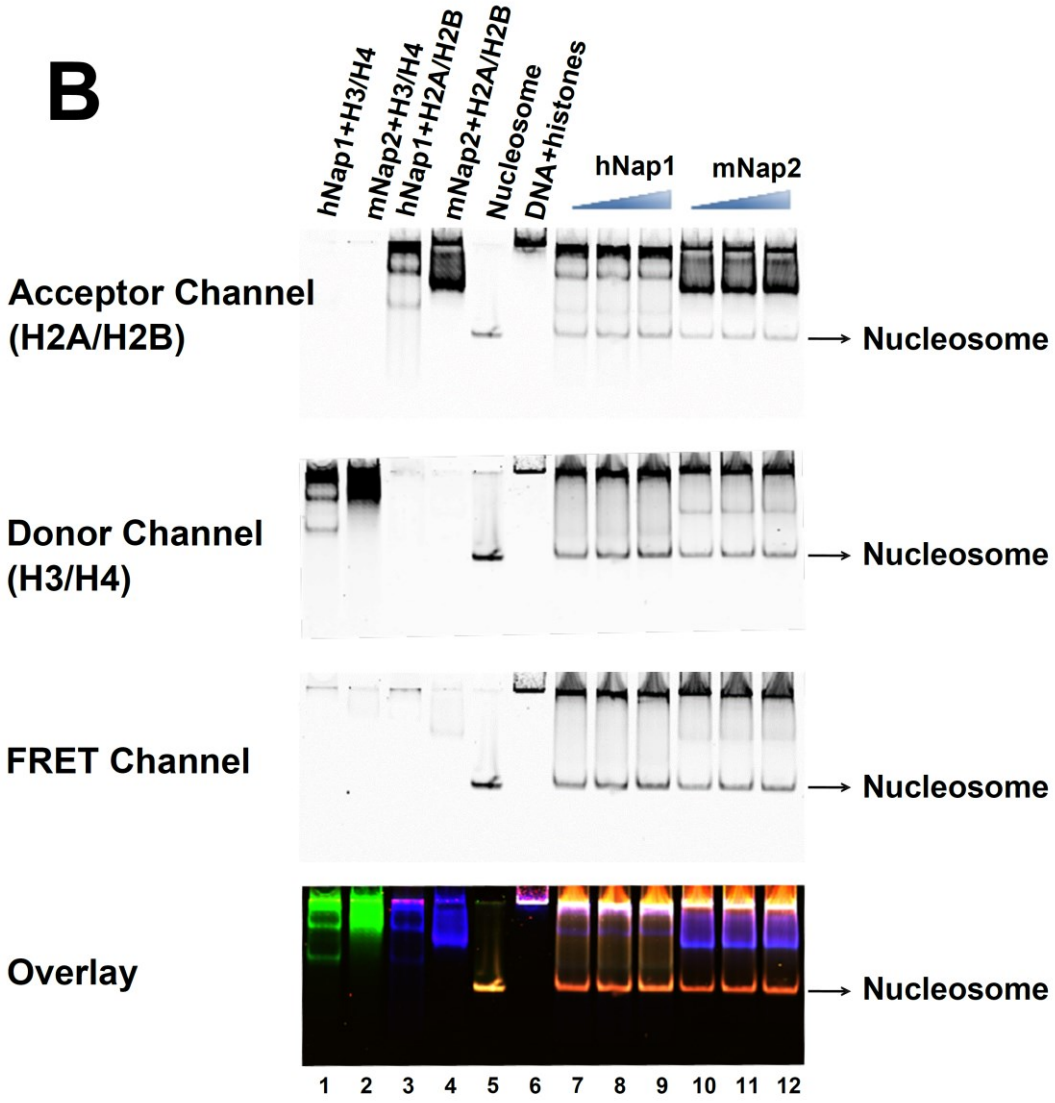

Figure 2.4. Nucleosome assembly activity of Nap1 family members shown by RAC assay. Stoichiometric amount of donor fluorophore-labeled H3/H4 and excessive amount of acceptor fluorophore-labeled H2A/H2B histones were mixed with DNA (lane 6), and histone chaperones yNap1, hSet, (A) hNap1 or mNap2 (B) was titrated into the DNA-histone mixture (A: for yNap1, lanes 7-9; for hSet, lanes 10-12; B: for hNap1, lanes 7-9; for mNap2, lanes 10-12) to recover nucleosome formation. The reactions were analyzed using 5% native gel electrophoresis, and scanned with the acceptor channel (top panel), donor channel (panel 2) and FRET channel (panel 3). An overlay of the signals is also shown (bottom panel). yNap1-H3/H4, hSet-H3/H4, (A) yNap1-H2A/H2B and mNap2-H2A/H2B (B) complexes are shown (lanes 1-4). Nucleosome reconstituted with labeled H2A/H2B and H3/H4 through salt dialysis method is also shown (lane 5).

we were able to obtain the stoichiometry of yNap1, hNap1, mNap2 and Set for H2A/H2B. The FRET signal of yNap1-H2A/H2B interaction peaks at 0.5 for fraction of yNap1, indicating a 1:1 binding stoichiometry (figure 2.5.A), or that one yNap1 monomer binds to one histone H2A/H2B dimer. This agrees with published data (D'Arcy et al, 2013). The signal for hNap1 binding to H2A/H2B also maximizes at 0.5, indicating 1:1 stoichiometry (figure 2.5.B). Nap2 has a 2:1 stoichiometry, as the peak is achieved at Nap2 fraction of ~0.7 (or Nap2:H2A/H2B ratio of 2:1) (figure 2.5.C). Set has a 1:2 stoichiometry, with the peak at Set fraction of ~0.35 (or Set:H2A/H2B ratio of 1:2) (figure 2.5.D).

2.5 Discussion

There are several Nap1 family members in eukaryotes, and their functional differences have been an intriguing question in the field. We compared several histone chaperones from the Nap1 family, including Nap1, Nap2 and Set. We found that Nap1 from different species, including yeast and humans, with only 58% sequence similarity (compared to 83% similarity for Nap1 and Nap2 in humans), behaves similarly to each other, with respect to histone binding affinities and stoichiometry, dissociation of non-nucleosomal complexes and nucleosome assembly activity. Nap2 and Set, although bind to histones with similar affinities as Nap1, do not dissociate non-nucleosomal complexes as efficiently as Nap1 does.

It was shown that yNap1 binds to H2A/H2B in a tetrameric conformation, blocks the binding surface of H2A/H2B to DNA, and directly competes for H2A/H2B from DNA

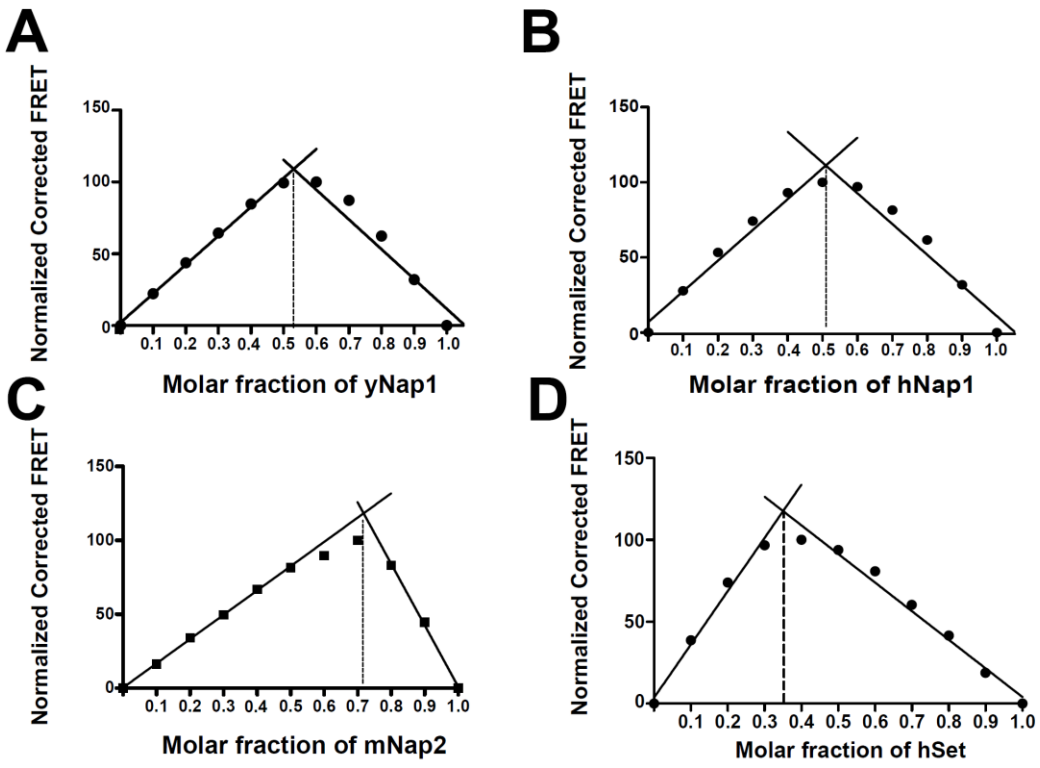

Figure 2.5. Stoichiometry of Nap-histone interactions using Job plot assays for (A) yNap1 (B) hNap1 (C) mNap2 (D) hSet. *X. laevis* H2A/H2B is labeled with donor fluorophore and chaperones are labeled with acceptor fluorophore. The total concentration of histone + chaperone was kept constant, with molar fraction of chaperone (X-axis) varied. Representative result from at least three replicates and for each replicate a duplicate was performed. Error bars are too small to be visible.

(Andrews et al, 2010; D'Arcy et al, 2013). Our stoichiometry data indicate thatNap2 binds to H2A/H2B with a different stoichiometry in our Job plot assays, and cannot dissociate non-nucleosomal complexes. It is thus plausible that the difference in stoichiometry causes the inability of Nap2 to compete for H2A/H2B with DNA. Another observation is that Set has different stoichiometry compared to Nap1 and Nap2, and cannot compete for H2A/H2B from DNA. It is also worth mentioning that Nap1 forms oligomers (Park et al, 2008a), so does Nap2 (unpublished data by Ling Zhang et al., see appendix V). It is possible that in Job plot assays, we observed the stoichiometry when histone chaperones are in certain oligomerization states. Nonetheless, these results indicate that the histone chaperones bind to histones with distinct conformations from each other. Crystal structures of Nap1 and Set have been solved, exhibiting similar structures. It is intriguing how structurally similar proteins display distinct properties. Crystallography trials and H/DX experiments can be carried out to study the binding surfaces of Nap2 and Set to H2A/H2B further investigate what conformations histones adopt upon binding to histone chaperones.

We have observed no difference for the histone chaperones with histone variants or different DNA sequences. The chaperones we tested showed similar affinity to canonical histones and variant histones, consistent with what was previously observed for yNap1 (Andrews et al, 2008). Nap1 can dissociate non-nucleosomal complexes containing canonical histones or histone variants, and from DNA with different sequences. Yet Nap2

and Set do not display these activities despite changes in histone types or DNA sequences.

Taken together, the data looks into the functional differences these histone chaperones may have *in vivo*. All of them bind to histones with high affinity, suggesting a histone binding or histone shuttling function. Yet they are different in their ability to disassemble non-nucleosomal complexes and assemble nucleosomes. Nucleosome reassembly during transcription was shown to be important in the proper regulation of transcription, and inefficiency to assemble nucleosomes can lead to cryptic transcription (Cheung et al, 2008; Kaplan et al, 2003; Silva et al, 2012). It is thus possible that these histone chaperones have quite distinct roles in transcription regulation, with Nap1 being more efficient than Nap2 or Set. Transcription regulation can then be fine-tuned with different types of histone chaperones.

It has been shown that both Nap1 and Nap2 are both polyglutamylated *in vivo*, on the C-terminal domain by the addition of a glutamate chain that includes up to 10 glutamate residues (Regnard et al, 2000). Data from our research group also indicated that the polyglutamylation of *Drosophila* Nap1 plays an important role in regulating the histone chaperone activity of Nap1 (Subramanian et al., data in preparation for submission). It is possible that the posttranslational modifications of Nap2 also play important roles by regulating the histone chaperone activity of Nap2. It is thus interesting to further

investigate what roles posttranslational modifications play in regulating the functions of nucleosome assembly proteins in the future.

PROJECT II.

TITLE: INTERACTION OF SPN1 WITH CHROMATIN COMPONENTS AND CHROMATIN REGULATORS

CHAPTER 3

REVIEW OF LITERATURE

3.1 Transcription regulation

Transcription is the first step of gene expression, in which DNA is transcribed into RNA by RNA polymerases. The process of transcription in eukaryotic cells is largely dependent on RNA polymerase II (RNAPII).

During transcription initiation, a preinitiation complex (PIC), composed of TATA-binding protein (TBP), general transcription factors, and RNAPII, is formed on the promoter (Svejstrup, 2004). For most of the well-studied promoters, formation of the PIC is the rate-limiting step during transcription process. These genes are thus referred to as recruitment-regulated genes (Kim et al, 2005). Some promoters are classified as regulated after recruitment of PIC, and genes with these promoters are classified as postrecruitment-regulated genes (Muse et al, 2007).

3.2 Post-recruitment-related transcription factor Spn1

Spn1 (suppresses postrecruitment functions gene number 1) is also known as Iws1 (interacts with Spt6). Spn1 is highly conserved throughout evolution (figure 3.1). It was identified as a transcription regulator that regulates post-recruitment of RNA polymerase II (RNAPII) in yeast (Fischbeck et al, 2002). Besides its physical and genetic interaction with Spt6 and physical interaction with RNAPII, Spn1 also has physical and genetic interaction with Spt4, physical interaction with TFIIS, and genetic interaction with TBP, which are factors involved in transcription initiation, elongation, processing and chromatin remodeling (Fischbeck et al, 2002; Lindstrom et al, 2003; Zhang et al, 2008).

Spt6 was originally identified as a factor that alters the expression of certain genes (Winston et al, 1984), and was later found to be involved in a variety of other biological processes, including chromatin maintenance (Bortvin & Winston, 1996) and RNA processing (Hartzog et al, 1998). The physical interaction of Spn1 with Spt6 has been reported in several species from yeast to humans (Li et al, 2010; Yoh et al, 2008; Zhang et al, 2008). The Spn1/Spt6 complex participates in transcription elongation (Yoh et al, 2008) and mRNA export (Yoh et al, 2007).

S. cerevisiae (yeast) *SPN1* is an essential gene for yeast viability. Yeast Spn1 is a 410-residue protein composed of a structured central domain (residues 141-305), which is highly conserved throughout evolution, and disordered acidic N- and basic C- terminal

domains. The central domain of Spn1 is sufficient for yeast viability (Pujari et al, 2010). The N- and C- terminal domains of Spn1 displays sequence variability in different species.

The crystal structure of the central domain of yeast and *Encephalitozoon cuniculi* Spn1, alone or in complex with a small region of Spt6 (a small N-terminal region of Spt6 that is sufficient for Spn1-Spt6 interaction), has been solved (Diebold et al, 2010; McDonald et al, 2010; Pujari et al, 2010) (figure 3.2).The central domain of Spn1 contains eight alpha helices, packing into a right-handed superhelical arrangement. The structure displays a surface-exposed cavity of Spn1, rimmed by conserved hydrophobic residues. The unique cavity of Spn1 has been shown to be critical for regulating RNAPII-mediated transcription (Pujari et al, 2010), since temperature-sensitive mutant residues are located on the rim of the cavity. The binding of a small region of Spt6 to Spn1 induces only minimal conformational changes in Spn1 (Diebold et al, 2010; McDonald et al, 2010).

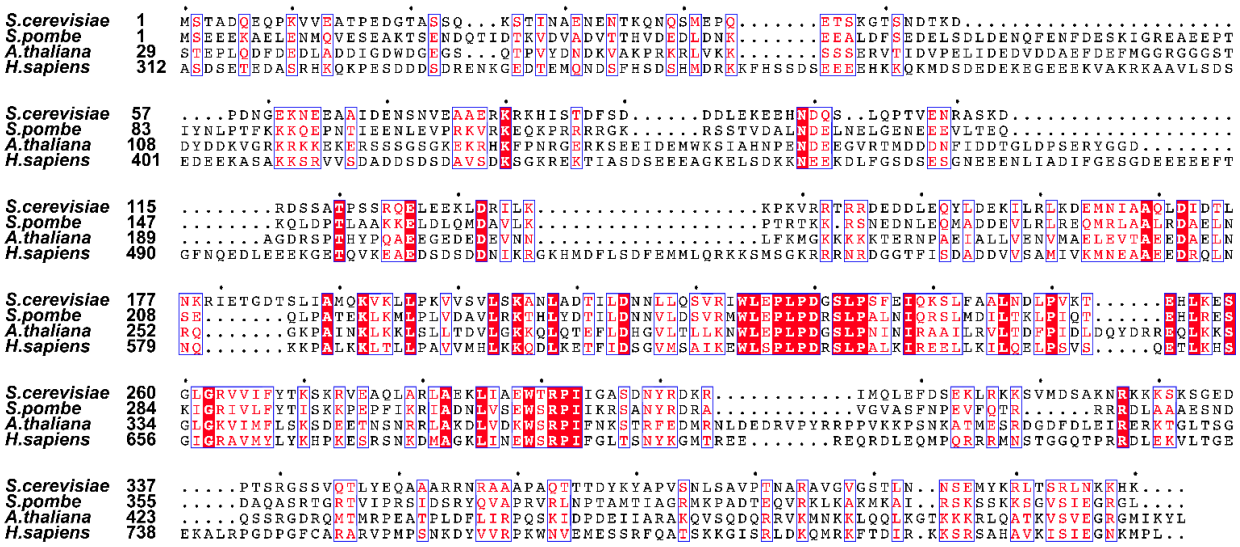

Figure 3.1. Spn1 is highly conserved throughout evolution. Amino acid sequence alignment of Spn1. Spn1 in *S. cerevisiae*, *Schizosaccharomyces pombe*, *Arabidopsis thaliana* and *Homo sapiens* are aligned. Alignments were performed using *Clustal X*, and visualized with *ESPript*. Blue boxes indicate >70% similarity between aligned sequences. Red indicates identical amino acids among all (shading) or most (letters) of aligned sequences.

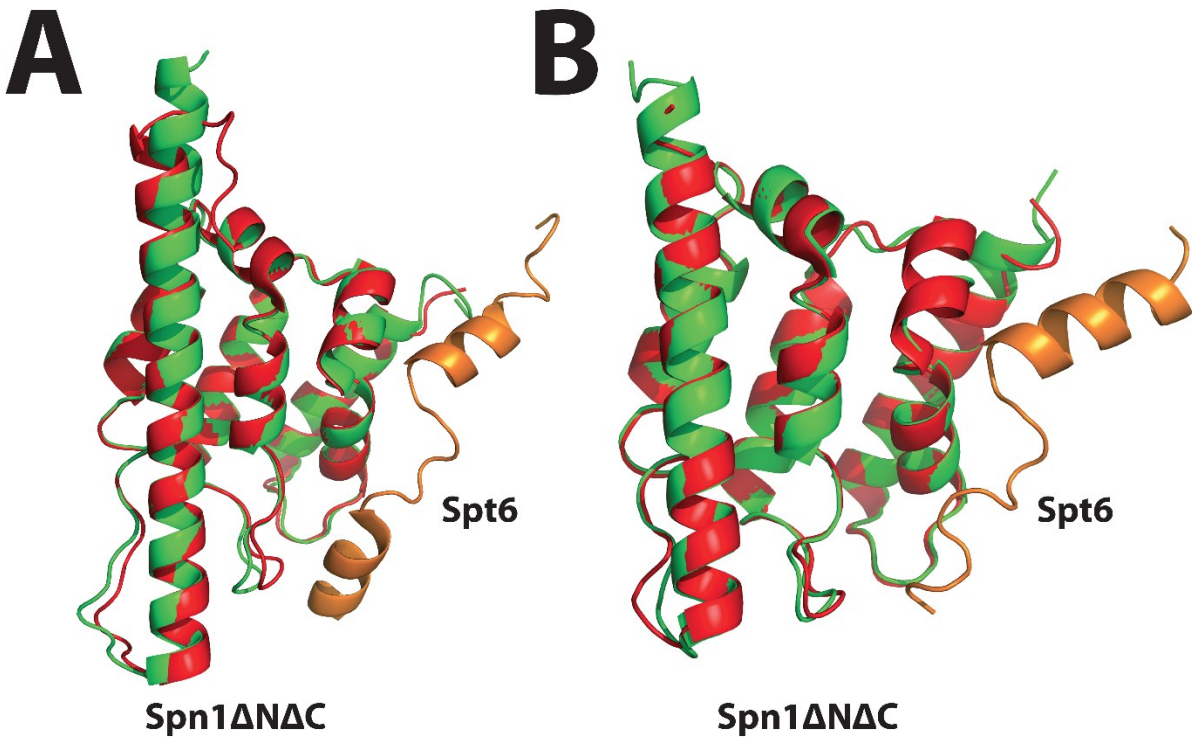

Figure 3.2. Crystal structure of Spn1 and Spn1-Spt6 complex, from yeast (figure A, PDB ID: 3NFQ and 3OAK) or *E. cuniculi* (figure B, PDB ID: 2XPL and 2XPP). The conserved central domain of Spn1 is shown in green for Spn1 alone or red in Spn1-Spt6 complex. Spt6 is shown in orange.

CHAPTER 4

Interaction of Spn1 with Chromatin Components and Chromatin Regulators[23]

4.1 Summary

Spn1 (suppresses postrecruitment functions gene number 1) was identified as a transcription regulator that regulates post-recruitment of RNA polymerase II (RNAPII) in yeast. Spn1 is highly conserved among eukaryotes ranging from yeast to humans (Fischbeck et al, 2002). Spn1 is involved in transcription repression by interacting with RNAPII and other transcription factors. Here we demonstrate that Spn1 binds to histones and to the histone chaperone Nap1, and also forms a ternary complex with histones and Nap1 *in vitro*. This was shown using several experimental approaches, including fluorescence-based binding assays, sucrose gradient sedimentation assays and electrophoretic mobility shift assays. Spn1 also assembles chromatin *in vitro*, as shown by a DNA supercoiling assay. The roles of N- and C- terminal tails of Spn1 in these

[2] Dr. Uma Muthurajan contributed figures 4.2 and 4.5. Ling Zhang contributed figures 4.1, 4.3, 4.4 to 4.11.

[3] **Disclaimer:**
New preparations of Spn1 have been made after the preparation of Chapters 4 and 5. Some of the experiments were repeated with the new preparations by members of the Stargell lab, but are not included in this thesis.

interactions are also discussed. This research looks into new functions of Spn1 on chromatin regulation by interacting directly with chromatin components and chromatin regulators.

4.2 Introduction

It was previously shown that the central domain of Spn1 is sufficient for performing the essential functions of Spn1 for viability of yeast cells (Pujari et al, 2010). However, N- and C-terminal tails appear to be required for yeast to grow under more stringent conditions (Almeida et al., unpublished data), such as varying temperatures and with the addition of caffeine into the medium with certain genetic backgrounds. These *in vivo* results suggest that N- and C- terminal tails of Spn1 (Spn1ΔN and Spn1ΔC) (figure 4.1) have potentially important functions, which cannot be explained by the interaction of Spn1 with RNAPII since the central domain of Spn1 is sufficient to maintain this interaction (Fischbeck et al, 2002). We thus sought for other chromatin-related activities in which Spn1 is involved. There is no published evidence for the interaction of Spn1 with nucleosome assembly proteins. In this research we examined the interaction of Spn1 with chromatin components and chromatin regulators, including histones and the histone chaperone Nap1, using several experimental approaches, including fluorescence-based binding assays, sucrose gradient sedimentation assays and EMSAs. We also show that Spn1 binds to both DNA and nucleosomes. The interaction of Spn1 with DNA and nucleosomes

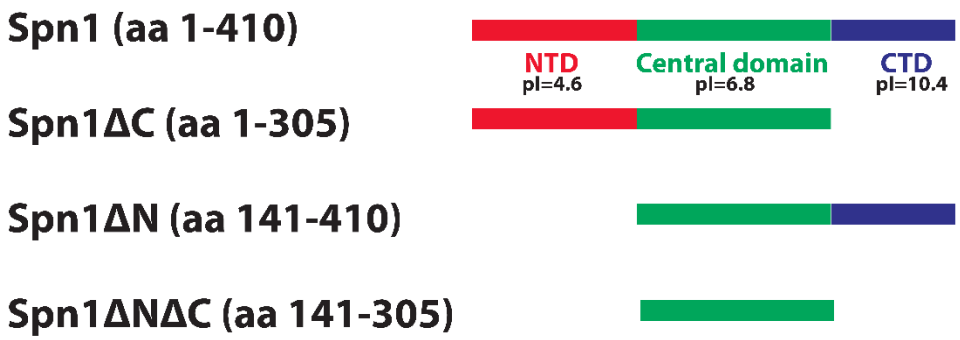

Figure 4.1. Yeast Spn1 constructs used in this research. N-terminal domain (NTD, shown in red), central domain (shown in green) and C-terminal domain (CTD, shown in blue) are indicated with individual pI for each domain. Full length Spn1 is 410 amino acids in length. Different tail deletion mutant constructs are also shown in colored diagrams, including C-terminal deletion construct (Spn1ΔC, amino acids 1-305), N-terminal deletion construct (Spn1ΔN, amino acids 141-410) and N- and C- terminal deletion construct (Spn1ΔNΔC, amino acids 141-305).

requires both N- and C- terminal tails. In addition, we show that Spn1 has nucleosome assembly activity using a DNA supercoiling assay. N- and C- terminal domains of Spn1 are important for these interactions and their roles are also discussed. This research looks into new functions of Spn1 on chromatin regulation by directly interacting with chromatin components and chromatin regulators.

4.3 Materials and Methods

4.3.1 Protein purification and nucleosome assembly

X. laevis histones H2A, H2B, H2BT112C, H3 and H4 were purified and refolded into H2A/H2B dimer, H2A/H2BT112C or $(H3/H4)_2$ tetramer as described (Dyer et al, 2004). H2A/H2B T112C and $(H3/H4E63C)_2$ was labeled as described (Andrews et al, 2008). *S. cerevisiae* Nap1 was purified as described (McBryant et al, 2003). Yeast Spn1 and Spn1 constructs were purified from *E. coli* using a pET15b vector and expressed with Rosetta 2 (DE3)pLysS cells at 30°C for 2 h (16°C overnight for miniSpn1). Cells were harvested by centrifugation at 4,000 rpm for 15 min and pellets were resuspended in 40 ml buffer containining 100 mM Tris-HCl, pH 7.5, 1 M NaCl, 10% glycerol, 50 mM imidazole and 500 µM. Cells were sonicated and centrifuged at 15,000 rpm for 40 min. Supernatant was then purified through Hi-Trap chelating column and eluted with buffer containing 50 to 500 mM imidazole, followed by Superdex 200 size-exclusion chromatography in buffer containing 25 mM MES pH 6.5, 200 mM NaCl, 10%glycerol. For full-length Spn1, an extra

step was performed by purification through Hi-Trap SP cation exchange column with buffer containing 25 mM MES, pH 6.5, 10% glycerol and 50 to 600 mM NaCl.

Nucleosomes were reconstituted as described (Dyer et al, 2004) on 147 bp (Nuc147) or 207 bp (Nuc207) DNA containing the 601 positioning sequence (Lowary & Widom, 1998).

4.3.2 Electrophoretic mobility shift assays of Spn1 binding to DNA or nucleosomes

5 μM of 601-147 bp or 601-207 bp DNA or nucleosomes assembled with *X. laevis* histone octamer on the same DNA fragments were incubated with 2 or 4 molar excess of various Spn1 constructs as indicated for 30 minutes at room temperature. The binding buffer was 50 mM Tris-HCl, pH 7.5, 50 mM NaCl and 2 mM arginine. The samples were analyzed on a 5% native PAGE. The gel was stained first with ethidium bromide followed by Coomassie blue.

4.3.3 Sucrose gradient sedimentation assay

100 μl of samples were loaded onto a 12 ml 5-25% sucrose gradient. The buffer also contains 150 mM NaCl, 10 mM Tris 7.5 and 1 mM DTT. Protein samples were prepared as follows: (1) 5 μM Spn1. (2) 5 μM H2A/H2B. (3) 5 μM Spn1 and 5 μM H2A/H2B. (4) 2.5 μM $(H3/H4)_2$. (5) 5 μM Spn1 and 2.5 μM $(H3/H4)_2$. Samples were then spun at 28,000 rpm for 18 h at 4°C. The gradients were fractionated into 50 μl from the top towards the bottom and every other fraction was analyzed on 4-12% precast Criterion XT SDS-

polyacrylamide gel (Bio-Rad 245-0124). Proteins were visualized with Sypro Ruby staining.

4.3.4 Microplate-based fluorescent assay

The fluorescence quenching assay was performed and data was analyzed as described (Hieb et al, 2012). In a 384-well, glass bottom microplate, 1-1000 nM Spn1 (for fluorescence-based de-quenching assays) or Spn1T185C-Atto647N (for FRET assays) was titrated into 1 nM Alexa488-labeled histone dimer H2A/H2BT112C, and the signal change was monitored using a standard Typhoon Trio multimode imager. Dissociation constants were calculated as described (Andrews et al, 2008). Reactions were carried out in buffers containing 150 mM KCl, 10 mM Tris 7.5, 5% glycerol, 0.035 mg/ml BSA, 0.01% Tween-20 and 1 mM DTT.

4.3.5 Chromatin assembly assay

The DNA supercoiling assay was carried out as described (Lusser & Kadonaga, 2004). Spn1, Spn1ΔN, Spn1ΔC or Spn1ΔNΔC was added into 25 pmol *X. laevis* histone octamer to reach a final Spn1 construct: histone octamer ratio of 0.5:1 and 1:1. Nap1 was added to histone octamer for a final ratio of 1:1 and 2:1. Reactions were incubated at 37°C for 10 min. The relaxed plasmid was added to the reaction and the reaction was incubated at 37°C for another hour in a buffer containing 10 mM Tris-HCl, pH 8.0, 100 mM NaCl, 1 mM $MgCl_2$, 1 mM EDTA and 100 µg/µl BSA. 8 units of wheat germ topoisomerase I (Promega) was then added and the reaction was incubated at 37°C for an additional hour.

Final concentrations of 0.5% SDS were added to inactivate topoisomerase followed by addition of 0.2mg/ml proteinase K. The reaction was then incubated at 55°C for 30 min. DNA was purified by phenol/chloroform extraction and ethanol precipitation. The final products were analyzed on a 1.2% agarose gel. For plasmid supercoiling assay in the absence of magnesium ions, Spn1, Spn1ΔNΔC or Nap1 was added into 30 pmol *X. laevis* histone octamer to reach a final Nap1 or Spn1 construct: histone octamer ratios of 1:1 or 2:1. The samples were processed in the absence of $MgCl_2$.

4.3.6 Chromatin assembly assay with excess H3/H4

90 nM $(H3/H4E63C)_2$-Alexa488, 80 nM H2A/H2BT112C-Atto647N was incubated with 80 nM yNap1 or 50, 100, 150, 200, 250, 300, 350 nM Spn1, and mixed with 10 nM DNA (165bp-601 sequence). No chaperone control was also carried out using the same condition, only in the absence of yNap1 or Spn1. Reaction buffer contained 200 mM NaCl, 10 mM Tris-HCl, pH 7.5, 5% glycerol, 0.05% NP-40, 0.05% CHAPS, 1 mM EGTA, 0.5 mM $MgAc_2$, 0.5 mM imidazole, 0.5 mM DTT, 0.5 mM PMSF, 0.05 µg/ml pepstatin A and 0.05 µg/ml leupeptin.

Reactions were incubated at room temperature for 15 min, and analyzed using 5% PAGE. Gels were scanned using Typhoon Trio multimode imager (GE healthcare) and scans were collected using 3 excitation/emission wavelengths: for donor channel, 488/520 nm; for acceptor channel, 633/670 nm; for FRET channel, 488/670 nm.

4.3.7 Chromatin assembly assay with excess H2A/H2B

48 nM $(H3/H4E63C)_2$-Alexa488, 300 nM H2A/H2BT112C-Atto647N was incubated with 1, 2, 3, 4, 5 or 6 μM Spn1, and mixed with 10 nM DNA (165bp-601 sequence). Reaction buffer contained 200 mM NaCl, 10 mM Tris-HCl, pH 7.5, 5% glycerol, 0.05% NP-40, 0.05% CHAPS, 1 mM EGTA, 0.5 mM $MgAc_2$, 0.5 mM imidazole, 0.5 mM DTT, 0.5 mM PMSF, 0.05 μg/ml pepstatin A and 0.05 μg/ml leupeptin.

The rest of the reactions were then carried out as described previously in 4.3.6.

4.3.8 Electrophoretic mobility shift assays of Spn1 binding to Nap1

EMSAs for interaction of Spn1 and Nap1 were performed using 2 μM Nap1 and 1, 2 or 4 μM Spn1, Spn1ΔN, Spn1ΔC or Spn1ΔNΔC. No chaperone control was carried out under the same condition, in the absence of Spn1 or Nap1. Components were mixed in a buffer containing 150 mM KCl, 10 mM Tris-HCl, pH 7.5, 5% glycerol, 0.01% CHAPS, 0.01% NP-40, 1 mM DTT. Reactions were incubated at 25°C for 15 min and analyzed on 5% polyacrylamide gel electrophoresis.

4.3.9 Electrophoretic mobility shift assays of Spn1 binding to Nap1 and histones

EMSAs for formation of Spn1-Nap1-histone complexes were performed using 1 μM Nap1, 1 μM H2A/H2B (or 0.5 μM $(H3/H4)_2$) and 1, 2 or 3 μM Spn1. Controls are: (1) 1 μM Nap1, (2) 1 μM Spn1, (3) 1 μM Nap1 and 2 μM Spn1. (4) 1 μM Nap1 and 1 μM H2A/H2B. (5) 1 μM Nap1 and 0.5 μM $(H3/H4)_2$. They were mixed in a buffer containing 150 mM

NaCl, 10 mM Tris-HCl, pH 7.5 and 1 mM DTT. Reactions were incubated at 25°C for 15 min and analyzed on 5% polyacrylamide gel electrophoresis.

4.4 Results

4.4.1 Spn1 binds to DNA

To examine if Spn1 binds to DNA, we applied EMSAs. A constant amount of 601-147 bp DNA was used, and Spn1 was titrated. With 2 to 4- fold excess of Spn1, we observed formation of Spn1-DNA complexes (figure 4.2, compare lanes 3 and 4 to lane 2), as indicated by the slower mobility of the complex band compared to DNA in native gel electrophoresis. In contrast, the deletion of the C-terminal domain of Spn1 resulted in an inability to bind to DNA (lanes 5, 6, 9 and 10). When the N-terminal domain of Spn1 is deleted, Spn1ΔN aggregates DNA to a certain extent (lanes 7 and 8), indicating that Spn1ΔN binding to DNA is altered compared to full length Spn1 binding to DNA.

4.4.2 Spn1 binds to histones

Attempts to use EMSA assays to examine Spn1-histone interactions were met with difficulties because neither Spn1 nor histones enter the PAGE gels. We decided to apply sucrose gradient sedimentation analysis to investigate whether Spn1 binds to histones. In the presence of Spn1, H3/H4 sedimented to lower fractions (figure 4.3, compare Aiv with Av, also indicated in graphic lines in Biii), indicating the formation of larger complexes, thus Spn1-H3/H4 complexes. The fractions containing the complex were analyzed on a 4-12% Criterion XT gel and H3/H4 as well as Spn1 band were found in the same fractions,

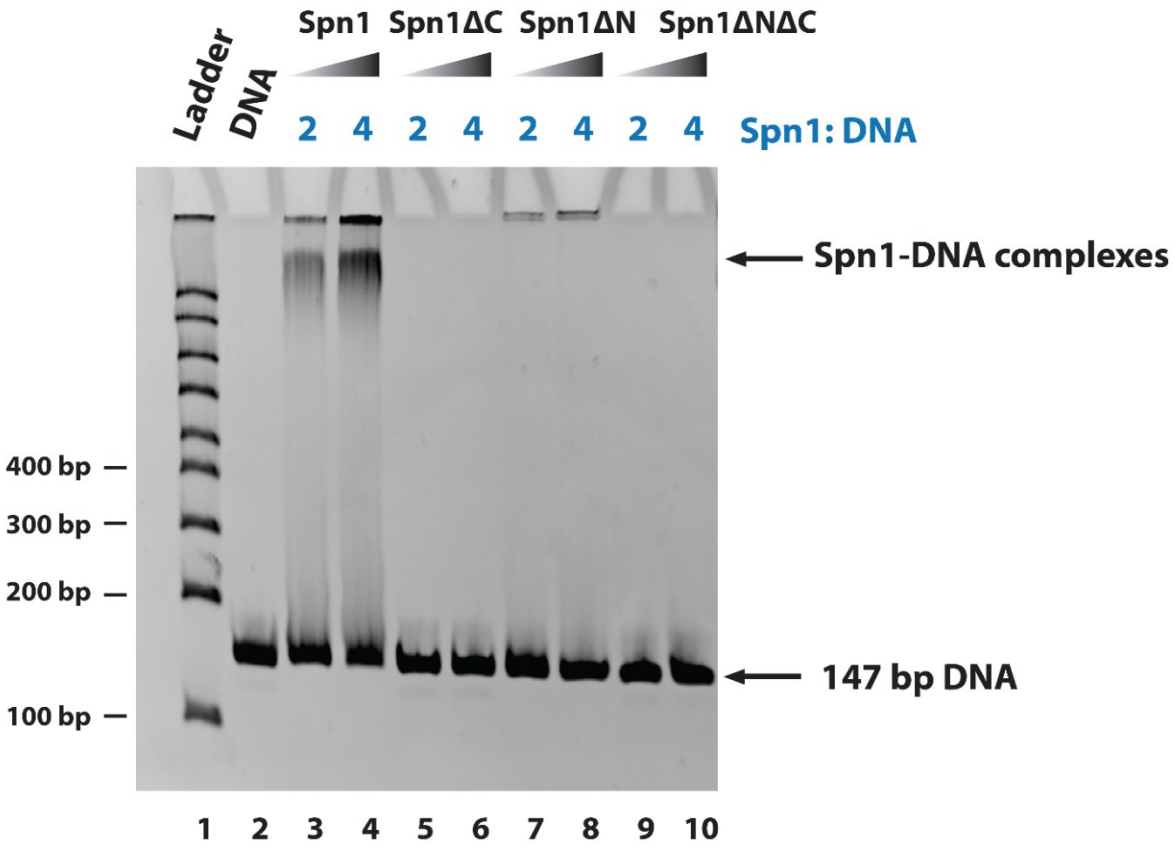

Figure 4.2. Binding of Spn1 to DNA. 5 μM 601-147 bp DNA was incubated with Spn1, Spn1ΔC, Spn1ΔN or Spn1ΔNΔC, The molar ratios of Spn1 constructs to DNA are 2:1 or 4:1. Samples were analyzed using 5% polyacrylamide gel electrophoresis and stained with ethidium bromide. Spn1 interacts with DNA, forming complexes with slower mobility (lanes 3-4). The C-terminal domain of Spn1 is required for binding to DNA, as shown by the fact that Spn1ΔC does not bind to DNA under the same conditions (lane 5-6). The N-terminal domain of Spn1 may play a role in DNA binding, as the migration of Spn1-DNA complexes is different in the absence of Spn1 N-terminal domain (lanes 7-8). There is no binding of Spn1ΔNΔC to DNA (lanes 9-10). 601-147 bp DNA control (lane 2) and DNA ladder (lane 1) are shown.

confirming the co-sedimentation of H3/H4 with Spn1. Sedimentation of H2A/H2B does not seem to change, indicating no formation of Spn1-H2A/H2B complexes. From sucrose gradient sedimentation analysis, we conclude that Spn1 binds to histone tetramer $(H3/H4)_2$ but not histone dimer H2A/H2B.

4.4.3 Affinity of Spn1-histone interactions

To investigate the affinity of Spn1 binding to histones, we applied a fluorescence-based binding assay. H2A/H2BT112C was labeled with Alexa488 fluorophore, and Spn1 was titrated. The titration of Spn1 resulted in a change in fluorescence, which can be quantified to yield the affinity of Spn1 binding to H2A/H2B (figure 4.4.A). Spn1 binds to H2A/H2B with an apparent K_d value larger than 166 nM, which is more than 10-fold weaker than most histone chaperone-H2A/H2B interactions that have been examined, including Nap1 (Andrews et al, 2008), VPS75 (Park et al, 2008b), Nap2, Set (this thesis) and FACT (Winkler et al, 2011).

Fluorescence-based binding assay was also performed using H3/H4E63C-Alexa488, but no fluorescent signal change was noticed upon titration of Spn1 (data not shown). This could mean that either Spn1 does not interact with H3/H4, or that the interaction of Spn1 with H3/H4 does not induce a fluorescence signal change. Since the possibility that Spn1 does not interact with H3/H4 would be in direct contradiction with our results from sucrose gradient assays, we think it is more likely that the interaction of Spn1 does not induce a fluorescence signal change when interacting with H3/H4 labeled with

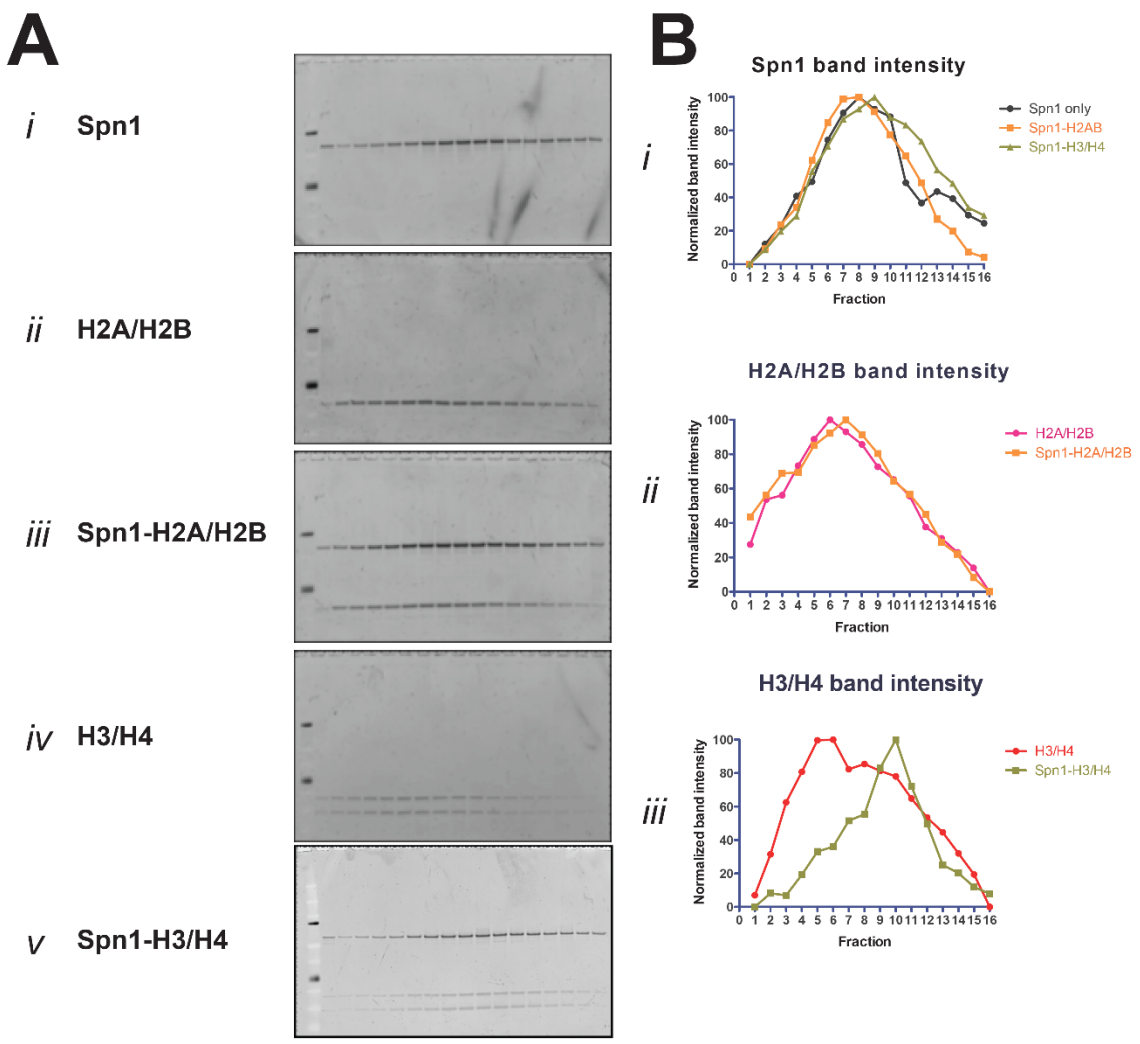

Figure 4.3. Spn1 binds to histone $(H3/H4)_2$ but not H2A/H2B. (A) Sucrose gradient sedimentation analysis was performed with i. Spn1 (5 μM), ii. H2A/H2B (5 μM), iii. Spn1-H2A/H2B (5 μM Spn1 - 5 μM H2A/H2B), iv. $(H3/H4)_2$ (2.5 μM) and v. Spn1-$(H3/H4)_2$ (5 μM Spn1 - 2.5 μM $(H3/H4)_2$). Fractions were analyzed on SDS PAGE and visualized with Sypro Ruby staining. (B) Quantification of sucrose gradient sedimentation analysis results. Band intensities were quantified for Spn1, H2A/H2B, H3/H4 in figure 4.3.A, normalized to 0-100%.

fluorohpores. To observe a fluorescent signal change in the fluorescence-based quenching assays, the binding of proteins have to cause change in conformation or environment change of the fluorophores, and there is the possibility that proteins bind, yet the change is not significant enough to induce a fluorescent signal change. FRET assay is thus a good alternative approach. For FRET assays, a FRET signal appears when two proteins come into proximity. So generally as long as the distance of the two fluorophores conjugated to proteins is within a critical distance, a FRET signal can be observed.

We next mutated wild-type Spn1 to introduce a cysteine residue for labeling with fluorophores in the sequence, so that FRET assay could be performed using both labeled Spn1 and labeled histones. Wild-type Spn1 does not contain cysteine residues in its native sequence. We carefully examined the sequence and structure of Spn1 to choose a residue for cysteine mutagenesis, which is least likely to disrupt the structure and function of Spn1. We decided that T185 is a good candidate since it is located in the loop region in the Spn1 structure and the mutation is unlikely to disrupt the structure of Spn1. After purification, Spn1T185C was labeled with Atto647 fluorophore and applied in FRET assays with H2A/H2BT112C-Alexa488 or H3/H4E63C-Alexa488. From the binding curves (figure 4.4.B), we conclude that Spn1 binds to H3/H4 with an affinity of 63.82 nM, whereas H2A/H2B binding to Spn1 does not result a plateau in the corrected FRET signal,

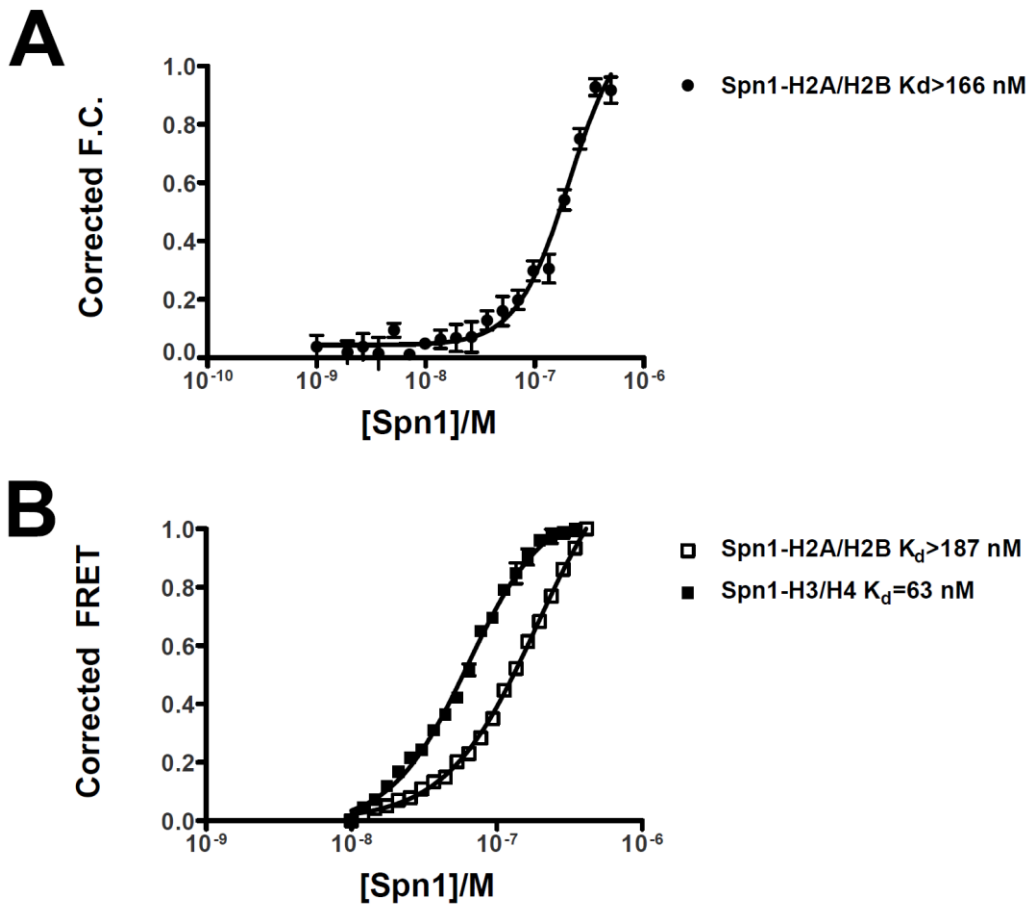

Figure 4.4. Fluorescence-based binding assays of Spn1-histone interaction. (A) Binding curves of fluorescent quenching assays for different Spn1 constructs-H2A/H2B interaction. Normalized fluorescence change (F.C.) is shown as a function of Spn1 concentration. (B) Binding curves of FRET assays for Spn1-H2A/H2B and Spn1-H3/H4 interaction. Normalized corrected FRET signals are shown as a function of Spn1 concentration in molar.

indicating again that Spn1 binds to H2A/H2B with low affinity, and/or that the binding of Spn1 to H2A/H2B is non-specific.

4.4.4 Spn1 binds to nucleosomes

We next investigated the binding of Spn1 to nucleosomes using gel shift assays. Nucleosomes were reconstituted with 147 bp DNA and *Xenopus laevis* histone octamer. Upon the addition of Spn1, bands with slower mobility were observed on a 5% native gel (figure 4.5, compare lanes 3 and 4 to lane 2), indicating formation of Spn1-nucleosome complexes. Deletion of the C-terminal domain of Spn1 resulted in the inability to bind to nucleosomes, as Spn1ΔC and Spn1ΔNΔC did not shift nucleosomes (lanes 4, 5, 9 and 10). Spn1ΔN can still bind to nucleosomes (lanes 6 and 7), yet the migration of the complexes seems to have changed from full length Spn1, as the complex seems to be altered as indicated by different mobility on the gel.

4.4.5 Spn1 has chromatin assembly activity

Given that Spn1 can bind histones, we next wanted to investigate whether Spn1 can assemble chromatin. To do that, we performed a DNA supercoiling assay, in which histones were incubated with relaxed plasmid DNA in the presence or absence of Spn1. Supercoiling is induced by nucleosome formation on the plasmid. After the removal of histones, DNA supercoiling is analyzed using agarose gel electrophoresis. When histones were added to plasmid DNA in the absence of histone chaperones, no supercoiling is induced (lane 5). More supercoiling was induced in the presence of Spn1 than in the

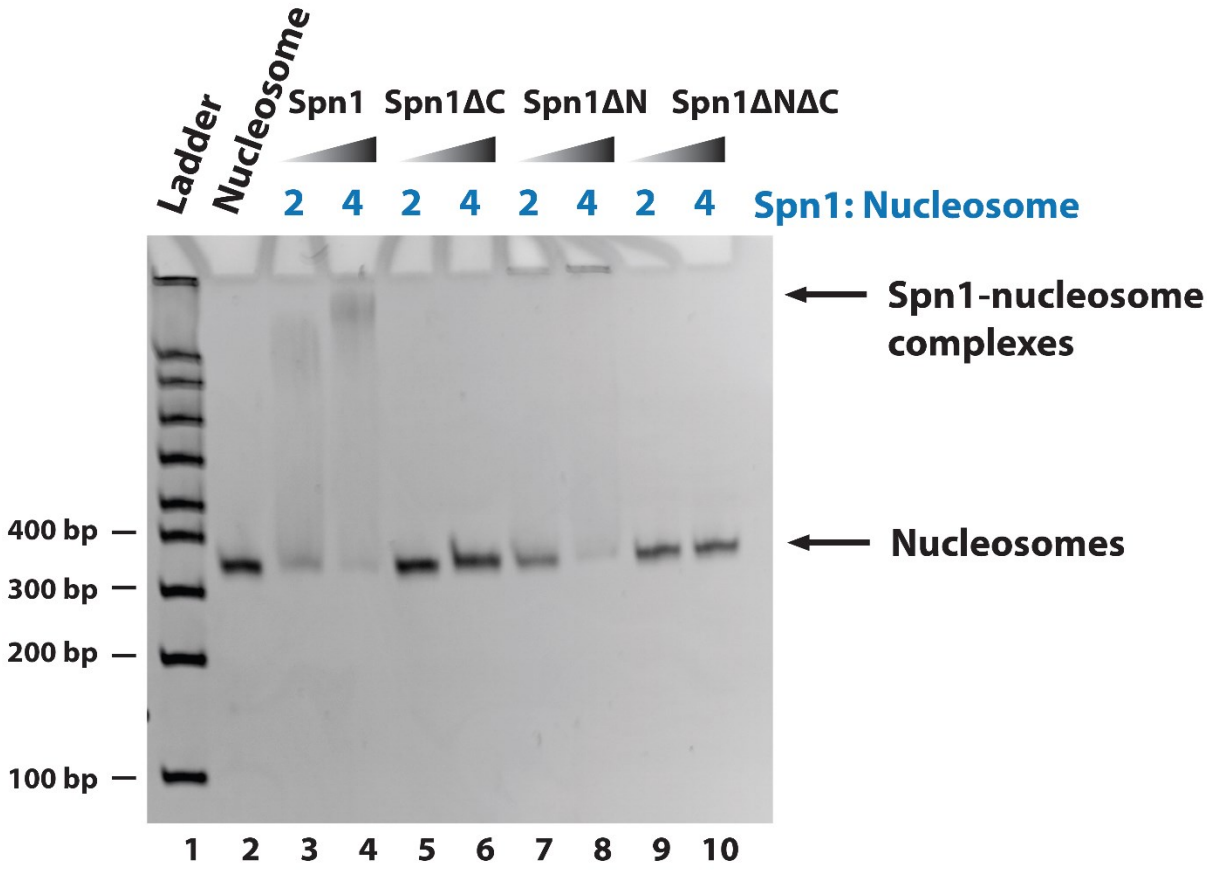

Figure 4.5. Binding of Spn1 to nucleosomes. Nucleosomes assembled with 601-147 bp DNA and *X. laevis* histones were incubated with a 2- or 4-fold molar excess of Spn1, Spn1ΔN, Spn1ΔC and Spn1ΔNΔC. Full lengthSpn1 interacts with nucleosomes, forming complexes with slower mobility (lanes 3-4). Deletion of the Spn1 C-terminal domain resulted in no binding of Spn1 to DNA (lane 5-6). The N-terminal domain of Spn1 also plays a role in nucleosome binding, as Spn1ΔN-nucleosome complexes show altered migration (lanes 7-8). There is no binding of Spn1ΔNΔC to nucleosomes (lanes 9-10). Nucleosome control (lane 2) and DNA ladder (lane 1) are shown.

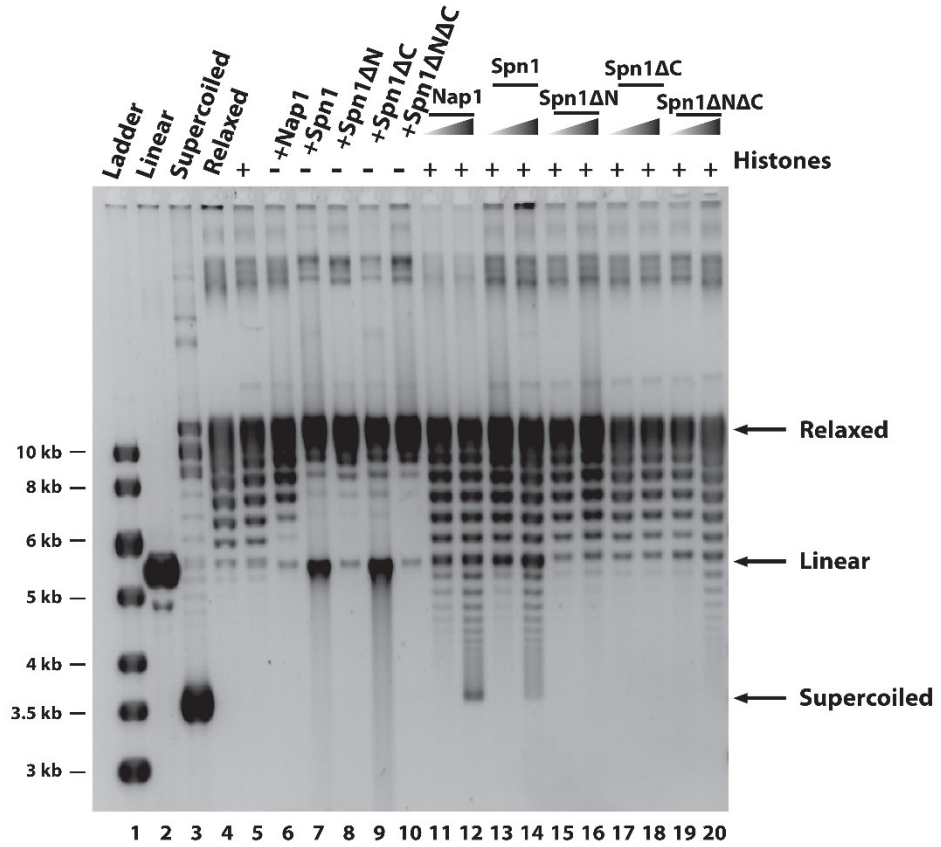

Figure 4.6. Chromatin assembly properties of Spn1. Nucleosomes were reconstituted by incubating relaxed plasmid with core histone octamer with or without Spn1 constructs. The nucleosome reconstitution was analyzed by examining formation of supercoiled DNA on an agarose gel. The molar ratio of Spn1 (lanes 13 and 14), Spn1ΔN (lanes 15 and 16), Spn1ΔC (lanes 17 and 18) and Spn1ΔNΔC (lanes 19 and 20) to histone octamer was 0.5:1 and 1:1. Nap1 was shown as a positive control (lanes 11 and 12). Controls of linear (lane 2), supercoiled (lane 3) and relaxed (lane 4) plasmids, with histones (lane 5), with only Nap1 (lane 6), Spn1 (lane 7), Spn1ΔN (lane 8), Spn1ΔC (lane 9) and Spn1ΔNΔC (lane 10) are shown. DNA ladder is indicated (lane 1).

absence of Spn1 (figure 4.6, compare lanes 13 and 14 with lane 5), indicating that Spn1 has nucleosome assembly activity. The nucleosome assembly activity of Spn1 is shown to be comparable to that of Nap1 (compare lanes 11-12 with lanes 13-14). But when either N- or C- terminal tails of Spn1 is truncated, the Spn1ΔN and Spn1ΔC constructs no longer have nucleosome assembly activity (lanes 15-18). Spn1ΔNΔC, in which both N- and C-terminal tails are truncated, also showed diminished nucleosome assembly activity (compare lanes 19 and 20 to lane 5).

We also performed plasmid supercoiling assays in the absence of magnesium ions to prevent the formation of linear plasmid products (see Chapter 5 for details). Similar results were obtained (figure 4.7). Without histone chaperones, there is low level of supercoiling (lane 7). Spn1 again showed assembly activity (lanes 12 and 13), although not as strong as yeast Nap1 (lanes 8 and 9), indicated by the enhanced DNA supercoiling compared to no chaperone control. Spn1ΔNΔC does not have chromatin assembly activity (lanes 10 and 11).

4.4.6 Spn1 recovers aggregated chromatin resulting from excess H3/H4

To confirm the chromatin assembly activity of Spn1, DNA was mixed with stoichiometric ratios of H2A/H2B and excess $(H3/H4)_2$ so an aggregation is noticed on native gel electrophoresis (figure 4.8, lane 2). H4 was labeled with donor fluorophore (Alexa488) and H2B was labeled with acceptor fluorophore (Atto647N). Reactions can then be analyzed using native gel electrophoresis. Nucleosomes reconstituted from the same

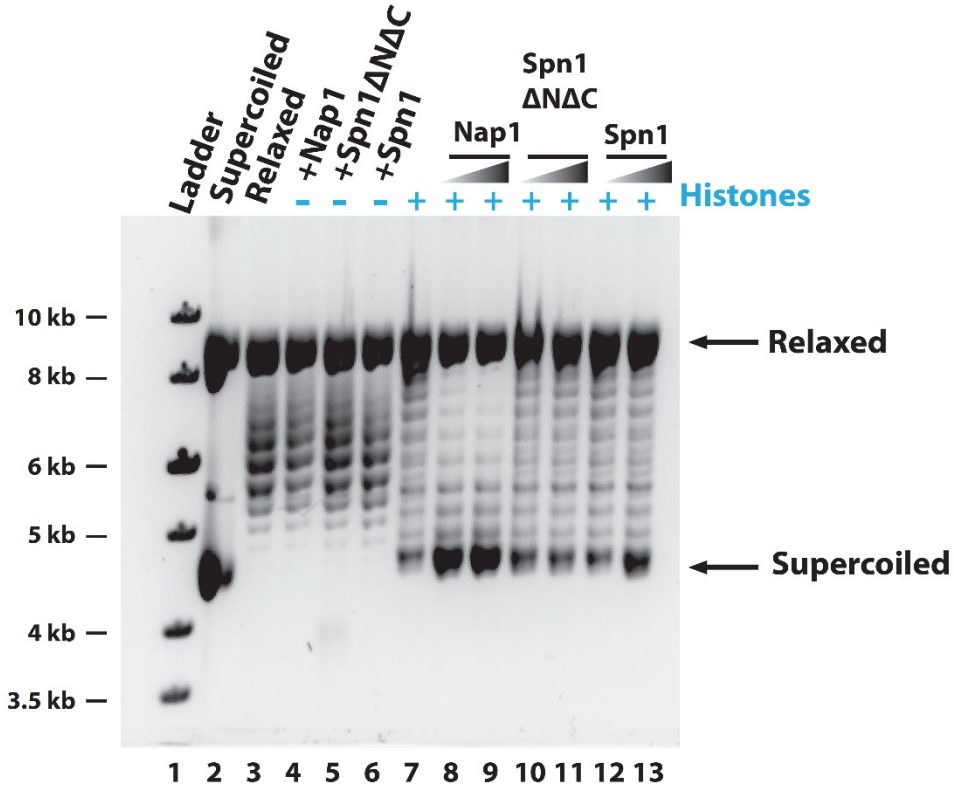

Figure 4.7. Plasmid supercoiling assay of Spn1 in the absence of magnesium ions. Spn1 has supercoiling activity (lanes 12 and 13), whereas Spn1 ΔNΔC does not (lanes 10 and 11), compared with no chaperone control (lane 7). Nap1 is shown as a positive control (lanes 8 and 9). Controls of supercoiled (lane 2) and relaxed (lane 3) plasmids, with only Nap1 (lane 4), Spn1 (lane 5), Spn1ΔNΔC (lane 6) and histones (lane 7) are shown. DNA ladder is indicated (lane 1).

fluorescently labeled histones using salt dialysis method can be used as a control. We can monitor the formation of nucleosome by examining the co-localization of donor and acceptor signals as well as the appearance of FRET signal. In the absence of histone chaperones, DNA aggregates in the presence of excess histones. If a histone chaperone has the ability to sequester the excess histones, this will lead to the formation of nucleosomes, indicated by FRET signals in the gel with the same mobility as the control nucleosomes in the gel. This assay, which we term 'RAC' (Recovery of Aggregated Chromatin) assay, is a good complementation to the plasmid supercoiling assay, as we can observe the formation of nucleosomes.

We first used DNA with stoichiometric amount of H2A/H2B and over-saturating amount of H3/H4. Spn1 was added to the DNA-histone mixture to recover the formation of nucleosome (figure 4.8, lanes 4-10). Spn1 was able to induce nucleosome formation (lane 6), yet the activity is much weaker compared to yeast Nap1.

Since our assays of Spn1-histone binding indicated that Spn1 is an H3/H4 chaperone, we hypothesized that Spn1 might be only able to recover aggregated chromatin resulting from excess H3/H4, but not excess H2A/H2B. We performed the experiment again using DNA with stoichiometric amount of H3/H4 and excess H2A/H2B. Spn1 did not induce nucleosome formation at all in this assay (figure 4.9, lanes 3-9). This further supported our previous data that Spn1 is an H3/H4-specific histone chaperone.

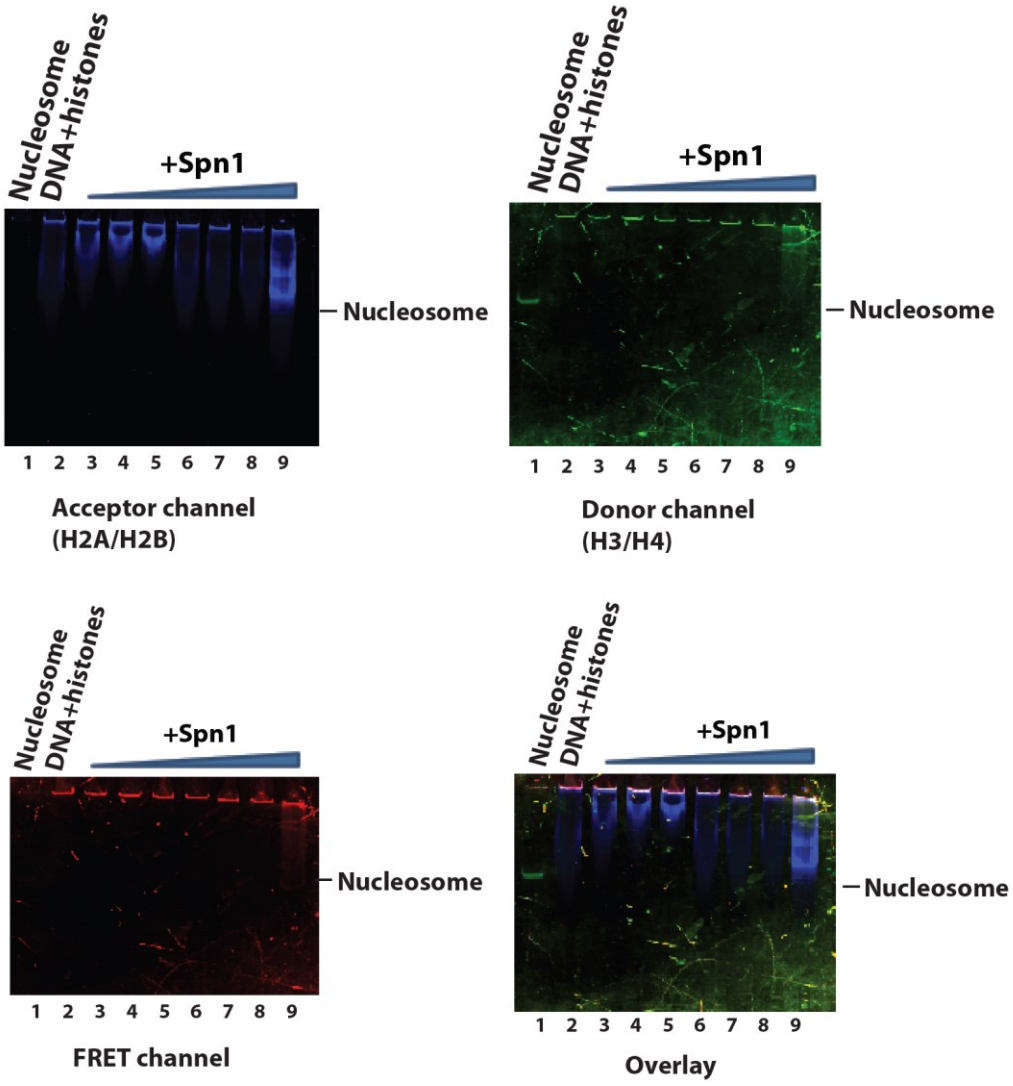

Figure 4.8. Spn1 recovers aggregated chromatin resulting from excess H3/H4. 10 nM DNA was incubated with non-saturating amount of H2A/H2BT112C-Atto647N and saturating amount of $(H3/H4E63C)_2$-Alexa488 with titration of Spn1 (lanes 4-10). With Spn1:H3/H4 ratios of 2:1, Spn1 shows optimal nucleosome assembly activity (lane 6). Reactions were analyzed using native gel electrophoresis and detected using acceptor, donor and FRET channels. Controls of aggregated chromatin with excess H3/H4 is shown (lane 2). Nucleosome control is shown (lane 1). Nap1 recovers aggregated chromatin efficiently (lane 3), and is thus used as a positive control.

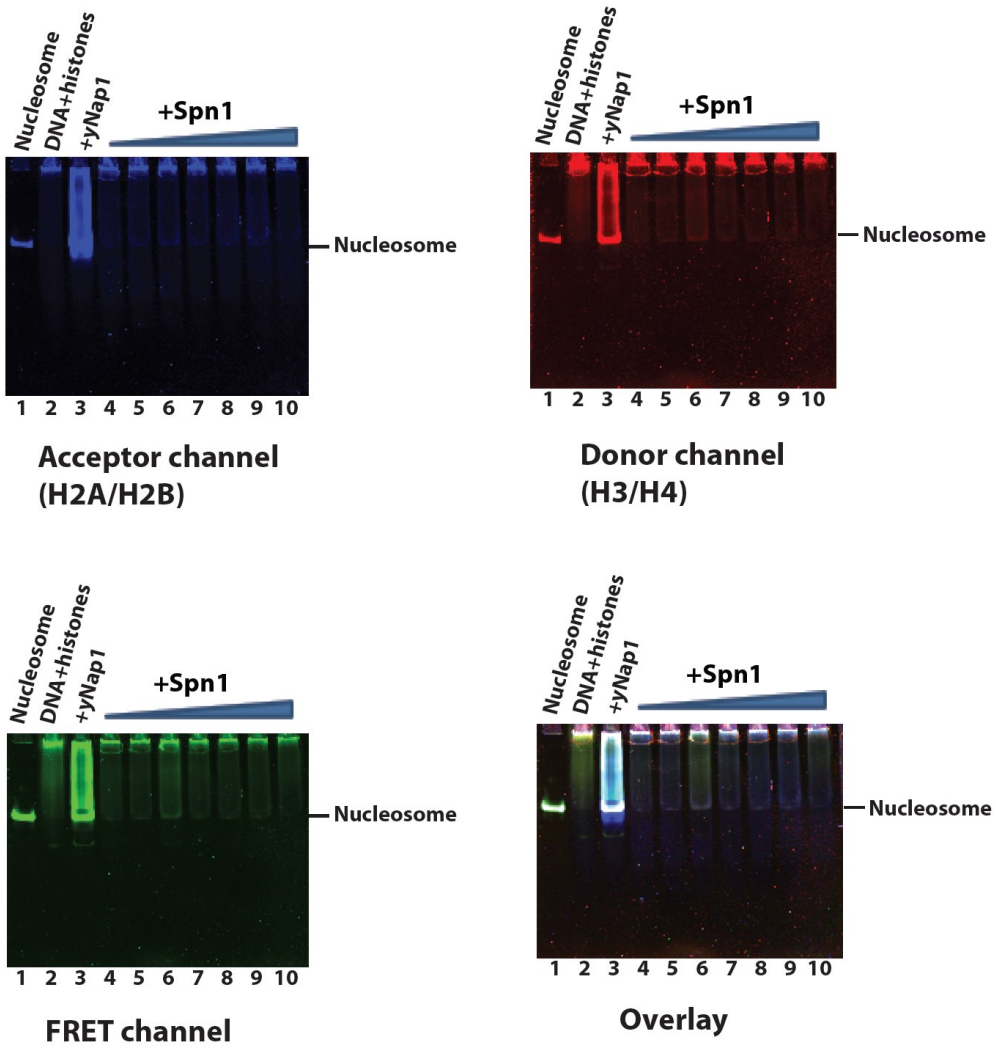

Figure 4.9. Spn1 does not recover aggregated chromatin resulting from excess H2A/H2B. 10 nM DNA was incubated with non-saturating amount of $(H3/H4E63C)_2$-Alexa488 and saturating amount of H2A/H2B-Atto647N with titration of Spn1 (lanes 3-10). Reactions were analyzed using native gel electrophoresis and detected using acceptor, donor and FRET channels. Controls of aggregated chromatin with excess H3/H4 is shown (lane 2), and Spn1 does not recover the aggregated chromatin (lane 3-10). Nucleosome control is shown (lane 1).

Taken together, our data indicate that Spn1 binds to H3/H4 specifically, and that Spn1 only recovers aggregated chromatin with excess H3/H4 but not excess H2A/H2B. We can conclude that our recovery of aggregated chromatin assay directly correlates with the histone chaperone activity of proteins, and also that it is a good assay to examine the nucleosome assembly activity of histone chaperones.

4.4.7 Spn1 binds to the histone chaperone Nap1

The observation of Spn1 interaction with chromatin components prompted us to wonder if it also interacts with chromatin regulators. Spn1 was shown to interact with histone chaperone Spt6 (McDonald et al, 2010). Here we tested for interaction with nucleosome assembly protein 1. The histone chaperone Nap1 has been shown to be important for proper nucleosome formation in yeast (Andrews et al, 2010). We investigated Spn1 interaction with Nap1 using EMSA. Nap1 was kept at a constant concentration, and Spn1 or tail deletion constructs were titrated. Complex formation was analyzed on native PAGE. As shown in figure 4.10, when full length Spn1 is added to Nap1, a distinct band with slower migration appears, accompanied by the disappearance of Nap1 band, indicating the formation of Spn1-Nap1 complex (figure 4.10.A, lanes 4-6). The addition of Spn1ΔC did not result in a disappearance of Nap1 band (figure 4.10.B, lanes 4-6), indicating that Spn1ΔC does not bind to Nap1. Both Spn1ΔN and Spn1ΔNΔC induced disappearance of Nap1 band, indicating an interaction of Spn1ΔN and Spn1ΔNΔC with Nap1 (figure 4.10.A, lanes 7-9 and figure 4.10.B, lanes 7-9). The results indicate that the binding of

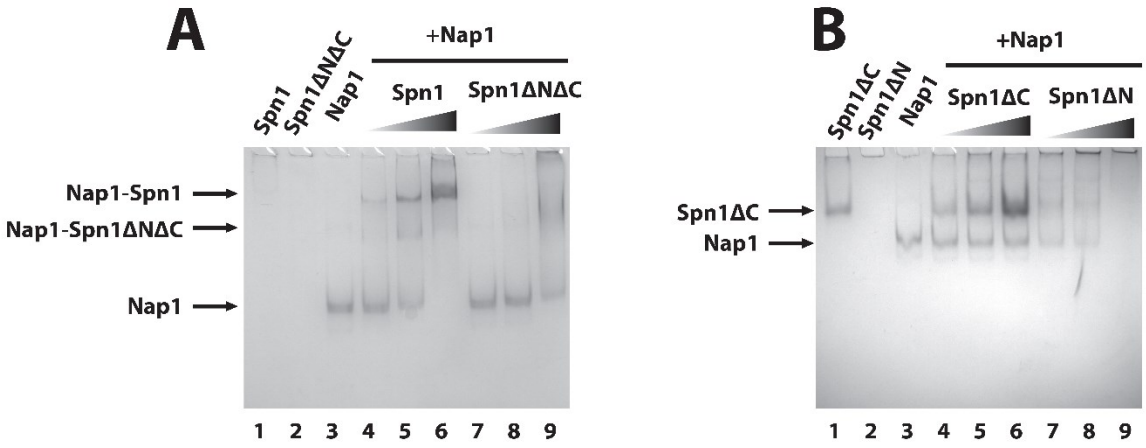

Figure 4.10. Binding of Spn1 to Nap1. 2 μM Nap1 was incubated with Spn1, Spn1ΔNΔC (figure A), Spn1ΔC or Spn1ΔN (figure B). The molar ratios of Spn1 constructs to Nap1 are 0.5:1, 1:1 and 2:1 (lanes 3-5 and 7-9). Spn1, Spn1ΔNΔC and Spn1ΔN interact with Nap1, forming complexes that migrate slower (figure A, lanes 4-6, lanes 7-9 and figure B, lanes 7-9). Spn1ΔC does not interact with Nap1 under the same conditions (figure B, lanes 4-6). Spn1 (figure A, lane 1), Spn1ΔNΔC (figure A, lane 2), Spn1ΔC (figure B, lane 1), Spn1ΔN (figure B, lane 2) and Nap1 (lane 3) controls are shown.

Spn1 to Nap1 is dependent on C-terminal tail, and is inhibited in the presence of N-terminal tail without C-terminal tail. Yet the deletion of N-terminal tail rescues the ability for Spn1ΔNΔC to bind to Nap1.

4.4.8 Spn1 forms ternary complexes with Nap1 and histones

In light of the fact that both Spn1 binds to both histones and Nap1, and also that Nap1 binds to histones, we next wanted to investigate if Spn1 can bind to Nap1 and histones simultaneously. To do that, we performed EMSA to examine the formation of Spn1-Nap1-histone triple complexes. As shown in figure 4.11, the titration of Spn1 into Nap1-H2A/B or Nap1-H3/H4 complex result in slower migrating bands (figure 4.11.A, lanes 7-9 and figure 11.B, lanes 7-9). These bands migrated slower than Nap1-H2A/H2B or Nap1-H3/H4 complexes (figure 4.11.A, lane 4 and figure 4.11.B, lane 4) and Nap1-Sp1 complex (figure 4.11.A, lane 5 and figure 4.11.B, lane 5), suggesting formation of Spn1-Nap1-H2A/B or Spn1-Nap1-H3/H4 ternary complexes. Further research needs to be carried out to confirm that Spn1 is mediating the formation of a ternary complex, and to investigate its stoichiometry.

4.5 Discussion

In this chapter, we showed that Spn1 binds to histones, DNA and nucleosomes, assembles nucleosomes, and binds to the histone chaperone Nap1. We also have an indication that Spn1 can also form ternary complexes with Nap1 and histones. Based on the Spn1-Nap1 interaction data, we hypothesize that Spn1 may function to recruit Nap1

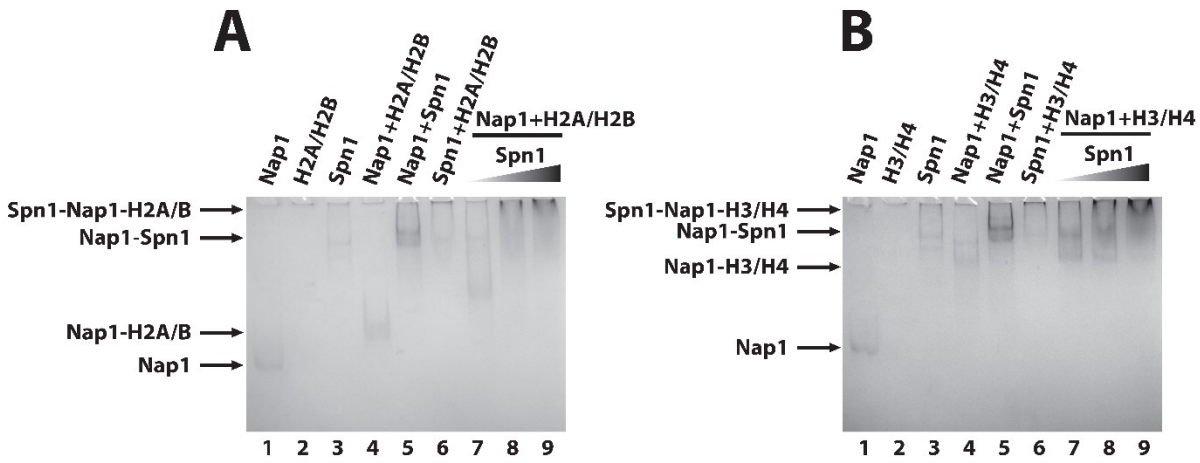

Figure 4.11. Formation of Spn1-Nap1-H2A/H2B complex (A) and Spn1-Nap1-H3/H4 complex (B). 1, 2 or 3 μM Spn1 was added to Nap1-H2A/H2B (1 μM Nap1 - 1 μM H2A/H2B) complexes (figure A, lanes 7-9) or Nap1-H3/H4 (1 μM Nap1 - 0.5 μM (H3/H4) 2) complexes (figure B, lanes 7-9). Controls of Nap1 (lane 1), H2A/H2B (figure A, lane 2), H3/H4 (figure B, lane 2), Spn1 (lane 3), Nap1-H2A/H2B complex (figure A, lane 4), Nap1-H3/H4 complex (figure B, lane 4), Nap1-Spn1 complex (lane 6) are shown. Samples were analyzed on 5% PAGE and stained with Imperial.

in vivo, which we will examine in future research. These data leads us to propose that Spn1 has an impact on chromatin dynamics by directly interacting with chromatin components and chromatin regulators. The N- and C-terminal tails of Spn1 have also been shown to be required for these activities. It was previously thought that the central domain is sufficient for the function of Spn1 in yeast (Pujari et al, 2010), yet N- and C-terminal tails of Spn1 are required for growth under several stringent conditions. Deletion of both N- and C- terminal tails of Spn1 dramatically increases the life span of yeast cells. These results lead us to re-evaluate about the roles of the N- and C- terminal tails of Spn1.

In this research, we have shown that N- and C- terminal tails are both required for its chromatin assembly property, as deletion of either the N- or C- terminal tail of Spn1 diminishes the chromatin assembly activity of Spn1. We have also shown that the C-terminal tail of Spn1 is required for binding to Nap1, whereas the N-terminal tail of Spn1 has a negative impact on Spn1-Nap1 interaction. Interestingly, deletion of both N- and C-terminal tails rescues the Spn1-Nap1 interaction. One possible explanation is that the N-terminal tail of Spn1 is highly negatively charged and thus may impair the binding of Spn1 to negatively charged Nap1.

Based on this and previous research, we propose a model for how Spn1 regulates transcription by interacting with histones and other factors and also assembling nucleosomes. In this model, Spn1 is involved in the reassembly of nucleosomes along the gene following RNAPII transcription. Since the nucleosome assembly activity of Spn1

requires the N- and C- terminal tails, Spn1ΔNΔC cannot reassemble nucleosomes as well as Spn1, resulting in elevated transcription levels.

Several factors that interact with Spn1 have been shown to also impact chromatin assembly and disassembly, including the nucleosome remodeling protein Spt6 (McDonald et al, 2010), Paf1 and SWI/SNF (Zhang et al, 2008), histone methyltransferase SET2 (Collins et al, 2007), and these factors are actively involved in transcription elongation. It is thus tempting to hypothesize that the interaction of Spn1 with these chromatin regulators can regulate the chromatin assembly activity of Spn1, which would have an impact on transcription.

In line with the model, it has been shown that activation of CYC1 gene modestly increases upon removal of both N- and C- terminal tails of Spn1 (Almeida et al., unpublished data). We will look for nucleosome deposition in Spn1 and Spn1ΔNΔC strains to validate this model. Based on this hypothesized model, we may also expect cryptic transcription of Spn1ΔNΔC strains (Ivanovska et al, 2011), which we will investigate in the future.

Combining with the *in vivo* data, this research provides strong evidence that Spn1 plays important roles in regulating chromatin dynamics, which further regulates transcription, for which N- and C- terminal tails of Spn1 are required.

CHAPTER 5

SPN1 HAS AN ASSOCIATED TOPOISOMERASE/NUCLEASE ACTIVITY[1]

5.1 Summary

While performing supercoiling assays with Spn1, to our surprise, we observed topoisomerase/nuclease activity of Spn1 samples, and this activity is correlated with the presence of the N-terminal domain of Spn1. This observation has been reproduced in the presence of Mg^{2+}. We were intrigued by the fact that Spn1 and Spn1ΔC samples have topoisomerase/nuclease activity, and decided to investigate this activity further. We found that Spn1 samples, highly purified from both *E. coli* and yeast, have topoisomerase/nuclease activity, which is either intrinsic or else tightly associated with the Spn1 protein. The activity is dependent on magnesium ions. The potential topoisomerase/nuclease activity we observed can also be associated with some Spn1-related phenotypes *in vivo*.

5.2 Introduction

Spn1 was first identified as a transcription factor that regulates post-recruitment of RNA polymerase II (Fischbeck et al, 2002). Another group also identified Spn1 as a factor

[1] Ling Zhang conducted the experiments. Ling Zhang and Karolin Luger designed the experiments and wrote this chapter.

that interacts with Spt6 (Krogan et al, 2002). SPN1 is an essential gene in yeast (Fischbeck et al, 2002). Spn1 is highly conserved throughout evolution and is a multi-functional protein. Besides its interaction with RNAPII (Zhang et al, 2008), Spn1 has also been reported to be involved in chromatin maintenance (Bortvin & Winston, 1996) and RNA processing (Hartzog et al, 1998). We recently identified Spn1 as a histone chaperone, and also interacts with nucleosomes, histone chaperone Nap1 and forms ternary complexes with histone chaperones and histones (chapter 4).

Here we report a potential novel function of Spn1 that has not been previously described. We identified the nuclease/topoisomerase activity of Spn1 samples, and this activity is dependent on the presence of Mg^{2+}, and requires the N-terminal domain of Spn1.

5.3 Materials and Methods

5.3.1 Preparation of reagents

Supercoiled DNA plasmids were amplified using the *E. coli* strain DH5α and prepared using Sigma GenElute plasmid miniprep kit. Spn1 purified from *E. coli* were prepared as described (Almeida, 2011). Plasmids were relaxed using *E. coli* topoisomerase I (Catalog # M0301), or linearized with the restriction enzymes EcoRI (Catalog # R0101) (linear #1) or NdeI (catalog # R0111) (linear #2).

For purification of Spn1 from yeast, yeast cells transfected with pJF201.1 (Spn1 subcloned into pJF201) plasmid or pJF201.2 (Spn1ΔNΔC subcloned into pJF201)

(Fischbeck et al, 2002) were incubated in YPD media to OD around 1.0, and harvested by centrifugation at 4,000 rpm for 20 min. Cell pellets were flash frozen using liquid nitrogen, and ground with a mortar and pestle. Cell lysate was then resuspended in lysis buffer containing 40 mM HEPES-KOH, pH 7.5, 10% glycerol, 350 mM NaCl, 0.1% Tween 20 and 1 mM EDTA, 1 mM DTT, 1 mM PMSF, 1 µg/ml pepstatin A and 1 µg/ml leupeptin. Cell lysate was then centrifuged at 18,000 rpm for 20 min in a JA 20 rotor, and the supernatant was centrifuged again at 28,800 rpm in a 50.2 Ti rotor. Supernatant was retrieved and incubated overnight incubation with IgG sepharose 6 fast flow (GE healthcare Catalog 17-0969-01) at 4°C. The beads were washed with lysis buffer three times, and resuspended in TEV cleavage buffer. TEV cleavage buffer contains 10 mM Tris-HCl, pH 7.5, 10% glycerol, 150 mM NaCl, 0.1% NP-40, 0.5 mM EDTA, 1 mM DTT, 1 mM PMSF, 1 µg/ml pepstatin A and 1 µg/ml leupeptin. TEV protease was added to a final concentration of 150 µg/ml, and reaction was incubated at 4°C overnight. The reaction was spun at 1,300 rpm for 1 min, and supernatant was then added to a calmodulin affinity resin (Agilent technologies, catalog 214303-52) and incubated at 4°C for overnight in CBP buffer containing 10 mM Tris-HCl, pH 7.5, 10% glycerol, 150 mM NaCl, 0.1% NP-40, 1mM $MgAc_2$, 2 mM $CaCl_2$, 1 mM imidazole, 1 mM DTT, 1 mM PMSF, 1 µg/ml pepstatin A and 1 µg/ml leupeptin. Beads were then washed three times with CBP buffer. CBP-Spn1 was eluted using buffer containing 10 mM Tris-HCl, pH 7.5, 10% glycerol, 150 mM NaCl, 0.1% NP-40, 1 mM $MgAc_2$, 2 mM EGTA, 1 mM imidazole, 1 mM DTT, 1 mM PMSF, 1 µg/ml

pepstatin A and 1 µg/ml leupeptin. See table 5.1 for comparison of purification procedures of Spn1 from *E. coli* and yeast.

5.3.2 Topoisomerase/nuclease activity assays

To test the topoisomerase/nuclease activity, 390 nmole of indicated Spn1 constructs were mixed with 500 ng of DNA plasmid in buffer containing 10 mM Tris-HCl, pH 8.0, 100 mM NaCl, 1 mM EDTA and 100 µg/µl BSA with or without 1 mM $MgCl_2$. NEB restriction buffer 4 (5 mM potassium acetate, 2 mM Tris-acetate, 1 mM Magnesium acetate, 0.1 mM DTT, pH 7.9) was also added where indicated. Total reaction volume is adjusted to 100 µl. Samples were incubated for 1, 2, 3 hours or overnight.

Phenol/chloroform extraction and ethanol precipitation was then performed. Samples were analyzed on 1% agarose gel electrophoresis.

5.3.3 Western blot analysis

Spn1 samples purified from yeast or *E. coli* were first analyzed using 15% SDS-PAGE and then transferred to a nitrocellulose membrane at 100 V for 1 hour. Western blot analysis was carried out using polyclonal anti-Spn1 antibody (1:10,000 dilution). Anti-mouse secondary antibody conjugated to IRDye 680 (LI-COR Biosciences) was used at 1:10,000 dilution and the emission was detected at 700 nm using Odyssey scanning system.

Table 5.1. Purification scheme of Spn1 from *E. coli* and yeast.

Source	*E. coli*	Yeast
Tag	In pET15b vector, His-tagged	TAP-tagged
Cell lysis	*Sonication* Lysis buffer: 100 mM Tris-HCl pH 7.5, 1 M NaCl, 10% glycerol, 50 mM imidazole and 0.5 mM PMSF	*Fluidizer* Lysis buffer: 40 mM Hepes-KOH pH 7.5, 10% glycerol, 350 mM NaCl, 0.1% tween-20, 1 mM EDTA, 1 mM DTT and protease inhibitors
1st column	*Hi-Trap chelating column* Buffer: 100 mM Tris-HCl pH 7.5, 1 M NaCl, 10% glycerol, imidazole gradient and 0.5 mM PMSF	*IgG Sepharose 6 fast flow* Binding Buffer: 40 mM Hepe-KOH pH 7.5, 10% glycerol, 350 mM NaCl, 0.1% tween-20, 1 mM EDTA, 1 mM DTT and protease inhibitors
Tag cleavage	None	IgG tag cleavage by TEV protease Buffer: 10 mM Tris-HCl pH 7.5, 10% glycerol, 150 mM NaCl, 0.1% NP-40, 0.5 mM EDTA, 1 mM DTT and protease inhibitors
2nd column	*Superdex 200 column* Buffer: 25 mM MES pH 6.5, 200 mM NaCl, 10% glycerol	*Calmodulin* Binding Buffer: 5 mM Tris-HCl pH 7.5, 5% glycerol, 75 mM NaCl, 0.05% NP-40, 1 mM $MgAc_2$, 2 mM CaCl2, 1 mM imidazole, 0.5 mM DTT and protease inhibitors
3rd column	*Hi-Trap SP cation exchange column* Buffer: 25 mM MES pH6.5, NaCl gradient and 10% glycerol	None
Final storage	Storage buffer: 50 mM Hepes-KOH pH 7.6, 10 mM EDTA, 10 mM $MgAc_2$, 100 mM KGlu, 20% glycerol, 1 mM DTT	Storage buffer: 10 mM Tris-HCl pH 7.5, 10% glycerol, 150 mM NaCl, 0.1% NP-40, 1 mM $MgAc_2$, 2 mM EGTA, 1 mM imidazole, 1 mM DTT and protease inhibitors

5.4 Results

5.4.1 The topoisomerase/nuclease activity is associated with the N-terminal domain of Spn1

While performing supercoiling assays with Spn1, we noticed that when we added Spn1 or Spn1ΔC into the reaction, pCR2.1-(CEN3+CEN6)$_4$ (Dechassa et al, 2011) plasmid was linearized, indicating that these samples contain topoisomerase/nuclease (figure 4.7, lanes 7 and 9). Spn1ΔN and Spn1ΔNΔC, which were prepared using the same approaches, did not show such activity (figure 4.7, lanes 8 and 10). This observation was reproducible in the presence of Mg^{2+}. All the Spn1 samples were highly purified with no observable contaminants (Almeida et al., unpublished data).

We also examined if other plasmid constructs can be digested by Spn1. We tested pBR322 plasmid, by incubating it with Spn1 (figure 5.1). Spn1 is also able to linearize pBR322 (lanes 10-13), indicating that the nuclease activity of Spn1 is not restricted to one specific type of plasmid.

Relaxed plasmid was used in the supercoiling assays, which can be digested by Spn1. We also examined and compared the effect of Spn1 on plasmids in different conformations, including supercoiled, relaxed and linear. We did the test on both pBR322 and pCEN8 plasmids. Spn1 is able to digest all these conformations of DNA. It digests linear DNA most efficiently (lanes 15-17 and 19-21), and digests relaxed plasmid more efficiently compared to supercoiled plasmid, indicated by more linear products (figure 5.1

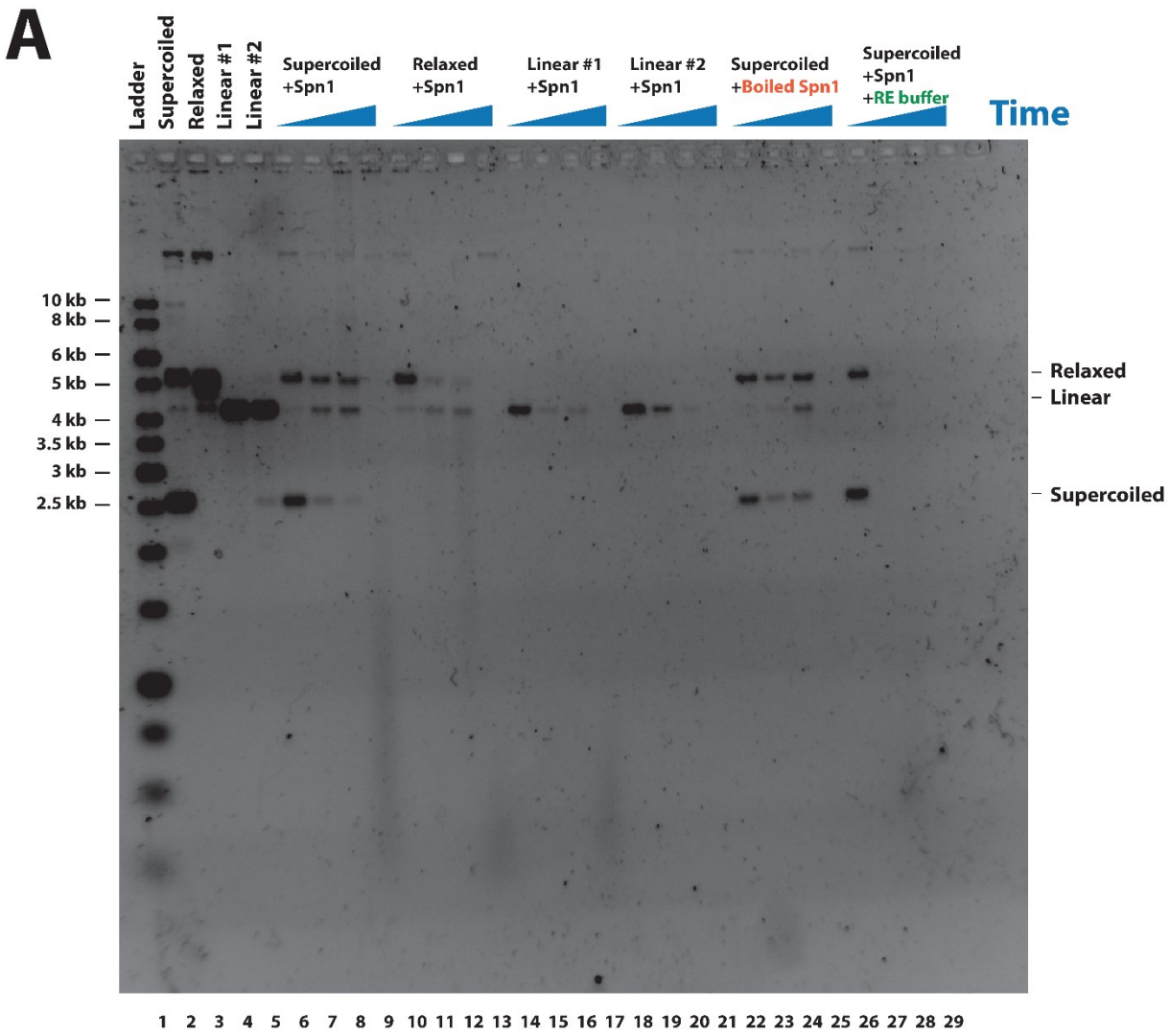
A
Ladder
Supercoiled
Relaxed
Linear #1
Linear #2
Supercoiled +Spn1
Relaxed +Spn1
Linear #1 +Spn1
Linear #2 +Spn1
Supercoiled +Boiled Spn1
Supercoiled +Spn1 +RE buffer
Time
10 kb
8 kb
6 kb
5 kb
4 kb
3.5 kb
3 kb
2.5 kb
Relaxed
Linear
Supercoiled
1 2 3 4 5 6 7 8 9 10 11 12 13 14 15 16 17 18 19 20 21 22 23 24 25 26 27 28 29

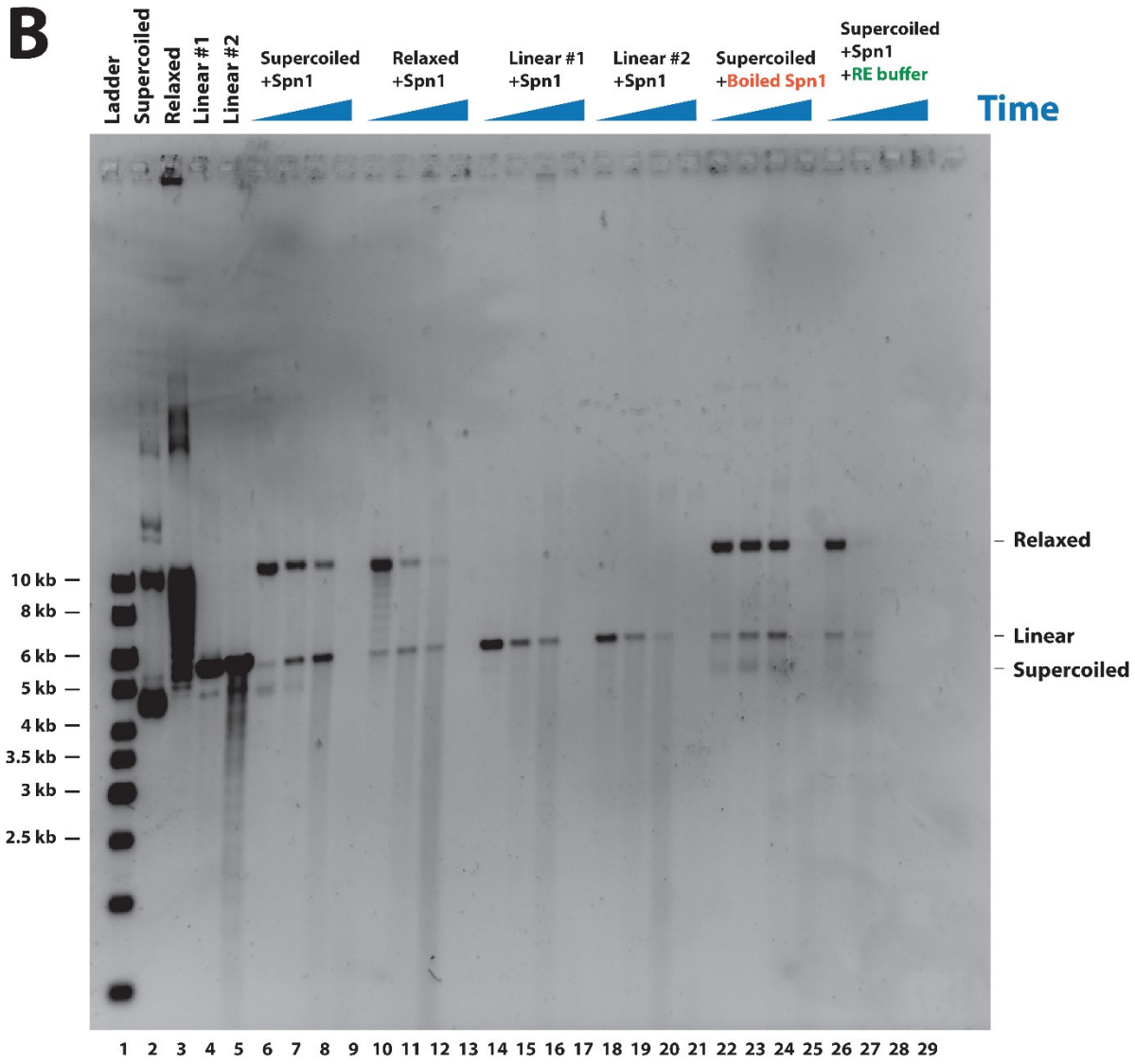

Figure 5.1. pBR322 (A) and pCEN8 (B) plasmids were digested by Spn1 samples. Spn1 was boiled for 30 min and then applied to the reaction. Supercoiled plasmid (lanes 6-9), relaxed plasmid (lanes 10-13), plasmid linearized at 2 different sites (lanes 14-17 and 18-21) were incubated with Spn1 for 0, 1, 3 and 24 hours, and the products were analyzed. Spn1 was boiled at 95°C for 30 min and also applied to the plasmid (lanes 22-25). NEB restriction enzyme buffer 4 was also added to the reaction to supply more Mg^{2+} (lanes 26-29). DNA ladder is shown (lane 1). Supercoiled, relaxed and linear plasmid controls are shown (lanes 2-5).

A and B, compare lanes 7-9 and 11-13). Boiled Spn1 has much lower nuclease activity, indicating that the nuclease activity is from Spn1 samples instead of other reagents used in the experiment. When using supercoiled plasmid as a substrate, plasmid first gets linearized (lane 7-8). With overnight incubation, DNA gets digested completely for all conformations (lanes 9, 13, 17 and 21).

All the data indicate that Spn1 samples have topoisomerase/nuclease activity. We were intrigued by the fact that Spn1 and Spn1ΔC samples have topoisomerase/nuclease activity, and decided to further investigate this activity and try to find out if this activity is intrinsic for the Spn1 protein.

5.4.2 The topoisomerase/nuclease activity is dependent on Mg^{2+}

A variety of topoisomerases and nucleases including restriction enzymes are dependent on Mg^{2+}. We examined if the topoisomerase/nuclease activity we noticed in the Spn1 samples is dependent on Mg^{2+}. We used EDTA as a chelating reagent for Mg^{2+}. After the addition of 25 mM EDTA, the topoisomerase/nuclease activity of Spn1 was inhibited (figure 5.2, lane 4-6), whereas for reactions in the absence of EDTA, Spn1 still digests the plasmid (lanes 7 and 8). Reactions without Mg^{2+} were also performed (figure 4.9), in which Spn1 does not digest the plasmid.

We also performed experiments with higher concentrations of Mg^{2+}, by supplying restriction enzyme buffer into the reactions. In these experiments, Spn1 digests the

plasmid with a much higher efficiency compared to experiments with less Mg^{2+} (figure 5.1, compare lanes 26-29 to 6-9).

These results all indicate that the topoisomerase/nuclease activity of Spn1 samples is dependent on magnesium, which is a common property of a variety of topoisomerases and nucleases.

5.4.3 Spn1 purified from yeast also has topoisomerase/nuclease activity

The Spn1 samples used above were prepared from *E. coli* cells. We reasoned that if the nuclease activity is a result of co-purified nuclease from *E. coli*, it is unlikely that we would notice the same nuclease activity in Spn1 purified from yeast. If Spn1 purified from yeast also has nuclease activity, then it is likely that this activity is intrinsic to Spn1 rather than a contaminant protein that was co-purified with Spn1.

Spn1 or Spn1ΔNΔC in pJF201.1 vector was transformed into yeast cells, and cells were tested for Spn1 expression. Western blot of purified products showed successful purification for both Spn1 and Spn1ΔNΔC (figure 5.3.A). For Spn1 purified from yeast, topoisomerase activity was detected (figure 5.3.B, lanes 5 and 6). Whereas Spn1ΔNΔC or the mock control did not digest DNA under the same conditions (lanes 7-10). Spn1 purified from yeast resulted in much lower yield compared to Spn1 purified from *E. coli*, thus not as much Spn1 had been applied to the reactions (~10 fold less). So less Spn1 is able to only relax the plasmid instead of relaxing and digesting the plasmid, thus the

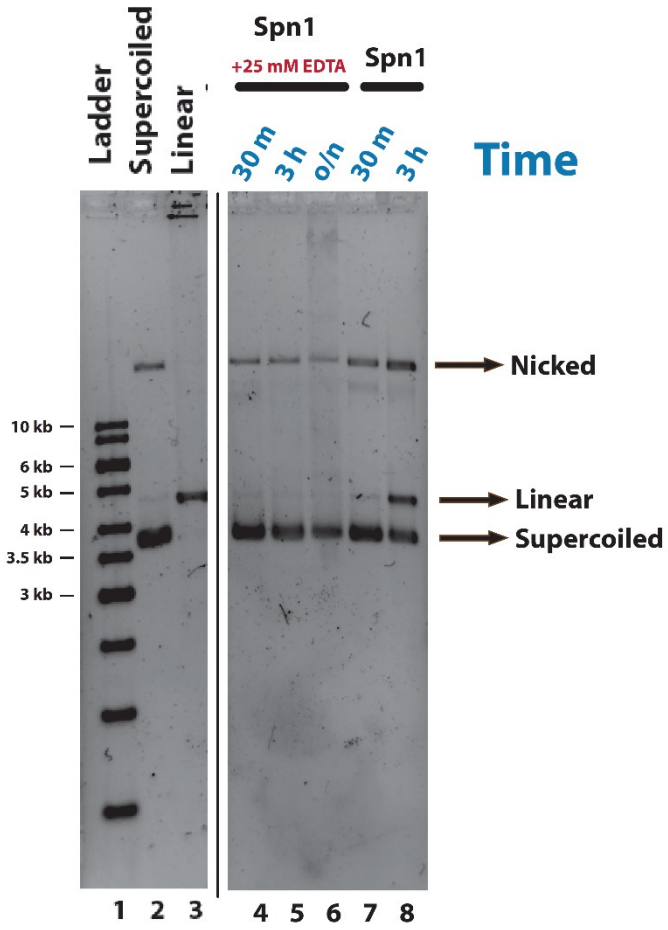

Figure 5.2. The topoisomerase/nuclease activity of Spn1 samples. Supercoiled plasmid was incubated with DNA plasmid in the presence (lanes 4-6) or absence (lanes 7 and 8) of 25 mM EDTA for 30 min, 3 h or overnight. Samples were deproteinized and analyzed on agarose gel electrophoresis. Supercoiled (lane 2) and linear (lane 3) plasmid are shown. DNA ladder is shown (lane 1).

digestion of DNA is not as efficient as Spn1 purified from *E. coli* (figure 5.3.B, compare lanes 11-12 to 5-6.).

Based on this result, we think that it is quite likely that the topoisomerase/nuclease activity of Spn1 samples is intrinsic for Spn1, given that Spn1 purified from both *E. coli* and yeast showed the activity. However, although highly unlikely, we still cannot exclude the possibility that a topoisomerase or nuclease binds tightly to Spn1 and co-purifies with Spn1 in all the purification replicates we performed.

5.5 Discussion

When investigating the properties of Spn1, we serendipitously noticed DNA relaxation and digestion by the Spn1 samples. We carried out several biochemical assays to examine the potential nuclease/topoisomerase activity of Spn1 samples.

Through our research, we found that this nuclease/topoisomerase activity has common properties as the other nucleases and topoisomerases. It is dependent on the availability of magnesium ions. With relaxed DNA, Spn1 samples also induced elevated DNA digestion. The potential nuclease/topoisomerase activity is also present in Spn1 samples purified from both *E.coli* and yeast. On the other hand, as a control, Spn1ΔNΔC samples purified using the same protocols did not exhibit nuclease/topoisomerase activity. According to the database for known interaction partners of Spn1, there is no known interaction for Spn1 with topoisomerase/nuclease (*Saccharomyces* genome database,

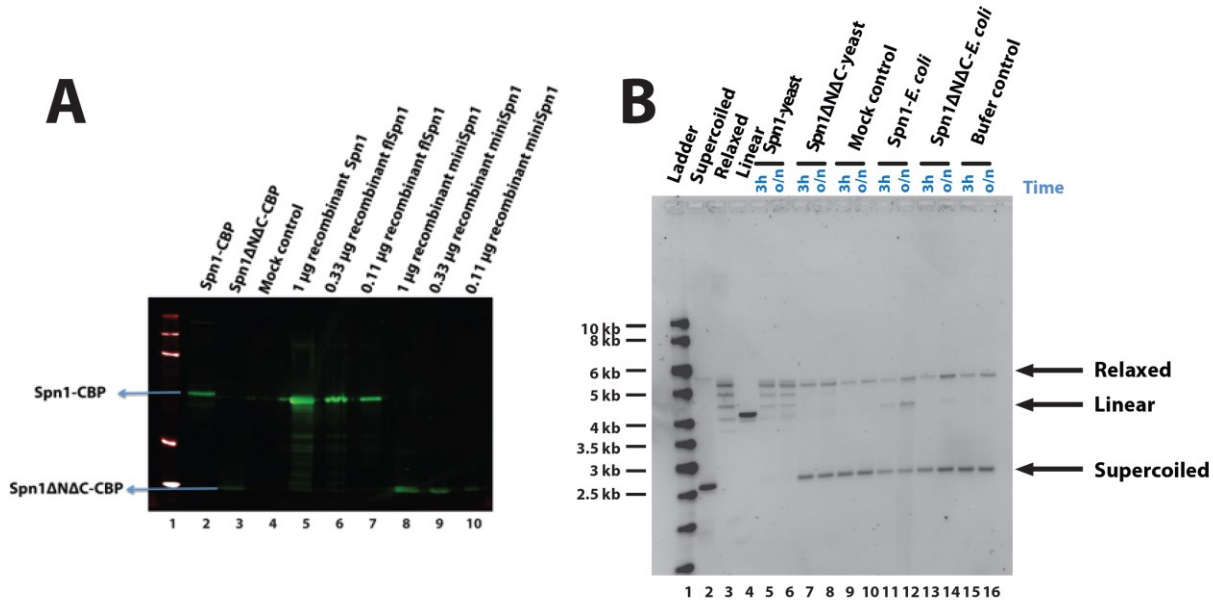

Figure 5.3. Spn1 purified from yeast has topoisomerase activity. (A) Western blot of Spn1 purified from yeast using TAP-purification. Spn1 (lane 2), Spn1ΔNΔC (lane 3) and mock controls (BY4741) (lane 4) are shown. For quantification and quality control purposes, Spn1 (lanes 5-7) and Spn1 ΔNΔC (lanes 8-10) purified from *E. coli* were also analyzed. (B) Spn1 (lanes 5 and 6) or Spn1ΔNΔC (lanes 7 and 8) or mock control (BY4741 yeast strain) (lanes 9 and 10) were purified via TAP-purification from yeast, and mixed with supercoiled DNA plasmid for 3 h or overnight. Spn1 (lanes 11 and 12) and Spn1 ΔNΔC (lanes 13 and 14) purified from *E. coli* are also included. Buffer control is also shown (lanes 15 and 16). Deproteinized samples were analyzed using agarose gel electrophoresis. Supercoiled, relaxed and linear plasmid controls are shown (lanes 2-4). DNA ladder is shown (lane 1).

Spn1/YPR133C). Based on these, it is possible that we have discovered a novel nuclease/topoisomerase activity of Spn1 that has not been described to date.

The topoisomerase/nuclease activity of Spn1 can also potentially answer questions raised by *in vivo* assays related to Spn1. Spn1 reduction-of-function yeast strains exhibit 'long' telomere phenotypes (Ungar et al, 2009), which can be a result of the reduced nuclease activity from Spn1. Telomere length is often correlated with lifespan. Agreeing with this, yeast strains in which Spn1 is replaced by Spn1ΔNΔC, which does not have nuclease activity, exhibited elongated lifespan (Almeida, 2011). In addition, this yeast strain also exhibits heat sensitivity (Sinha et al, 2008) and sensitivity to MMS (Svensson et al, 2011), a chemical that causes DNA damaging, which also indicates that Spn1 is involved in the maintenance of DNA *in vivo*.

This associated novel property of Spn1 can be of great importance. The future direction of the project would be to first confirm that this nuclease/topoisomerase activity is intrinsic to Spn1 protein. Then, whole genome assays, such as ChIP-seq can be carried out to further look at how disruption of Spn1 affects the integrity of the whole genome.

CHAPTER 6

SUMMARY AND FUTURE DIRECTIONS

This thesis focuses on the biochemical, biophysical and functional characterization of histone chaperones, and elucidates the roles of histone chaperones in the regulation of chromatin dynamics.

In the first project, we investigated the functional studies and comparison of nucleosome assembly protein family members. We focused on biochemical and biophysical characterization of Nap1, Nap2 and Set, comparing various aspects of their functions including interaction with histones and nucleosome assembly/disassembly activities.

In the second project, we focused on the identification and characterization of the interaction of Spn1 with chromatin components and chromatin regulators. Several previously unidentified interaction partners of Spn1 were identified, including histones, nucleosomes and Nap1. N- and C- terminal domains were also found to play important roles in these interactions. Also, we have observed a topoisomerase and nuclease activity associated with Spn1, which is a potential intrinsic function of Spn1 that had not been described. A summary of results with different Spn1 constructs is shown in table 6.1.

Table 6.1. Summary of functions of different Spn1 constructs. 'N.A.' indicates results not available. '++' indicates the activity of full length Spn1, whereas '+' indicates weaker activity compared to full length Spn1. '-' indicates no activity observed.

	Spn1ΔC	Spn1ΔNΔC	Spn1ΔN	flSpn1
DNA binding	-	-	+	++
Histone binding		N.A.		++
Nucleosome binding	-	-	+	++
Nucleosome assembly	-	-	+	++
Nap1 binding	-	+	+	++
Nuclease/Topoisomerase	++	-	-	++

There are a few interesting questions pending to be answered. The first question would be how nucleosome assembly protein family members carry out distinct functions despite their high degree of conservation, both in sequence and in structure. To answer this question, it is helpful to characterize the structures of nucleosome assembly protein-histone complexes. Although the structures of nucleosome assembly proteins, such as Nap1 and Set, are similar to each other, they may go under conformational changes upon binding to histones. It is through these confirmations that histone chaperones adopt different roles in chromatin regulation.

It will also be interesting to further investigate roles of N- and C- terminal domains of Spn1 in its histone chaperone and nuclease/topoisomerase activities under *in vivo* settings. Our *in vitro* assays indicated the requirement of the N- and/or the C- terminal domain(s) of Spn1 in its DNA, histone, nucleosome interaction, nucleosome assembly and associated nuclease/topoisomerase activity. Previous research indicated that N- and C- terminal domains are required for yeast to grow under more stringent conditions; also Spn1ΔNΔC strain exhibits elongated lifespan. To fully understand how the terminal domains of Spn1 are involved in chromatin regulation, we will need to look into detailed information on how nucleosome deposition and DNA regulation changes *in vivo* using Spn1 tail-deletion strains.

REFERENCES

Adachi Y, Pavlakis GN, Copeland TD (1994) Identification and characterization of SET, a nuclear phosphoprotein encoded by the translocation break point in acute undifferentiated leukemia. *J Biol Chem* **269:** 2258-2262

Almeida A (2011) Spn1, a highly conserved and essential node of RNA polymerase II dependent functions. *Biochemistry and Molecular Biology, Colorado State University, Fort collins*

Andrews AJ, Chen X, Zevin A, Stargell LA, Luger K (2010) The histone chaperone Nap1 promotes nucleosome assembly by eliminating nonnucleosomal histone DNA interactions. *Molecular cell* **37:** 834-842

Andrews AJ, Downing G, Brown K, Park YJ, Luger K (2008) A thermodynamic model for Nap1-histone interactions. *The Journal of biological chemistry* **283:** 32412-32418

Armache KJ, Garlick JD, Canzio D, Narlikar GJ, Kingston RE (2011) Structural basis of silencing: Sir3 BAH domain in complex with a nucleosome at 3.0 A resolution. *Science* **334:** 977-982

Avvakumov N, Nourani A, Cote J (2011) Histone chaperones: modulators of chromatin marks. *Molecular cell* **41:** 502-514

Bohm V, Hieb AR, Andrews AJ, Gansen A, Rocker A, Toth K, Luger K, Langowski J (2011) Nucleosome accessibility governed by the dimer/tetramer interface. *Nucleic Acids Res* **39:** 3093-3102

Bortvin A, Winston F (1996) Evidence that Spt6p controls chromatin structure by a direct interaction with histones. *Science* **272:** 1473-1476

Bowman A, Ward R, Wiechens N, Singh V, El-Mkami H, Norman DG, Owen-Hughes T (2011) The histone chaperones Nap1 and Vps75 bind histones H3 and H4 in a tetrameric conformation. *Mol Cell* **41:** 398-408

Burgess RJ, Zhang Z (2013) Histone chaperones in nucleosome assembly and human disease. *Nature structural & molecular biology* **20:** 14-22

Cairns BR (2005) Chromatin remodeling complexes: strength in diversity, precision through specialization. *Current opinion in genetics & development* **15:** 185-190

Calvert ME, Keck KM, Ptak C, Shabanowitz J, Hunt DF, Pemberton LF (2008) Phosphorylation by casein kinase 2 regulates Nap1 localization and function. *Mol Cell Biol* **28:** 1313-1325

Chakravarthy S, Gundimella SK, Caron C, Perche PY, Pehrson JR, Khochbin S, Luger K (2005) Structural characterization of the histone variant macroH2A. *Mol Cell Biol* **25:** 7616-7624

Cheung V, Chua G, Batada NN, Landry CR, Michnick SW, Hughes TR, Winston F (2008) Chromatin- and transcription-related factors repress transcription from within coding regions throughout the Saccharomyces cerevisiae genome. *PLoS biology* **6:** e277

Choi YC, Gu W, Hecht NB, Feinberg AP, Chae CB (1996) Molecular cloning of mouse somatic and testis-specific H2B histone genes containing a methylated CpG island. *DNA and cell biology* **15:** 495-504

Choy MK, Movassagh M, Goh HG, Bennett MR, Down TA, Foo RS (2010) Genome-wide conserved consensus transcription factor binding motifs are hyper-methylated. *BMC Genomics* **11:** 519

Clapier CR, Cairns BR (2009) The biology of chromatin remodeling complexes. *Annu Rev Biochem* **78:** 273-304

Clapier CR, Chakravarthy S, Petosa C, Fernandez-Tornero C, Luger K, Muller CW (2008) Structure of the Drosophila nucleosome core particle highlights evolutionary constraints on the H2A-H2B histone dimer. *Proteins* **71:** 1-7

Collins SR, Miller KM, Maas NL, Roguev A, Fillingham J, Chu CS, Schuldiner M, Gebbia M, Recht J, Shales M, Ding H, Xu H, Han J, Ingvarsdottir K, Cheng B, Andrews B, Boone C, Berger SL, Hieter P, Zhang Z, Brown GW, Ingles CJ, Emili A, Allis CD, Toczyski DP, Weissman JS, Greenblatt JF, Krogan NJ (2007) Functional dissection of protein complexes involved in yeast chromosome biology using a genetic interaction map. *Nature* **446:** 806-810

Craig JM, Wong NC (2011) Epigenetics: A Reference Manual

D'Arcy S, Martin KW, Panchenko T, Chen X, Bergeron S, Stargell LA, Black BE, Luger K (2013) Chaperone Nap1 shields histone surfaces used in a nucleosome and can put H2A-H2B in an unconventional tetrameric form. *Molecular cell* **51:** 662-677

Daganzo SM, Erzberger JP, Lam WM, Skordalakes E, Zhang R, Franco AA, Brill SJ, Adams PD, Berger JM, Kaufman PD (2003) Structure and function of the conserved core of histone deposition protein Asf1. *Current biology : CB* **13:** 2148-2158

Dechassa ML, Wyns K, Li M, Hall MA, Wang MD, Luger K (2011) Structure and Scm3-mediated assembly of budding yeast centromeric nucleosomes. *Nat Commun* **2:** 313

Demeler B, van Holde KE (2004) Sedimentation velocity analysis of highly heterogeneous systems. *Anal Biochem* **335:** 279-288

Diebold ML, Koch M, Loeliger E, Cura V, Winston F, Cavarelli J, Romier C (2010) The structure of an Iws1/Spt6 complex reveals an interaction domain conserved in TFIIS, Elongin A and Med26. *EMBO J* **29:** 3979-3991

Dutta S, Akey IV, Dingwall C, Hartman KL, Laue T, Nolte RT, Head JF, Akey CW (2001) The crystal structure of nucleoplasmin-core: implications for histone binding and nucleosome assembly. *Molecular cell* **8:** 841-853

Dyer PN, Edayathumangalam RS, White CL, Bao Y, Chakravarthy S, Muthurajan UM, Luger K (2004) Reconstitution of nucleosome core particles from recombinant histones and DNA. *Methods Enzymol* **375:** 23-44

Eitoku M, Sato L, Senda T, Horikoshi M (2008) Histone chaperones: 30 years from isolation to elucidation of the mechanisms of nucleosome assembly and disassembly. *Cellular and molecular life sciences : CMLS* **65:** 414-444

Elsasser SJ (2013) A common structural theme in histone chaperones mimics interhistone contacts. *Trends Biochem Sci* **38:** 333-336

Fan Z, Beresford PJ, Oh DY, Zhang D, Lieberman J (2003) Tumor suppressor NM23-H1 is a granzyme A-activated DNase during CTL-mediated apoptosis, and the nucleosome assembly protein SET is its inhibitor. *Cell* **112:** 659-672

Fischbeck JA, Kraemer SM, Stargell LA (2002) SPN1, a conserved gene identified by suppression of a postrecruitment-defective yeast TATA-binding protein mutant. *Genetics* **162:** 1605-1616

Frenster JH, Allfrey VG, Mirsky AE (1963) Repressed and Active Chromatin Isolated from Interphase Lymphocytes. *Proc Natl Acad Sci U S A* **50:** 1026-1032

Fujii-Nakata T, Ishimi Y, Okuda A, Kikuchi A (1992) Functional analysis of nucleosome assembly protein, NAP-1. The negatively charged COOH-terminal region is not necessary for the intrinsic assembly activity. *J Biol Chem* **267:** 20980-20986

Gill J, Yogavel M, Kumar A, Belrhali H, Jain SK, Rug M, Brown M, Maier AG, Sharma A (2009) Crystal structure of malaria parasite nucleosome assembly protein: distinct modes of protein localization and histone recognition. *J Biol Chem* **284:** 10076-10087

Gouet P, Courcelle E, Stuart DI, Metoz F (1999) ESPript: analysis of multiple sequence alignments in PostScript. *Bioinformatics* **15:** 305-308

Govin J, Caron C, Lestrat C, Rousseaux S, Khochbin S (2004) The role of histones in chromatin remodelling during mammalian spermiogenesis. *European journal of biochemistry / FEBS* **271:** 3459-3469

Govin J, Escoffier E, Rousseaux S, Kuhn L, Ferro M, Thevenon J, Catena R, Davidson I, Garin J, Khochbin S, Caron C (2007) Pericentric heterochromatin reprogramming by new histone variants during mouse spermiogenesis. *J Cell Biol* **176:** 283-294

Grewal SI, Elgin SC (2002) Heterochromatin: new possibilities for the inheritance of structure. *Curr Opin Genet Dev* **12:** 178-187

Hansen JC (2002) Conformational dynamics of the chromatin fiber in solution: determinants, mechanisms, and functions. *Annu Rev Biophys Biomol Struct* **31:** 361-392

Hansen JC, Nyborg JK, Luger K, Stargell LA (2010) Histone chaperones, histone acetylation, and the fluidity of the chromogenome. *J Cell Physiol* **224:** 289-299

Harp JM, Hanson BL, Timm DE, Bunick GJ (2000) Asymmetries in the nucleosome core particle at 2.5 A resolution. *Acta Crystallogr D Biol Crystallogr* **56:** 1513-1534

Hartzog GA, Wada T, Handa H, Winston F (1998) Evidence that Spt4, Spt5, and Spt6 control transcription elongation by RNA polymerase II in Saccharomyces cerevisiae. *Genes Dev* **12:** 357-369

Henikoff S (2010) Summary: The nucleus--a close-knit community of dynamic structures. *Cold Spring Harb Symp Quant Biol* **75:** 607-615

Henikoff S, Furuyama T, Ahmad K (2004) Histone variants, nucleosome assembly and epigenetic inheritance. *Trends in genetics : TIG* **20:** 320-326

Hieb AR, D'Arcy S, Kramer MA, White AE, Luger K (2012) Fluorescence strategies for high-throughput quantification of protein interactions. *Nucleic Acids Res* **40:** e33

Hsu TC (1962) Differential rate in RNA synthesis between euchromatin and heterochromatin. *Exp Cell Res* **27:** 332-334

Hu H, Liu Y, Wang M, Fang J, Huang H, Yang N, Li Y, Wang J, Yao X, Shi Y, Li G, Xu RM (2011) Structure of a CENP-A-histone H4 heterodimer in complex with chaperone HJURP. *Genes & development* **25:** 901-906

Hu RJ, Lee MP, Johnson LA, Feinberg AP (1996) A novel human homologue of yeast nucleosome assembly protein, 65 kb centromeric to the p57KIP2 gene, is biallelically expressed in fetal and adult tissues. *Human molecular genetics* **5:** 1743-1748

Hwang I, Chae CB (1989) S-phase-specific transcription regulatory elements are present in a replication-independent testis-specific H2B histone gene. *Molecular and cellular biology* **9:** 1005-1013

Ishimi Y, Yasuda H, Hirosumi J, Hanaoka F, Yamada M (1983) A Protein Which Facilitates Assembly Of Nucleosome-Like Structures Invitro In Mammalian-Cells. *Journal of biochemistry* **94:** 735-744

Ito T, Tyler JK, Kadonaga JT (1997) Chromatin assembly factors: a dual function in nucleosome formation and mobilization? *Genes Cells* **2:** 593-600

Ivanovska I, Jacques PE, Rando OJ, Robert F, Winston F (2011) Control of chromatin structure by spt6: different consequences in coding and regulatory regions. *Mol Cell Biol* **31:** 531-541

Jin J, Cai Y, Li B, Conaway RC, Workman JL, Conaway JW, Kusch T (2005) In and out: histone variant exchange in chromatin. *Trends in biochemical sciences* **30:** 680-687

Kamakaka RT, Biggins S (2005) Histone variants: deviants? *Genes & development* **19:** 295-310

Kaplan CD, Laprade L, Winston F (2003) Transcription elongation factors repress transcription initiation from cryptic sites. *Science* **301:** 1096-1099

Kepert JF, Mazurkiewicz J, Heuvelman GL, Toth KF, Rippe K (2005) NAP1 modulates binding of linker histone H1 to chromatin and induces an extended chromatin fiber conformation. *J Biol Chem* **280:** 34063-34072

Kim TH, Barrera LO, Zheng M, Qu C, Singer MA, Richmond TA, Wu Y, Green RD, Ren B (2005) A high-resolution map of active promoters in the human genome. *Nature* **436:** 876-880

Kleinschmidt JA, Seiter A, Zentgraf H (1990) Nucleosome assembly in vitro: separate histone transfer and synergistic interaction of native histone complexes purified from nuclei of Xenopus laevis oocytes. *EMBO J* **9:** 1309-1318

Kouzarides T (2007) Chromatin modifications and their function. *Cell* **128:** 693-705

Krogan NJ, Kim M, Ahn SH, Zhong G, Kobor MS, Cagney G, Emili A, Shilatifard A, Buratowski S, Greenblatt JF (2002) RNA polymerase II elongation factors of Saccharomyces cerevisiae: a targeted proteomics approach. *Mol Cell Biol* **22:** 6979-6992

Laskey RA, Honda BM, Mills AD, Finch JT (1978) Nucleosomes are assembled by an acidic protein which binds histones and transfers them to DNA. *Nature* **275:** 416-420

Li L, Ye H, Guo H, Yin Y (2010) Arabidopsis IWS1 interacts with transcription factor BES1 and is involved in plant steroid hormone brassinosteroid regulated gene expression. *Proc Natl Acad Sci U S A* **107:** 3918-3923

Li M, Makkinje A, Damuni Z (1996) The myeloid leukemia-associated protein SET is a potent inhibitor of protein phosphatase 2A. *J Biol Chem* **271:** 11059-11062

Li M, Strand D, Krehan A, Pyerin W, Heid H, Neumann B, Mechler BM (1999) Casein kinase 2 binds and phosphorylates the nucleosome assembly protein-1 (NAP1) in Drosophila melanogaster. *J Mol Biol* **293:** 1067-1084

Lindstrom DL, Squazzo SL, Muster N, Burckin TA, Wachter KC, Emigh CA, McCleery JA, Yates JR, 3rd, Hartzog GA (2003) Dual roles for Spt5 in pre-mRNA processing and transcription elongation revealed by identification of Spt5-associated proteins. *Mol Cell Biol* **23:** 1368-1378

Loven MA, Muster N, Yates JR, Nardulli AM (2003) A novel estrogen receptor alpha-associated protein, template-activating factor Ibeta, inhibits acetylation and transactivation. *Mol Endocrinol* **17:** 67-78

Lowary PT, Widom J (1998) New DNA sequence rules for high affinity binding to histone octamer and sequence-directed nucleosome positioning. *Journal of molecular biology* **276:** 19-42

Loyola A, Almouzni G (2004) Histone chaperones, a supporting role in the limelight. *Biochimica et biophysica acta* **1677:** 3-11

Lu X, Simon MD, Chodaparambil JV, Hansen JC, Shokat KM, Luger K (2008) The effect of H3K79 dimethylation and H4K20 trimethylation on nucleosome and chromatin structure. *Nat Struct Mol Biol* **15:** 1122-1124

Luebben WR, Sharma N, Nyborg JK (2010) Nucleosome eviction and activated transcription require p300 acetylation of histone H3 lysine 14. *Proceedings of the National Academy of Sciences of the United States of America* **107:** 19254-19259

Luger K (2003) Structure and dynamic behavior of nucleosomes. *Curr Opin Genet Dev* **13:** 127-135

Luger K, Dechassa ML, Tremethick DJ (2012) New insights into nucleosome and chromatin structure: an ordered state or a disordered affair? *Nat Rev Mol Cell Biol* **13:** 436-447

Luger K, Hansen JC (2005) Nucleosome and chromatin fiber dynamics. *Curr Opin Struct Biol* **15:** 188-196

Luger K, Mader AW, Richmond RK, Sargent DF, Richmond TJ (1997) Crystal structure of the nucleosome core particle at 2.8 A resolution. *Nature* **389:** 251-260

Lusser A, Kadonaga JT (2004) Strategies for the reconstitution of chromatin. *Nat Methods* **1:** 19-26

Makde RD, England JR, Yennawar HP, Tan S (2010) Structure of RCC1 chromatin factor bound to the nucleosome core particle. *Nature* **467:** 562-566

Matsumoto K, Nagata K, Ui M, Hanaoka F (1993) Template activating factor I, a novel host factor required to stimulate the adenovirus core DNA replication. *J Biol Chem* **268:** 10582-10587

McBryant SJ, Park YJ, Abernathy SM, Laybourn PJ, Nyborg JK, Luger K (2003) Preferential binding of the histone (H3-H4)2 tetramer by NAP1 is mediated by the amino-terminal histone tails. *J Biol Chem* **278:** 44574-44583

McBryant SJ, Peersen OB (2004) Self-association of the yeast nucleosome assembly protein 1. *Biochemistry* **43:** 10592-10599

McDonald SM, Close D, Xin H, Formosa T, Hill CP (2010) Structure and biological importance of the Spn1-Spt6 interaction, and its regulatory role in nucleosome binding. *Molecular cell* **40:** 725-735

Moore LD, Le T, Fan G (2013) DNA methylation and its basic function. *Neuropsychopharmacology* **38:** 23-38

Muse GW, Gilchrist DA, Nechaev S, Shah R, Parker JS, Grissom SF, Zeitlinger J, Adelman K (2007) RNA polymerase is poised for activation across the genome. *Nat Genet* **39:** 1507-1511

Muto S, Senda M, Akai Y, Sato L, Suzuki T, Nagai R, Senda T, Horikoshi M (2007) Relationship between the structure of SET/TAF-Ibeta/INHAT and its histone chaperone activity. *Proc Natl Acad Sci U S A* **104:** 4285-4290

Natsume R, Eitoku M, Akai Y, Sano N, Horikoshi M, Senda T (2007) Structure and function of the histone chaperone CIA/ASF1 complexed with histones H3 and H4. *Nature* **446:** 338-341

Ohara-Imaizumi M, Nakamichi Y, Nishiwaki C, Nagamatsu S (2002) Transduction of MIN6 beta cells with TAT-syntaxin SNARE motif inhibits insulin exocytosis in biphasic insulin release in a distinct mechanism analyzed by evanescent wave microscopy. *J Biol Chem* **277:** 50805-50811

Okuwaki M, Nagata K (1998) Template activating factor-I remodels the chromatin structure and stimulates transcription from the chromatin template. *J Biol Chem* **273:** 34511-34518

Olson EJ, Buhlmann P (2011) Getting more out of a Job plot: determination of reactant to product stoichiometry in cases of displacement reactions and n:n complex formation. *J Org Chem* **76:** 8406-8412

Oudet P, Gross-Bellard M, Chambon P (1975) Electron microscopic and biochemical evidence that chromatin structure is a repeating unit. *Cell* **4:** 281-300

Park YJ, Chodaparambil JV, Bao Y, McBryant SJ, Luger K (2005) Nucleosome assembly protein 1 exchanges histone H2A-H2B dimers and assists nucleosome sliding. *J Biol Chem* **280:** 1817-1825

Park YJ, Luger K (2006a) Structure and function of nucleosome assembly proteins. *Biochemistry and cell biology = Biochimie et biologie cellulaire* **84:** 549-558

Park YJ, Luger K (2006b) The structure of nucleosome assembly protein 1. *Proceedings of the National Academy of Sciences of the United States of America* **103:** 1248-1253

Park YJ, McBryant SJ, Luger K (2008a) A beta-hairpin comprising the nuclear localization sequence sustains the self-associated states of nucleosome assembly protein 1. *Journal of molecular biology* **375:** 1076-1085

Park YJ, Sudhoff KB, Andrews AJ, Stargell LA, Luger K (2008b) Histone chaperone specificity in Rtt109 activation. *Nat Struct Mol Biol* **15:** 957-964

Pujari V, Radebaugh CA, Chodaparambil JV, Muthurajan UM, Almeida AR, Fischbeck JA, Luger K, Stargell LA (2010) The transcription factor Spn1 regulates gene expression via a highly conserved novel structural motif. *J Mol Biol* **404:** 1-15

Regnard C, Desbruyeres E, Huet JC, Beauvallet C, Pernollet JC, Edde B (2000) Polyglutamylation of nucleosome assembly proteins. *J Biol Chem* **275:** 15969-15976

Rodriguez P, Pelletier J, Price GB, Zannis-Hadjopoulos M (2000) NAP-2: histone chaperone function and phosphorylation state through the cell cycle. *J Mol Biol* **298:** 225-238

Rogner UC, Spyropoulos DD, Le Novere N, Changeux JP, Avner P (2000) Control of neurulation by the nucleosome assembly protein-1-like 2. *Nature genetics* **25:** 431-435

Seo SB, McNamara P, Heo S, Turner A, Lane WS, Chakravarti D (2001) Regulation of histone acetylation and transcription by INHAT, a human cellular complex containing the set oncoprotein. *Cell* **104:** 119-130

Sharma N, Nyborg JK (2008) The coactivators CBP/p300 and the histone chaperone NAP1 promote transcription-independent nucleosome eviction at the HTLV-1 promoter. *Proc Natl Acad Sci U S A* **105:** 7959-7963

Silva AC, Xu X, Kim HS, Fillingham J, Kislinger T, Mennella TA, Keogh MC (2012) The replication-independent histone H3-H4 chaperones HIR, ASF1, and RTT106 co-operate to maintain promoter fidelity. *The Journal of biological chemistry* **287:** 1709-1718

Sinha H, David L, Pascon RC, Clauder-Munster S, Krishnakumar S, Nguyen M, Shi G, Dean J, Davis RW, Oefner PJ, McCusker JH, Steinmetz LM (2008) Sequential elimination of major-effect contributors identifies additional quantitative trait loci conditioning high-temperature growth in yeast. *Genetics* **180:** 1661-1670

Suto RK, Clarkson MJ, Tremethick DJ, Luger K (2000) Crystal structure of a nucleosome core particle containing the variant histone H2A.Z. *Nat Struct Biol* **7:** 1121-1124

Svejstrup JQ (2004) The RNA polymerase II transcription cycle: cycling through chromatin. *Biochim Biophys Acta* **1677:** 64-73

Svensson JP, Pesudo LQ, Fry RC, Adeleye YA, Carmichael P, Samson LD (2011) Genomic phenotyping of the essential and non-essential yeast genome detects novel pathways for alkylation resistance. *BMC Syst Biol* **5:** 157

Tachiwana H, Kagawa W, Osakabe A, Kawaguchi K, Shiga T, Hayashi-Takanaka Y, Kimura H, Kurumizaka H (2010) Structural basis of instability of the nucleosome containing a testis-specific histone variant, human H3T. *Proc Natl Acad Sci U S A* **107:** 10454-10459

Tachiwana H, Osakabe A, Kimura H, Kurumizaka H (2008) Nucleosome formation with the testis-specific histone H3 variant, H3t, by human nucleosome assembly proteins in vitro. *Nucleic Acids Res* **36:** 2208-2218

Talbert PB, Henikoff S (2010) Histone variants--ancient wrap artists of the epigenome. *Nature reviews Molecular cell biology* **11:** 264-275

Tan M, Luo H, Lee S, Jin F, Yang JS, Montellier E, Buchou T, Cheng Z, Rousseaux S, Rajagopal N, Lu Z, Ye Z, Zhu Q, Wysocka J, Ye Y, Khochbin S, Ren B, Zhao Y (2011) Identification of 67 histone marks and histone lysine crotonylation as a new type of histone modification. *Cell* **146:** 1016-1028

Tan S, Davey CA (2011) Nucleosome structural studies. *Curr Opin Struct Biol* **21:** 128-136

Tang Y, Meeth K, Jiang E, Luo C, Marmorstein R (2008) Structure of Vps75 and implications for histone chaperone function. *Proc Natl Acad Sci U S A* **105:** 12206-12211

Thompson JD, Higgins DG, Gibson TJ (1994) CLUSTAL W: improving the sensitivity of progressive multiple sequence alignment through sequence weighting, position-specific gap penalties and weight matrix choice. *Nucleic Acids Res* **22:** 4673-4680

Tsunaka Y, Kajimura N, Tate S, Morikawa K (2005) Alteration of the nucleosomal DNA path in the crystal structure of a human nucleosome core particle. *Nucleic Acids Res* **33:** 3424-3434

Ungar L, Yosef N, Sela Y, Sharan R, Ruppin E, Kupiec M (2009) A genome-wide screen for essential yeast genes that affect telomere length maintenance. *Nucleic Acids Res* **37:** 3840-3849

Vasudevan D, Chua EY, Davey CA (2010) Crystal structures of nucleosome core particles containing the '601' strong positioning sequence. *J Mol Biol* **403:** 1-10

von Lindern M, van Baal S, Wiegant J, Raap A, Hagemeijer A, Grosveld G (1992) Can, a putative oncogene associated with myeloid leukemogenesis, may be activated by fusion of its 3' half to different genes: characterization of the set gene. *Molecular and cellular biology* **12:** 3346-3355

White CL, Suto RK, Luger K (2001) Structure of the yeast nucleosome core particle reveals fundamental changes in internucleosome interactions. *EMBO J* **20:** 5207-5218

Winkler DD, Luger K, Hieb AR (2012) Quantifying chromatin-associated interactions: the HI-FI system. *Methods in enzymology* **512:** 243-274

Winkler DD, Muthurajan UM, Hieb AR, Luger K (2011) Histone chaperone FACT coordinates nucleosome interaction through multiple synergistic binding events. *J Biol Chem* **286:** 41883-41892

Winston F, Chaleff DT, Valent B, Fink GR (1984) Mutations affecting Ty-mediated expression of the HIS4 gene of Saccharomyces cerevisiae. *Genetics* **107:** 179-197

Wu F, Caron C, C DER, Khochbin S, Rousseaux S (2008) Testis-Specific Histone Variants H2AL1/2 Rapidly Disappear from Paternal Heterochromatin after Fertilization. *J Reprod Dev*

Yang C, van der Woerd MJ, Muthurajan UM, Hansen JC, Luger K (2011) Biophysical analysis and small-angle X-ray scattering-derived structures of MeCP2-nucleosome complexes. *Nucleic Acids Res* **39:** 4122-4135

Yoh SM, Cho H, Pickle L, Evans RM, Jones KA (2007) The Spt6 SH2 domain binds Ser2-P RNAPII to direct Iws1-dependent mRNA splicing and export. *Genes Dev* **21:** 160-174
Yoh SM, Lucas JS, Jones KA (2008) The Iws1:Spt6:CTD complex controls cotranscriptional mRNA biosynthesis and HYPB/Setd2-mediated histone H3K36 methylation. *Genes Dev* **22:** 3422-3434

Zalensky AO, Siino JS, Gineitis AA, Zalenskaya IA, Tomilin NV, Yau P, Bradbury EM (2002) Human testis/sperm-specific histone H2B (hTSH2B). Molecular cloning and characterization. *The Journal of biological chemistry* **277:** 43474-43480

Zentner GE, Henikoff S (2013) Regulation of nucleosome dynamics by histone modifications. *Nat Struct Mol Biol* **20:** 259-266

Zhang L, Fletcher AG, Cheung V, Winston F, Stargell LA (2008) Spn1 regulates the recruitment of Spt6 and the Swi/Snf complex during transcriptional activation by RNA polymerase II. *Mol Cell Biol* **28:** 1393-1403

Zhou Z, Feng H, Hansen DF, Kato H, Luk E, Freedberg DI, Kay LE, Wu C, Bai Y (2008) NMR structure of chaperone Chz1 complexed with histones H2A.Z-H2B. *Nature structural & molecular biology* **15:** 868-869

Zhou Z, Feng H, Zhou BR, Ghirlando R, Hu K, Zwolak A, Miller Jenkins LM, Xiao H, Tjandra N, Wu C, Bai Y (2011) Structural basis for recognition of centromere histone variant CenH3 by the chaperone Scm3. *Nature* **472:** 234-237

Zlatanova J, Seebart C, Tomschik M (2007) Nap1: taking a closer look at a juggler protein of extraordinary skills. *FASEB journal : official publication of the Federation of American Societies for Experimental Biology* **21:** 1294-1310

APPENDICES

APPENDIX I

NUCLEOSOME ASSEMBLY ACTIVITY OF ONCOPROTEIN DEK

Introduction:

Using supercoiling assay, we investigated the nucleosome assembly activity of the oncoprotein human DEK. DEK undergoes phosphorylation *in vivo*. Phosphorylated DEK exhibited nucleosome assembly activity (figure S.1, lanes 10-11). Dephosphorylation of DEK resulted in a complete loss of this activity (lanes 13-14).

Materials and Methods:

Chromatin assembly assay

The DNA supercoiling assay was done as described in *(Alexandra Lusser & James T Kadonaga, Nature methods, 2004)*. For each reaction, 1.2 ug of DNA plasmid was relaxed with 3 units of E. coli topoisomerase I (NEB) for 2 h at 37°C. 25 pmol histone octamer and 50 or 100 pmol of yNap1 or DEK were incubated at 37°C for 10 min. Then the relaxed plasmid was added and the reaction was incubated at 37°C for 1 h in buffer containing 10 mM Tris pH 8.0, 100 mM NaCl, 1 mM EDTA and 100 µg/µl BSA. 8 units of wheat germ topoisomerase I (Promega) was then added and the reaction was incubated at 37°C for

an additional 1 h. Final concentrations of 0.5% SDS and 0.2 mg/ml proteinase K were added and the reaction was incubated at 55°C for 30 min. DNA was purified by phenol/chloroform extraction and ethanol precipitation. The final products were analyzed on a 1.2% agarose gel running at 50 V for 15 h.

Publication:

The data was published as a collaboration project in the following paper:

F. Kappes, T. Waldmann, V. Mathew, J. Yu, L. Zhang, M.S. Khodadoust, A.M. Chinnaiyan, K. Luger, S. Erhardt, R. Schneider, D.M. Markovitz, (2011) The DEK oncoprotein is a Su(var) that is essential to heterochromatin integrity, *Genes and Development* 25, 673-678.

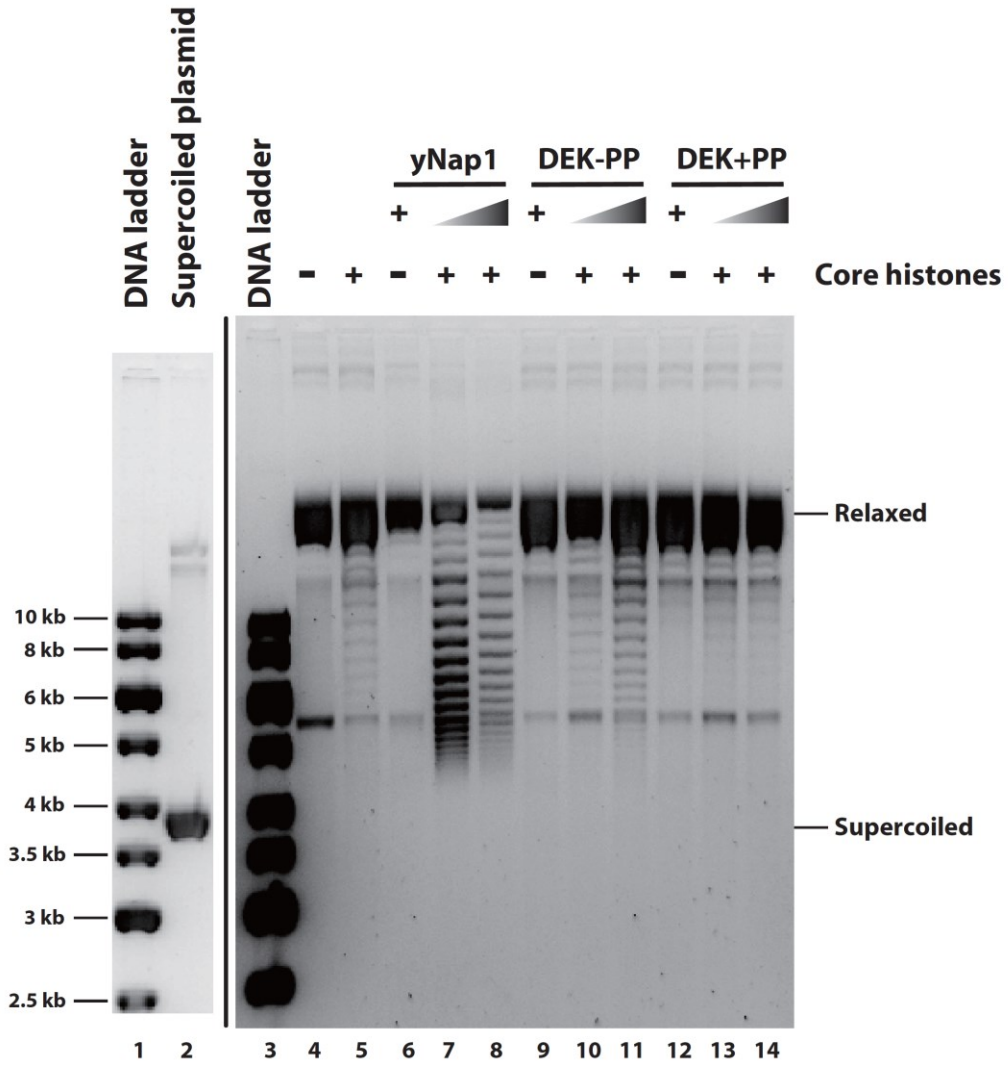

Figure S.1. Phosphorylation alters the chromatin assembly property of DEK. Nucleosome was reconstituted by incubating relaxed plasmid with core histone octamer and yeast Nap1 (lanes 7-8), DEK without phosphatase treatment (DEK-PP, lanes 10-11) or after phosphatase treatment (DEK+PP, lanes 13-14). The nucleosome reconstitution was analyzed by plasmid supercoiling assay on 1.2% agarose gel. The molar ratio of Nap1/DEK to histone octamer is 2:1 or 4:1. Controls of supercoiled plasmids (lane 2), relaxed plasmids (lane 4), with histones (lane 5), yNap1 (lane 6), DEK-PP (lane 9) or DEK+PP (lane 12) added are shown. DNA ladder is indicated (lanes 1 and 3, same DNA ladder for both gels).

APPENDIX II

NUCLEOSOME ASSEMBLE ACTIVITY OF DROSOPHILA NAP1

Introduction:

We investigated the effects of posttranslational modification of drosophila Nap1 (dNap1) on its nucleosome assembly activity. *In vivo*, E342 residue of dNap1 is polyglutamylated with the addition of up to 10 glutamyl units. To mimic the polyglutamylated dNap1, we inserted 10 glutamate residues between residues 342 and 343 of dNap1 (dNap1 342-10E). The nucleosome assembly of wild-type dNap1 is less efficient compared to dNap1 342-10E, as indicated using both supercoiling assay (figure S.2, compare lanes 5-7 to 8-10) and RAC assay (figure S.3, compared lanes 9-10 with 11-12). The deletion of C-terminal domain of dNap1 abolishes the ability to assemble nucleosomes under the same experimental conditions (figure S.2, lanes 11-13 and figure S.3, lanes 13-14).

Materials and Methods:

DNA supercoiling assay:

dNap1 wt, dNap1 342-10E, dNap1ΔC was added into 52 pmol *X. laevis* histone octamer to reach a final dNap1 construct: histone octamer ratios of 2:1, 4:1 or 8:1. Yeast Nap1 was added to histone octamer for a final yNap1:histone octamer ratio of 2:1. Reactions were incubated at 37°C for 10 min. 1.2 µg of relaxed plasmid was then added

to the reaction and the reaction was incubated at 37°C for 1 h. Wheat germ topoisomerase I was added and the reaction was incubated at 37°C for an additional 1 h. Final concentrations of 0.5% SDS were added to inactivate topoisomerase followed by addition of 0.2 mg/ml proteinase K. The reaction was then incubated at 55°C for 30 min. DNA was purified by phenol/chloroform extraction and ethanol precipitation. The final products were analyzed on a 1% agarose gel.

RAC assay:

48 nM $(H3/H4E63C)_2$-Alexa488, 300 nM H2A/H2BT112C-Atto647N was incubated with 300 or 450 μM yNap1 or dNap1 constructs, and mixed with 10 nM DNA (165bp-601 sequence). Control reactions were performed using 48 nM $(H3/H4E63C)_2$-Alexa488 and 48 nM yNap1 or dNap1 constructs; or 300 nM H2A/H2BT112C-Atto647N and 300 nM yNap1 or dNap1 constructs. Reaction buffer contained 200 mM NaCl, 10 mM Tris-HCl, pH 7.5, 5% glycerol, 0.05% NP-40, 0.05% CHAPS, 1 mM EGTA, 0.5 mM $MgAc_2$, 0.5 mM imidazole, 0.5 mM DTT, 0.5 mM PMSF, 0.05 μg/ml pepstatin A and 0.05 μg/ml leupeptin.

Reactions were incubated at room temperature for 15 min, and analyzed using 5% PAGE. Gels were scanned using Typhoon Trio multimode imager (GE healthcare) and collected using 3 excitation/emission wavelengths: for donor channel, 488/520 nm; for acceptor channel, 633/670 nm; for FRET channel, 488/670 nm.

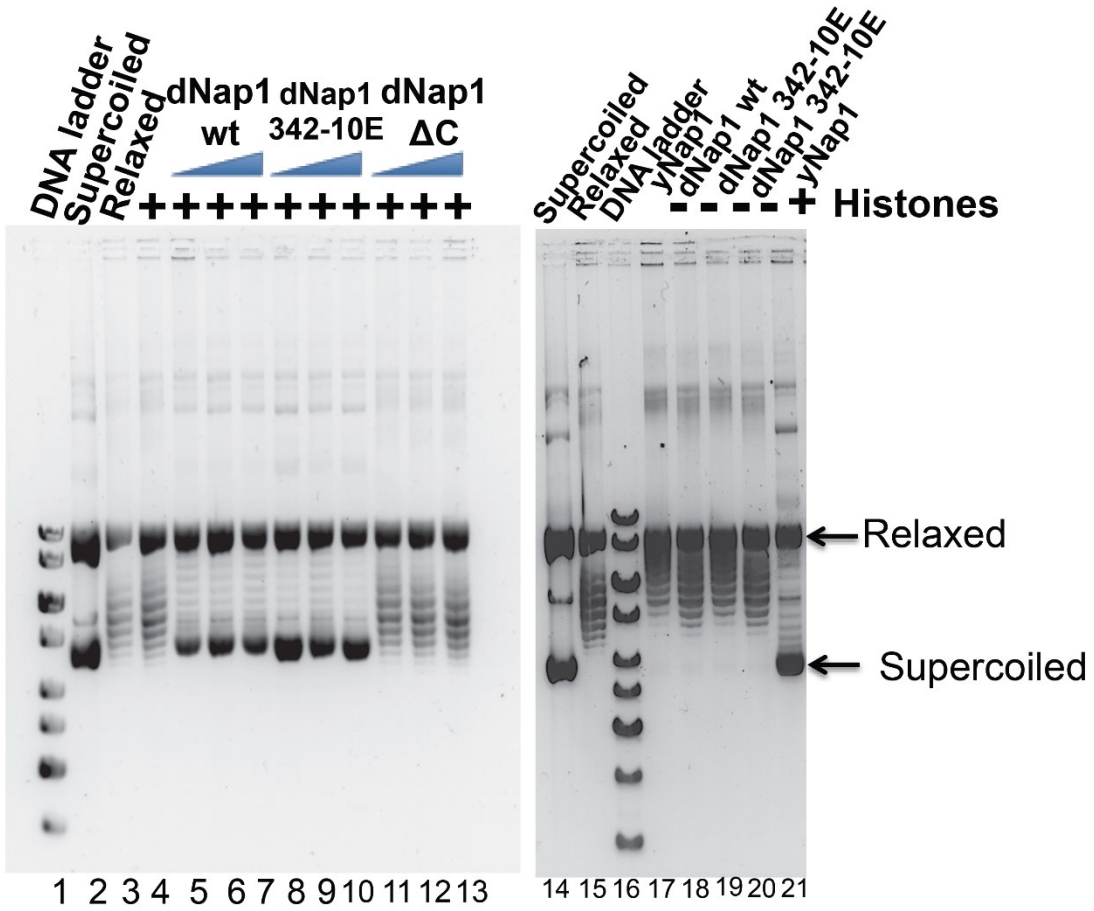

Figure S.2. Plasmid supercoiling assay with *Drosophila* Nap1 (dNap1). dNap1 wt (lanes 5-7) and 342-10E (lanes 8-10) both showed chromatin assembly activity. dNap1ΔC (lanes 11-13) does not have chromatin assembly activity. yNap1 is used as a positive control (lane 21). Supercoiled plasmid (lane 2 and 14) and relaxed plasmid (lane 3 and 15) are shown. yNap1, dNap1 wt, dNap1 343-10E, dNap1ΔC do not induce DNA supercoiling in the absence of histones (lanes 17-20). Histones do not induce DNA supercoiling either, without histone chaperones (lane 4).

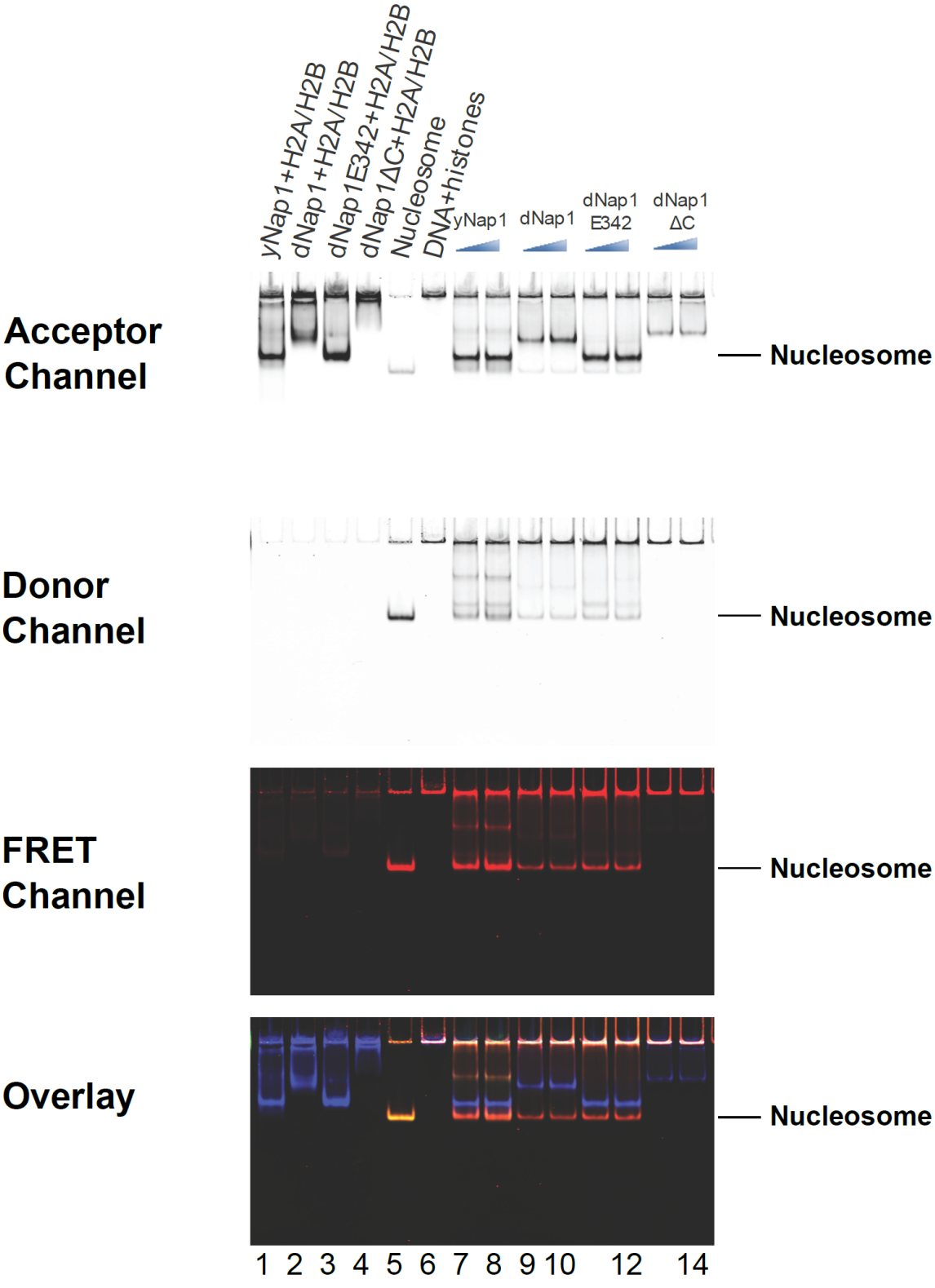
yNap1+H2A/H2B
dNap1+H2A/H2B
dNap1E342+H2A/H2B
dNap1ΔC+H2A/H2B
Nucleosome
DNA+histones
yNap1
dNap1
dNap1 E342
dNap1 ΔC
Acceptor Channel
Nucleosome
Donor Channel
Nucleosome
FRET Channel
Nucleosome
Overlay
Nucleosome
1 2 3 4 5 6 7 8 9 10 12 14

Figure S.3. Rescue of aggregated chromatin (RAC) assay with dNap1. DNA was incubated with stoichiometric amount of $(H3/H4)_2$ labeled with donor fluorophore and excess amount of H2A/H2B labeled with acceptor fluorophore. In the absence of histone chaperone, DNA and histones form aggregation that does not run into the gel (lane 6). In the presence of yNap1, nucleosome formation was rescued (lanes 7 and 8). Addition of wild type dNap1 does not induce nucleosome formation as efficiently as yNap1 (lanes 9 and 10). Addition of 10 glutamate residues in dNap1 sequence enhanced nucleosome formation (lanes 11 and 12), whereas deletion of C-terminal domain of dNap1 completely abolishes the formation of nucleosome. Controls of nucleosome reconstituted via salt dialysis (lane 5) and H2A/H2B bound to different Nap1 constructs are shown (lane 1-4).

APPENDIX III

NAP1 REARRANGES DNA-H3/H4 COMPLEXES

Introduction:

Using electrophoretic mobility shift assay (EMSA), we observed that yeast Nap1 rearranges DNA-H3/H4 complexes. When H3/H4 is mixed with DNA (207 bp-'601' sequence (Lowary & Widom, 1998)) and analyzed on native gels, DNA-H3/H4 form complexes with a gradient of mobility, indicated by smeary bands on the gel (figure S.4, lanes 4-6). With the addition of Nap1 to the complexes, more distinct bands are observed (lanes 7-9), indicating that Nap1 rearranges DNA-H3/H4 complexes.

Materials and Methods:

Electrophoretic mobility shift assays:

EMSAs were performed using 7.5 μM yNap1, 1.5 μM 207 bp 601 DNA, and 0.375, 0.75 or 1.5 μM $(H3/H4)_2$. Reaction buffer contains 20 mM Tris-HCl, pH 7.5, 100 mM NaCl and 0.35 mM EDTA. Reactions were incubated at 25°C for 15 min and then analyzed using 5% polyacrylamide gel electrophoresis.

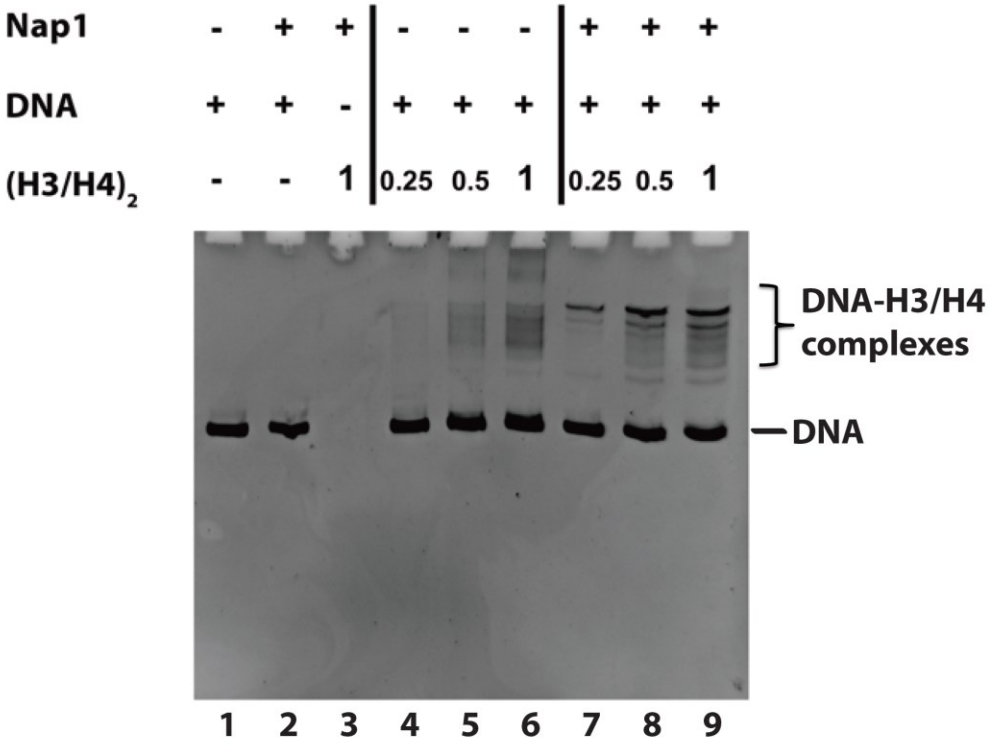

Figure S.4. Nap1 rearranges DNA-H3/H4 complexes, $(H3/H4)_2$ was added to 1.5 μM DNA. The molar ratios of $(H3/H4)_2$ to DNA are 0.25:1, 0.5:1 and 1:1 (lanes 4-6). Nap1 was added in five-fold excess to DNA (lanes 7-9). Nap1 does not interact with DNA (lane 2). DNA control (lane 1) and Nap1-$(H3/H4)_2$ (lane 3) are shown. Gels visualized with ethidium bromide staining. The addition of Nap1 into DNA-H3/H4 complexes rearranges the complexes, as indicated by changes in mobility.

APPENDIX IV

THE IC50 VALUES OF NAP1 COMPETITION ASSAYS CHANGE WITH DIFFERENT LIGAND CONCENTRATIONS

Introduction:

In this section we analyzed the IC50 values for Nap1 competition for H2A/H2B from DNA. IC50 value is obtained when we have a complex with two components, and use a third molecule to compete for a component in the complex. IC50 value is calculated as the concentration of the competitor for which reaction is half saturated. Theoretically, Ki values obtained from IC50 values should represent the binding affinity of the competitor and its binding partner. Yet when we use unlabeled Nap1 to for labeled H2A/H2B from labeled Nap1 (FRET pair), we observed discrepancies of the Ki values with the Nap1-H2A/H2B affinity with non-saturating concentrations of Nap1, which is resolved if we have Nap1 concentration that is oversaturating of H2A/H2B.

For the explanation for this observation, our hypothesis is that the oligomerization state of Nap1 (Park et al, 2008a) also affect the binding of H2A/H2B. When we have 10 nM H2A/H2B with 10-100 nM Nap1, most of Nap1 is occupied by H2A/H2B, and is in a different oligomerization state compared to the titrated, or competitor Nap1. Whereas when we have 1 nM H2A/H2B with 50 nM Nap1, most of Nap1 is free to oligomerize, and

is thus in the same oligomerization state as the competitor Nap1. To test this hypothesis, we can apply mutants of Nap1 that affect the oligomerization (Park et al, 2008a), and investigate if the binding affinity to H2A/H2B is altered with these Nap1 mutants.

Materials and Methods:

Reactions were performed in a 384-well microplate with glass bottom. H2A/H2BT112C-Alexa488 was mixed with yeast Nap1 labeled with Atto647N fluorophore. Reaction buffer contained 300 mM NaCl, 10 mM Tris-HCl, pH 7.5, 5% glycerol, 0.01% CHAPS, 0.01% NP40 and 1 mM DTT. 207 bp-601 DNA was titrated and the disappearance of FRET signal was monitored using Typhoon imager and collected using 3 excitation/emission wavelengths: for donor channel, 488/520 nm; for acceptor channel, 633/670 nm; for FRET channel, 488/670 nm. FRET signals were corrected as described in (Hieb et al, 2012). IC50 value was calculated using equation: $f=f_{max}*(1-(x\text{^}h/(x\text{^}h+IC50\text{^}h)))+f_{min}$, with f indicating the FRET signal, f_{max} and f_{min} indicating maximum and minimum FRET, x indicating the concentration of titrated DNA. Five sets of probe concentrations were used: 1. 10 nM H2A/H2B and 10 nM Nap1; 2. 10 nM H2A/H2B and 20 nM Nap1; 3. 10 nM H2A/H2B and 50 nM Nap1; 4. 10 nM H2A/H2B and 100 nM Nap1; 5. 1 nM H2A/H2B and 50 nM Nap1. At least two repeats were performed for each setting, and the average of IC50 value is shown in the table. Ki was calculated using equation: $Ki=IC50/(1+[Nap1]/K_{d(Nap1\text{-}H2A/H2B)})$.

Table S.1. Observed IC50 values and calculated Ki values for DNA competing for H2A/H2B with Nap1. Varying probe concentrations are indicated, with respective IC50 and Ki values indicated in nM. Ki values drop with the increasing Nap1 concentrations or decreasing H2A/H2B concentrations.

Observed Kd value for H2A/H2B binding to 601 DNA is 10.46 nM, which is the close to the Ki values obtained with the probe 1 nM H2A/H2B and 50 nM Nap1.

Probe	Average IC50 / nM	Ki/nM
10 nM H2A/H2B+**10** nM Nap1	214.85	67.09
10 nM H2A/H2B+**20** nM Nap1	174.5	32.28
10 nM H2A/H2B+**50** nM Nap1	267.4	22.26
10 nM H2A/H2B+**100** nM Nap1	382.35	16.6
1 nM H2A/H2B+**50** nM Nap1	107.6	8.96

A

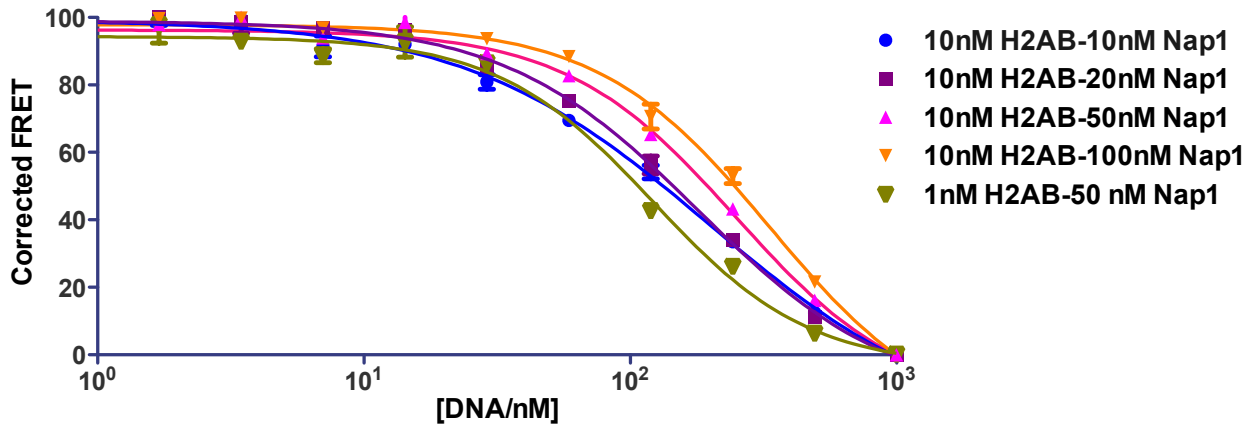

B

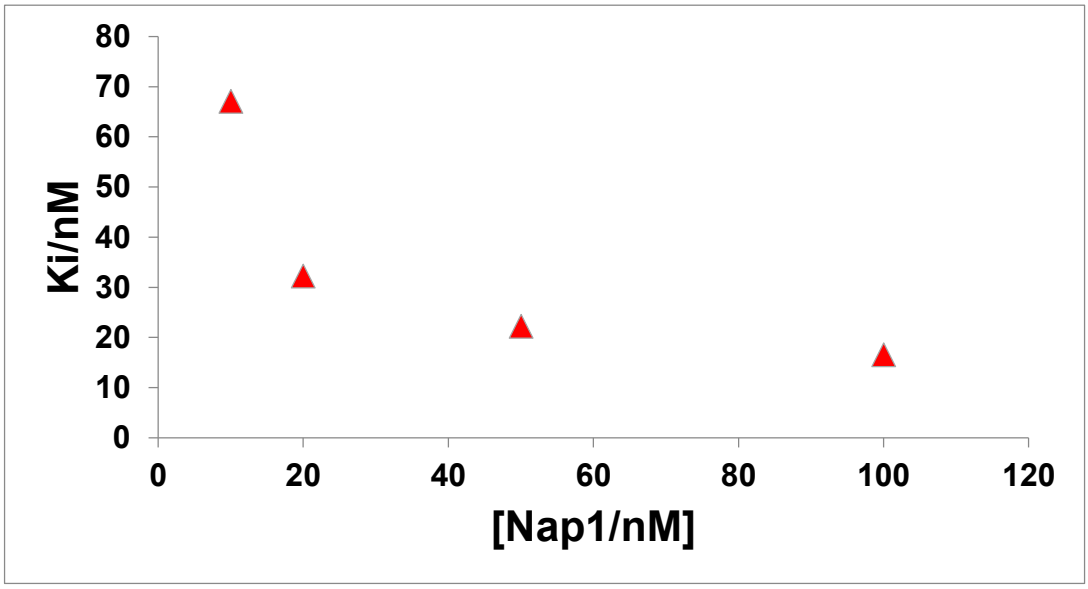

Figure S.5. (A) Curves for FRET competition assays of DNA competing for H2A/H2B with Nap1. DNA concentration (in nM) is shown on the X-axis with a log scale. Normalized corrected FRET values are shown on the Y-axis. (B) Trend of K_i values with increasing Nap1 concentrations. Calculated IC50 values in the presence of 10 nM H2A/H2B was shown on the Y-axis, and the Nap1 concentration (in nM) was shown on the X-axis.

APPENDIX V

NAP2 EXHIBITS SELF-ASSOCIATION BEHAVIOR

Introduction:

It has been previously shown that yNap1 self-associates with the basic state of yNap1 being a stable dimer. This dimer self associates into a mixture of oligomeric species at physiological ionic strength (McBryant & Peersen, 2004; Park et al, 2008a). The role of yNap1 oligomerization *in vivo*, however, is not well understood. Given the similarity between yNap1 and Nap2, the self-association status of Nap2 was examined, using both size exclusion chromatography-multi-angle light scattering (SEC-MALS) and analytical ultracentrifugation (AUC).

Light scattering experiments were performed with Nap2 in a buffer containing physiological salt concentrations (100 mM NaCl). The molar mass of Nap2 was determined to be between 200 kDa and 500 kDa (Fig.S.6). Considering the theoretical molecular weight of a Nap2 monomer is 42.5 kDa, the range of its association state can be estimated to be a pentamer to a decamer.

As shown in fig.S.7, using 3.6 μM Nap2, the sedimentation coefficient increases as the concentration of NaCl decreases, indicating self-association of Nap2 into larger oligomers. With NaCl concentration of above 350 mM, the sedimentation of Nap2 revealed a nearly

homogeneous species with a sedimentation coefficient of approximately 4.5 S. With 200 mM NaCl, Nap2 has an S value of ~6-9 S, while with 100 mM NaCl it has an S value of ~8-12 S. The range of the S value indicates the heterogeneity of Nap2.

Increasing the concentration of Nap2 can also drive self-association. By increasing the Nap2 concentration about 6-fold, the S value at 350 mM NaCl increases by about 1 S. Also, the sedimentation coefficient at 100 mM NaCl increases to 8-15 S, indicating the existence of bigger oligomers. Comparing to Nap2 at lower concentration, Nap2 at higher concentration shows a higher degree of heterogeneity.

Materials and Methods:

Size-exclusion chromatography/multi-angle light scattering

Size exclusion chromatography combined with multi-angle light scattering (SEC-MALS) is used in the determination of the molar mass of proteins in solution. SEC-MALS of Nap2 was performed using 100 μl of 0.5 mg/mL Nap2 in a buffer containing 100 mM NaCl, 20 mM Tris-HCl, pH 7.5, 1 mM EDTA and 0.2 mM TCEP. Samples were loaded onto Sephadex 200 (24 ml, GE Healthcare) size-exclusion column combined with a multi-angle light scattering instrument (Wyatt technologies). The scattered light was collected and analyzed by ASTRA software.

Analytical ultracentrifugation

Sedimentation velocity experiments were performed as described in (McBryant & Peersen, 2004). 400 μl of Nap2 or buffer control samples were applied onto a Beckman

XL series analytical ultracentrifugation system. Centrifugation was performed at 23°C using 40,000 rpm for 5 h with a total of 90 scans. Buffers contained 20 mM Tris-HCl, pH7.5, 0.2 mM TCEP or 200 mM/350 mM/500 mM NaCl. Data obtained were processed using Demeler-van Holde method with Ultrascan software (Demeler & van Holde, 2004).

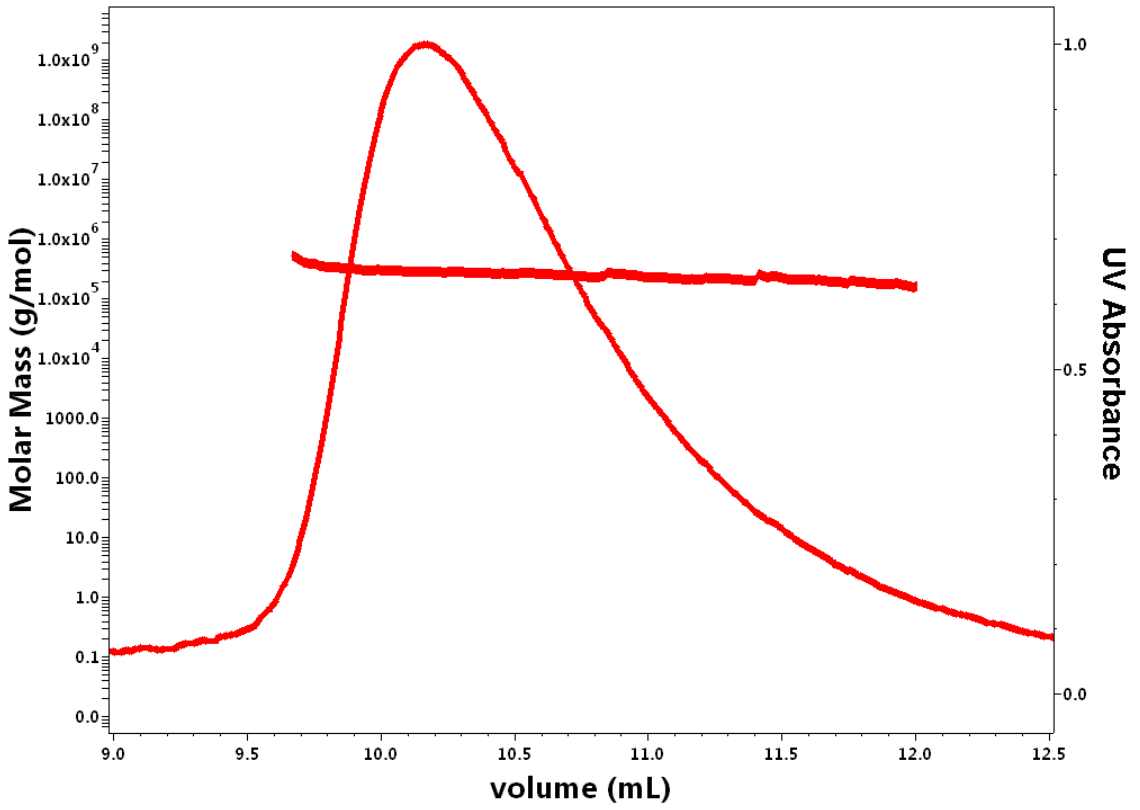

Figure S.6. SEC-MALS profile indicating self-association state of Nap2 with 100 mM NaCl. The size exclusion chromatography trace is shown as a continuous curve. The flat line shows molecular weight range of Nap2 (indicated on the left y-axis).

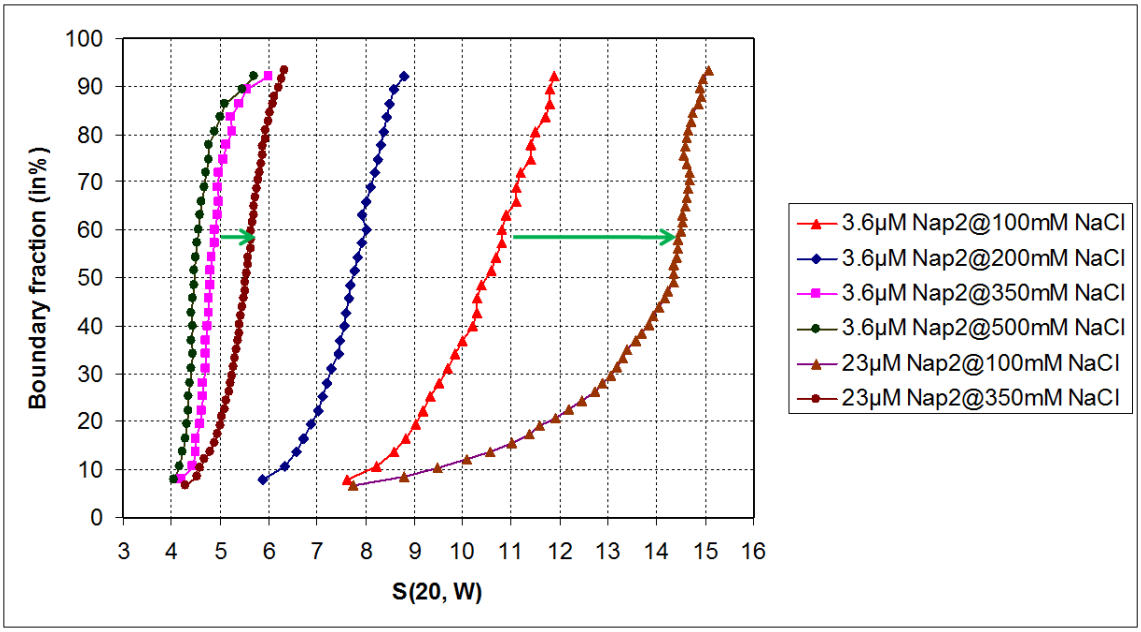

Figure S.7. G(s) plot of sedimentation velocity data showing changes in self-association state of Nap2 under different ionic strength. Data was collected and analyzed using two Nap2 concentrations (3.6 μM and 23 μM) and four NaCl concentrations (100 mM, 200 mM, 350 mM and 500 mM). Green arrows indicate the change with increased concentration of Nap2 at two salt concentrations.